

## ABSTRACT

Title of Dissertation:           EFFICIENT SPECTRUM MANAGEMENT FOR  
MOBILE AD HOC NETWORKS

Leo Henry Jones, Jr., Doctor of Philosophy, 2010

Dissertation directed by:    Professor Gregory B. Baecher

Department of Civil and Environmental Engineering

The successful deployment of advanced wireless network applications for defense, homeland security, and public safety depends on the availability of relatively interference-free spectrum. Setup and maintenance of mobile networks for military and civilian first-response units often requires temporary allocation of spectrum resources for operations of finite, but uncertain, duration. As currently practiced, this is a very labor-intensive process with direct parallels to project management. Given the wide range of real-time local variation in propagation conditions, spatial distribution of nodes, and evolving technical and mission priorities current human-in-the loop conflict resolution approaches seem untenable.

If the conventional radio regulatory structure is strictly adhered to, demand for spectrum will soon exceed supply. Software defined radio is one technology with

potential to exploit local inefficiencies in spectrum usage, but questions regarding the management of such network have persisted for years.

This dissertation examines a real-time spectrum distribution approach that is based on principles of economic utility and equilibrium among multiple competitors for limited goods in a free market. The spectrum distribution problem may be viewed as a special case of multi-objective optimization of a constrained resource. A computer simulation, described in Appendix A, was developed to create hundreds of cases of local spectrum crowding, to which simultaneous perturbation simulated annealing (SPSA) was applied as a nominal optimization algorithm. Two control architectures were modeled for comparison, one requiring a local monitoring infrastructure and coordination (“top down”) the other more market based (“bottom up”). The analysis described herein indicates that in both cases “hands-off” local spectrum management by trusted algorithms is not only feasible, but that conditions of entry for new networks may be determined a priori, with a degree of confidence described by relatively simple algebraic formulas.

The network simulation results confirm the assertions of 2009 Nobel laureate economist Elinor Ostrom (Ostrom & Dietz, 2002) that locally autonomous groups and individuals are as capable of managing a common resource as any external authority.

EFFICIENT SPECTRUM MANAGEMENT FOR MOBILE AD HOC NETWORKS

By

Leo Henry Jones, Jr.

Dissertation submitted to the Faculty of the Graduate School of the  
University of Maryland, College Park, in partial fulfillment  
of the requirements for the degree of  
Doctor of Philosophy  
2010

Advisory Committee:  
Professor Gregory B. Baecher, Chair  
Professor Stuart D. Milner  
Professor Christopher Davis  
Professor Qibin Cui  
Professor S. Raghavan

© Copyright by

Leo Henry Jones, Jr.

2010

## **Dedication**

I would like to thank my father, Leo Jones, Sr., for his inspiration and my wife Gioia and our children for their considerable patience during this project.

## Contents

Dedication .....	ii
List of Tables.....	v
List of Figures .....	vi
List of Abbreviations.....	ix
Chapter 1: Problem Definition and Scope.....	1
Spectrum Management and Project Management.....	6
Chapter 2: Survey of Related Literature and Prior Research .....	11
Chapter 3: Proposed Solution.....	17
Spectrum Utility .....	21
Local Spectrum Constraints .....	25
Previous Research on Spectrum Management for SDR.....	26
Basic Research Questions .....	33
Models of Physical Processes .....	39
Radio Node Model .....	39
Network Connectivity .....	40
Network Geometry and Motion .....	41
Radio Propagation Model.....	44
Signal Spectrum Model.....	45
Interference Model .....	47
Receiver Noise Power .....	49
SINR Calculation .....	51
Application of SPSA to Spectrum Adjudication.....	52
Chapter 4: Design of Simulation Experiment .....	57
Distribution of Input Variables .....	60
Time-Series Output .....	62
Chapter 5: Analysis of Simulation Results .....	67
Kolmogorov-Smirnov Test of SINR Residuals .....	83

Investigation of Heteroskedasticity in SINR Prediction Errors .....	86
Gaussian Frequency Dependent Integration.....	87
Chapter 6: Potential Applications .....	96
Chapter 7: Extensions of Interference Models .....	103
Time Diversity Interference Model .....	103
Code Diversity Interference Model .....	104
Spatial Diversity Interference Model .....	105
Chapter 8: Conclusions .....	110
Appendix A: Spectrum Management Simulation .....	115
Program Structure .....	115
MATLAB Source Code .....	118
Appendix B: Sample Case Input .....	131
Appendix C: Sample Case Output .....	133
Appendix D: Timing Estimate for Autonomous Spectrum Allocation.....	139
Appendix E: List of Symbols .....	142
Bibliography .....	143

## List of Tables

Table 1: Inputs for MANET simulation .....	59
Table 2: MLS Coefficients for Minimum SINR, Homogeneous MANET .....	69
Table 3: Multivariate Least Squares: Case H0 (Homogeneous Nets).....	69
Table 4: MLS Analysis: Case H1 (Heterogeneous Nets).....	70
Table 5: Statistics for MANET Prior Prediction Fit: Case H3 (Mixed).....	70
Table 6: Coefficients for Prior Estimate of SINR Standard Error .....	80
Table 7: Results of K-S Test for Normally Distributed Residuals.....	85
Table 8: Simulation Inputs for Sample Case.....	132
Table 9: Simulation Case Output .....	133



## List of Figures

Figure 1: Spectrum Management organization for U.S. Army units operating outside the continental United States (FM 24-2, 1991) .....	8
Figure 2: Software defined radio can help negotiate “spectrum commons” .....	18
Figure 3: Adaptive spectrum management as a microeconomics problem.....	19
Figure 4: Components of a nominal spectrum utility objective function.....	24
Figure 5: SIMULINK model of interactions between three adjacent SDR nets .....	28
Figure 6: SIMULINK model of cognitive radio tuning .....	29
Figure 7: OSE-driven frequency (MHz) evolution (Jones, 2001).....	30
Figure 8: OSE-driven bandwidth (MHz) evolution (Jones, 2001).....	30
Figure 9: OSE-constrained power (dBW) evolution (Jones, 2001) .....	31
Figure 10: Each network tries to optimize its utility function (Jones, 2001) .....	31
Figure 11: Evolution of a "spectrum rich" (100 MHz) four-net OSE distribution..	32
Figure 12: Evolution of a "spectrum-starved" (40 MHz) four-net distribution .....	33
Figure 13: Top-down model of automated spectrum management.....	35
Figure 14: Bottom-up model of automated spectrum management .....	36
Figure 15: Geometric “stacking” model for spectrum provisioning.....	38
Figure 16: Conceptual model for adaptive radio nodes .....	40
Figure 17: Notional MANET Layout.....	42
Figure 18: Gaussian spectrum model for signals and interference .....	46
Figure 19: Two adjacent MANET must deal with mutual interference.....	48
Figure 20: Example of FDI for Gaussian passband model .....	51
Figure 21: Distributions of selected input parameters for simulation.....	61
Figure 22: Histogram of cases for low geometric loading .....	62
Figure 23: A nominal “top-down” spectrum solution.....	63
Figure 24: A nominal “bottom-up” spectrum solution.....	64
Figure 25: Spectrum utility for top-down and bottom-up solutions.....	65
Figure 26: Networks attempt to minimize overall spectrum occupancy.....	66
Figure 27: MLS curve fit for top-down spectrum adaptation .....	71

Figure 28: MLS curve fit for bottom-up spectrum adaptation .....	72
Figure 29: Divergence of Top-Down and Bottom-Up minimum SINR .....	75
Figure 30: Potential for chaotic top-down SINR behavior .....	76
Figure 31: Potential for chaotic bottom-up SINR behavior .....	77
Figure 32: Risk-based spectrum access architecture (nominal) .....	77
Figure 33: Exponential bound for Top-down SINR residuals .....	79
Figure 34: Exponential bound for Bottom-up SINR residuals.....	80
Figure 35: MLS regression model results for low density of MANET .....	81
Figure 36: Histogram of top-down prediction residuals .....	82
Figure 37: Histogram of bottom-up prediction residuals .....	82
Figure 38: Cumulative distribution functions for simulated residuals .....	83
Figure 39: Log-linear behavior of FDI derivative.....	89
Figure 40: Idealized alternative passband functions .....	90
Figure 41: Nominal FDI functions for idealized passbands.....	91
Figure 42: FDI derivative for several passband models.....	92
Figure 43: FDI response for Gaussian and rectangular passbands.....	94
Figure 44: Comparison of Residuals for Gaussian and Rectangular passbands .....	95
Figure 45: Spectrum Provisioning for Top-Down Autonomous Management.....	98
Figure 46: Spectrum management model for engineering analysis .....	100
Figure 47: Derived confidence metric for top-down minimum SINR .....	101
Figure 48: Derived confidence metric for bottom-up minimum SINR.....	102
Figure 49: Gain pattern for a nominal directional antenna array .....	106
Figure 50: Directional antennas can enable angular discrimination .....	109
Figure 51: Architecture diagram of spectrum management simulation .....	115
Figure 52: SPSA algorithm for spectrum management .....	117
Figure 53: MANET node distribution generated for Sample Case.....	134
Figure 54: Top-Down Spectrum Solution for Sample Case 104 .....	135
Figure 55: Bottom-Up Spectrum Solution for Sample Case 104.....	136
Figure 56: Spectrum Utility Evolution for Sample Case 104 .....	137

Figure 57: Playbox Occupancy Evolution for Sample Case 104 ..... 138

## List of Abbreviations

3G	Third generation communication service
BER	Bit error rate
BPSK	Binary phase shift keying
CDF	Cumulative distribution function
CR	Cognitive radio
DARPA	Defense Advanced Research Projects Agency
dB	Decibel
dBm	Decibel relative to one milliwatt (0.001 watt)
DHS	Department of Homeland Security
DSP	Digital signal processor
EM	Electromagnetic
EMC	Electromagnetic compatibility
EMCON	Emission control
EMI	Electromagnetic interference
EW	Electronic warfare
FCC	Federal Communications Commission
FDI	Frequency dependent integration
FDR	Frequency dependent rejection
GHz	Gigahertz ( $10^9$ cycles/sec)
INR	Interference-to-Noise Ratio
IPv6	Internet Protocol Version 6
ITU	International Telecommunications Union
ISL	Integrated side lobe level
JTRS	Joint Tactical Radio System
kHz	Kilohertz ( $10^3$ cycles/sec)
MANET	Mobile ad hoc network
MHz	Megahertz ( $10^6$ cycles/sec)
MIMO	Multiple-input, multiple-output
MLS	Multivariate least squares
NTIA	National Telecommunications and Information Administration
PHY	Physical layer
PSD	Power spectral density
RF	Radio frequency
SDR	Software defined radio
SINR	Signal-to-Interference-plus-Noise Ratio $S/(I+N)$
SNBU	Signal-to-Interference-plus-Noise Ratio (Bottom-Up)
SNTD	Signal-to-Interference-plus-Noise Ratio (Top-Down)
SPSA	Simultaneous perturbation simulated annealing
UBU	Utility (Bottom-Up)
UTD	Utility (Top-Down)
WCDMA	Wideband code division multiple access
XG	Next Generation Communications Program



## **Chapter 1: Problem Definition and Scope**

The military services of the United States, along with many civilian and public safety agencies of the federal, state, and municipal governments, have embraced modern communications network technology in an effort to improve the efficiency and effectiveness of their core operations. Concepts such as “net-centricity”, and “network-centric operations” are currently subjects of intense study in government-sponsored think tanks. Most of the anticipated benefits of net-centric operation are expected to come from improvements in the location and coordination of highly mobile assets (e.g., soldiers, police, firefighters and long-haul trucks), each of which would ideally have access to sufficient information (often called “situational awareness”) to accomplish the mission while minimizing casualties.

While the precise nature of the relationship between information availability and tactical performance remains a matter of continued analysis and debate, there is general agreement that given the current state of operations “more is better”. The imperatives of mobility and situational awareness drive defense and public safety operations to ever increasing dependence on wireless networks, which in turn leads to increased demands for radio-frequency (RF) spectrum to support advanced network applications.

Normally, increased demand for a commodity induces suppliers to produce more to meet the demand. The electromagnetic (EM) spectrum is a special commodity, in that "Mother Nature" through the laws of physics produces the available spectrum. EM spectrum is a truly scarce resource. Current / historic methods of spectrum allocation assign the available spectrum bands to individuals and groups, without regard to their

actual rate of use on a moment by moment basis. Creating a market mechanism that would allow underutilized spectrum to be accessed by individuals and groups who greatly desire to communicate will increase the efficiency of the commodity's utilization. While the laws of physics determine the available spectrum, the efficiency of the market system determines the effective spectrum available for communications.

As the network becomes more critical to the success of future deployments, the potential impact of network failure has gained significant attention. For example, J. Peha's testimony before the FCC (Peha, 2005) alleges that problems with interoperability between radio networks contributed to first-responder casualties during the World Trade Center attack on September 11, 2001.

*“The worst failure occurred in the World Trade Center’s North Tower. At 9:59AM on September 11, 2001, the first of several announcements was transmitted to emergency responders ordering them to evacuate the North Tower. Police inside the building heard the order on their radios, and most left safely. However, firefighters were using incompatible communications equipment that could not receive the order. People watching television at home knew that the unimaginable had already occurred - that the World Trade Center’s South Tower had collapsed - but many firefighters inside the North Tower would never learn of this. When the North tower fell 29 minutes after that first evacuation order, 121 firefighters were still inside. None survived. At the same time, two hundred miles away, more communications failures were making it harder to contain fires at the Pentagon, where another plane had crashed. These failures put more lives at risk.”*

The inadequacy of the current U.S. government approaches for allocating and managing radio spectrum for public safety applications has been the subject of expert testimony over nearly a decade, yet debate continues regarding the nature of the needed change.

*“The FCC and DHS have different perspectives on radio technology and infrastructure. DHS policies favor reliability and familiarity in their requirements and guidelines for technology and in their emphasis on training and repeated use of equipment. Spectrum policy at the FCC promotes spectrum efficiency and competition among commercial license-holders. Neither the FCC nor the DHS agencies that support public safety communications appear to have considered preparing public safety communications for the coming generations of wireless technology.” (Moore, 2009)*

The military services face a similar array of communication resource issues. The U.S. Army estimates that without significant technological advancement in efficient spectrum usage, it will soon face a bandwidth shortage that could significantly hamper future operations. In response, the outgoing Army procurement chief has commissioned studies to estimate the extent of the projected shortfall and to evaluate the benefits of technological and regulatory strategies.

*“Battlefield radio networks that allow friendly forces to exchange voice, data and video signals will be key to an Army equipped with 27-ton Future Combat Systems vehicles instead of 70-ton Abrams tanks. Even with Joint Tactical Radio Systems (JTRS) that move bits hundreds of times faster than earlier radios, the needs of an information-powered force are poised to overwhelm the available bandwidth.*

*“We have enough to do the job today, but I am not convinced we have enough to do the job I see coming five years from now,” Claude Bolton, the outgoing assistant Army secretary for acquisition, logistics and technology, said in an exit interview.*

*Beginning in 2010 and continuing for several decades, the Army will introduce elements of an ever-more-networked force that moves vast amounts of data from soldier-mounted sensors, aerial and ground robots, manned vehicles and more.” (Osborn, 2008)*

There are documented instances from the current wars in Iraq and Afghanistan where physical-layer communications problems such as electromagnetic interference (EMI) from friendly sources, or spotty connectivity—“outrunning the net”—have compromised the advantage of U.S. and allied combat units. One Army battalion



commander describes a network capacity reduced to low rate text and locating his adversary the old-fashioned way, by running into him:

*As night fell, the situation grew threatening. [Lieutenant Colonel Ernest] Marcone arrayed his battalion in a defensive position on the far side of the bridge and awaited the arrival of bogged-down reinforcements. One communications intercept did reach him: a single Iraqi brigade was moving south from the airport. But Marcone says no sensors, no network, conveyed the far more dangerous reality, which confronted him at 3:00 a.m. April 3. He faced not one brigade but three: between 25 and 30 tanks, plus 70 to 80 armored personnel carriers, artillery, and between 5,000 and 10,000 Iraqi soldiers coming from three directions. This mass of firepower and soldiers attacked a U.S. force of 1,000 soldiers supported by just 30 tanks and 14 Bradley fighting vehicles. The Iraqi deployment was just the kind of conventional, massed force that's easiest to detect. Yet "We got nothing until they slammed into us," Marcone recalls. (Talbot, 2004)*

This increase in institutional demand has unfortunately coincided with a steady decrease in the amount of spectrum allocated to military and public safety applications due to commercial occupation or statutory restriction of technically advantageous bands. In the regulatory scheme employed by the Federal Communications Commission (FCC), the National Telecommunications and Information Administration (NTIA) and the International Telecommunications Union (ITU) the rights to a particular band are awarded to a license holder or limited to a particular set of applications. All secondary users of the band have subordinate rights, if any, and must operate on a not-to-interfere basis with the primary users.

The rationale for this approach is rooted in the relatively embryonic radio technology of the 1930s. One notable consequence is that spectrum planning and resource management remains a very labor intensive process in the 21<sup>st</sup> century, even for public safety agencies and expeditionary military units. Consider the battlefield spectrum

management process as depicted in Figure 1, excerpted from a (recently superseded) U.S. Army field manual on spectrum management (FMI 6-20.70 (FM 24-2) , 2006).

*The division network planners design the network, and the spectrum manager uses this design to determine the spectrum requirements necessary for the communications network. In the emerging force structure there are two spectrum managers per division. Normally, one spectrum manager will be responsible for the network to include satellite requirements while the other spectrum manager will handle combat net radio (CNR) and other systems requirements to include fires, EW, radar, and other systems. The brigade spectrum manager performs all of these functions and is located at the S-6 in order to have visibility of all spectrum related matters at the brigade.*

On an organizational chart this arrangement more closely resembles the structure of a commercial firm preparing to defend itself against a lawsuit than an army prepared for rapidly changing conditions in network-centric operations.

Yet the entire spectrum regulatory infrastructure cannot be thrown to the winds, with all radio spectrum declared to be unlicensed. Certain critical safety applications (e.g., air traffic control radar) and commercial enterprises (broadcast or satellite radio) rely on guaranteed spectrum availability and widespread technical compatibility, and thus would have nothing to gain by adopting agile radio technology. On the other hand, few if any terrestrial license holders need or can afford to project a persistent, omnipresent signal. This fact, coupled with regulatory provisions for unlicensed and multipurpose bands, allows for the existence of local spatial-temporal pools of available spectrum, the so called “white spaces”, which can and should be exploited for national defense and public safety applications.

Despite the necessary technical content that follows, this thesis is primarily a feasibility study for potential improvements to the spectrum management process under

conditions where the timeliness and quality of the solution will translate into lives rather than money saved. It is intended as an engineering-based resource management treatise rather than a design document for a new radio protocol.

### **Spectrum Management and Project Management**

As currently practiced, spectrum management is a very labor-intensive process with direct parallels to project management, several a few of which are relevant to this study:

- *Temporary arrangements* - Maintenance of mobile radio networks for military and civilian first-response units usually involves a temporary allocation of valuable spectrum resources for operations of finite, but uncertain, duration.
- *Complex organizational dependencies* - The quality of service in the networks has a direct impact on the flow of information, which affects the quality and timeliness of coordination and decision-making processes among the various teams, which in turn affects the probability of success for the entire operation.
- *Conflict resolution* – Spectrum managers try to avoid service disruptions due to interference from friendly sources (“spectrum fratricide”) and so must consider the electromagnetic compatibility (EMC) of the radio equipment used by all units. Military spectrum managers must also consider emission control (EMCON) constraints which attempt to prevent signal intercept and exploitation by adversaries.
- *Specific time and place* - The matter is further complicated by the fact that the availability of spectrum is often highly dependent upon the time and location of

the emergency, while the utility of the available bands may be constrained by local propagation conditions such as terrain, vegetation and weather.

- *Regulatory, legal and economic constraints* - During peacetime local and international radio regulations must be respected, as well as the contractual rights of commercial network operators. Consequently, a spectrum plan developed for a military exercise at Fort Irwin, California may bear little relevance to a plan for operations in South Korea involving the same brigades.

Even highly skilled military frequency managers armed with the latest in conventional spectrum planning and conflict resolution software (e.g., Spectrum XXI<sup>1</sup> and JEET<sup>2</sup>) may take days to develop an acceptable frequency plan and hours to re-plan around Clausewitz's "fog of war", using an "incumbent/exclusionary" spectrum allocation model. Meanwhile conditions in the battlefield electromagnetic environment may change by the minute.

---

<sup>1</sup> Spectrum XXI software was developed by Alion Science and Technology under the direction of the Department of Defense Joint Spectrum Center (JSC) and the National Telecommunications and Information Administration (NTIA) to help automate and standardize the spectrum management processes throughout the Federal Government.

<sup>2</sup> Joint E3 Evaluation Tool (JEET) is a PC-based intersite electromagnetic compatibility (EMC) analysis program that examines the potential for electromagnetic interference (EMI) between a system of interest and its operational electromagnetic environment.

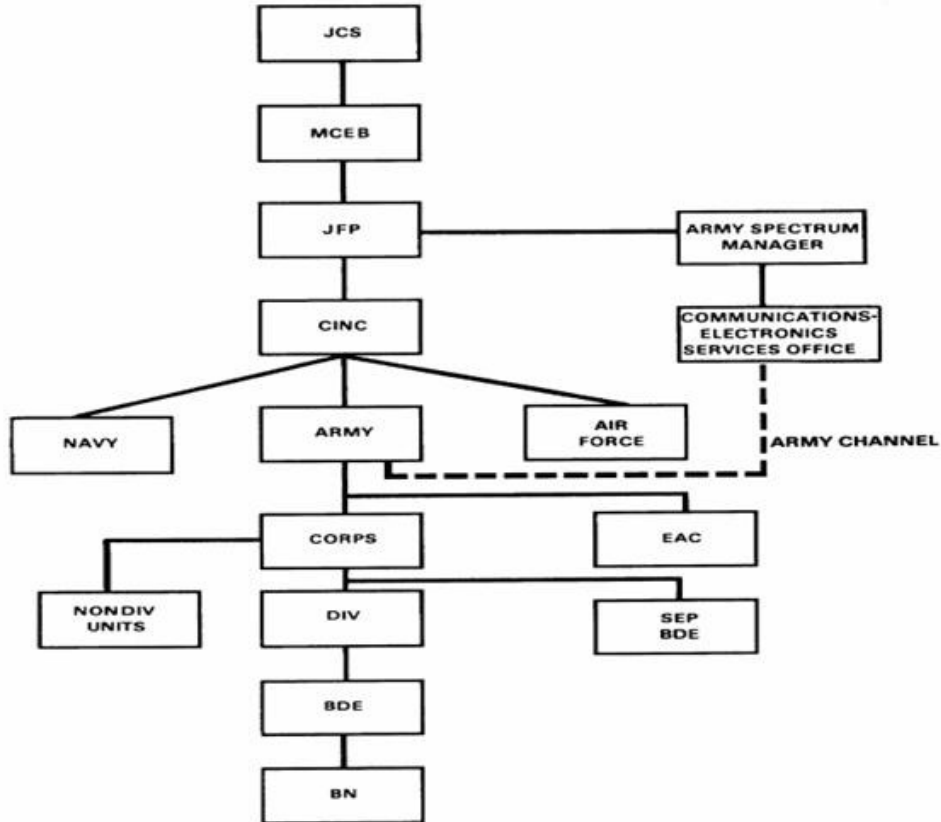


**Figure 1: Spectrum Management organization for U.S. Army units operating outside the continental United States (FM 24-2, 1991)**

Man-in-the-loop frequency resolution processes cannot adequately cope with real-time changes in local conditions. If the current “single purpose band” radio regulatory structure is strictly adhered to, demand for spectrum will soon exceed supply, a trend already recognized by the military services.

Recent advances in radio technology have the potential to serve as the building blocks of a more efficient spectrum management process. Many have faced significant regulatory challenges to their deployment. Notable examples include:

- *Mobile ad hoc networks (MANET)* – An ensemble of mobile radio nodes that must maintain communication and collaborate while constantly reorganizing itself in response to changes the external environment, all without benefit of a preexisting infrastructure. Future Army and Marine ground tactical networks are expected to include a large number of MANET.
- *Software defined radio (SDR)* – A radio in which some or all of the physical layer functions that are typically set by hardware (e.g., mixers, filters, amplifiers and modulator/demodulators) may be defined or reconfigured by software. The SDR concept was first described by Joseph Mitola (Mitola, 1992). SDR programs with significant near-term impact include the Joint Tactical Radio System (JTRS) and the Next Generation Communications (XG) project sponsored by the Defense Advanced Research Projects Agency (DARPA).
- *Cognitive Radio (CR)* – This technological descendent of SDR allows a network to change its transmission or reception parameters to more effectively communicate by avoiding interference from other networks, based on the active monitoring of several factors, e.g., radio frequency spectrum, user behavior and network state.
- *Multiple-input multiple-output (MIMO) systems* – A combination of multiple-aperture antennas and advanced signal processing can take advantage of urban multi-path radio propagation to define new channels, as opposed to suffering severe performance degradation.

U.S. military units operating around the world must contend with the telecommunications infrastructure of host nations, many of which have chosen to leapfrog the wired stage of network deployment in their efforts to modernize. The electromagnetic environment encountered during these operations will be even more complex and varied than that faced during domestic training or by public safety responders, where the license holders and frequency assignments can in principle be known far in advance. Market forces continue to make military-reserved radio frequency bands attractive targets for commercial and political speculation. Given such rapidly evolving conditions new, less manpower-intensive approaches are needed to ease transition of adaptive network technology into the defense establishment, to minimize adverse impacts to friendly legacy systems, and to develop automated management strategies to deal with complex real-time interactions.

## Chapter 2: Survey of Related Literature and Prior Research

The issues of spectrum management are not new. A great deal of ink has already been expended on the subject, with increasing attention since the 1990s. The major themes in this body of literature are the legal and political framework for spectrum allocation; arguments for regulatory change on the basis of economics, to include game theory; and finally, appeals to technology to modernize spectrum management by removing much of the entropy and delay associated with human intervention.

Three documents in particular provide a useful background in current spectrum management policy and practice from the perspective of an ITU member nation, the U. S. government, and the Department of Defense, respectively:

- The ITU *Handbook on National Spectrum Management* describes the procedures for regulating radio transmissions within the borders of a participating country. Particular attention is given to the definition and relationships between technical parameters that “if not controlled, could cause interference to other systems and adversely impact the efficient use of the frequency spectrum”, including: carrier frequencies, transmitter power, frequency tolerance, bandwidth, unwanted emissions, inter-modulation products, and receiver sensitivity (ITU Radiocommunication Bureau, 2005). Chapter 7 of this handbook describes the transition to automated spectrum management, although the automation considered is of the spreadsheet-and-database variety and requires significant human participation.



- The most recent edition of the NTIA *Manual of Regulations and Procedures for Federal Frequency Management* (aka, “the Red Book”) defines spectrum management policy as applied to U.S. military and other federal agencies, including general channel allocations for land, nautical, aviation and satellite communications (National Telecommunications and Information Administration, 2008).
- In a MITRE<sup>3</sup> technical report for the Office of the Assistant Secretary of Defense for Networks and Information Infrastructure (OSD NII) titled *Spectrum 101: An Introduction to Spectrum Management*, John Stine and David Portigal provide an excellent overview of the current spectrum management process from a DoD perspective, plus a tutorial on the implications of emerging radio technologies (Stine & Portigal, Spectrum 101, 2004).

The economic aspects of spectrum availability have long been recognized, dating back to the issuance of the first radio broadcast licenses. Recent attention has been given to the process of resolving spectrum property rights disputes between commercial enterprises, or between commercial and public interests:

- A survey of theoretical economic approaches to long term spectrum allocation problems, such as Network Utility Maximization (Yi & Chiang,

---

<sup>3</sup> MITRE is a federally funded research and development center (FFRDC).

2008), shows that spectrum optimization concerns for institutional users date back to at least 1998. These studies primarily sought to optimize the revenue streams available to commercial cellular providers and other primary spectrum licensees.

- To help moderate private sector lobbying for what was then deemed an abundance of spectrum allocated to government and public usage, Mark Bykowsy and Michael Marcus of the FCC proposed the creation of an electronic market for “callable” spectrum. In this scheme the risk of technical unsuitability of a given portion of the spectrum due to chance events (“performance risk”) could be transferred from the public sector to a prospective lessee or license holder (Byowsky & Marcus, 2002).
- As described by Yochai Benkler (Benkler, 2002), calls for greater spectrum allocation efficiency, in economic terms, fall into two camps – one advocating distribution of permanent property rights to spectrum according to some formulation that maximizes public good, the other declaring that advances in technology (e.g., software defined radio) would enable the public good to be even further enhanced by an open market approach with high levels of spatial and temporal granularity. Benkler also explores the economic and regulatory implications of some of then-state-of-the art radio technologies, such as ultra-wideband (UWB).

- Gerald Faulhaber, a Wharton economics professor and former chief economist for the FCC, has long advocated marrying economic theory to modern radio technology to derive greater public good from the public airwaves (Faulhaber G. R., 2005). In a more recent paper, Faulhaber describes the legal and economic implications of deploying cognitive, spectrum-sensing radios with opportunistic access to pools of unlicensed spectrum, a concept very similar to the decentralized “bottom up” spectrum management approach examined in this study. Faulhaber acknowledged both the disruptive and positive potential of cognitive radio, while leaving engineers to work out the technical details (Faulhaber G. R., 2008).

Theoretical work in spectrum management of course begs the question of practical implementation, and the engineering community has not been found lacking in activity:

- The concept of quantifying spectrum efficiency for mobile radio networks was described by R. J. Matheson for the NTIA. His detailed technical analysis showed that single user voice applications have inherent opportunities for frequency reuse (Matheson, 1994).
- John Stine has recently developed a method for determining spectrum access rights based on location and knowledge of local conditions for radio propagation (Stine, A Location-Based Method for Specifying RF Spectrum Rights, 2007). In an earlier paper, Stine documented automated spectrum management for an ad hoc network, based on a modification of an existing node state routing (NSR) protocol (Stine, 2006).

- Steven Silverman and Anne Wells at Raytheon used an OPNET<sup>4</sup> simulation to demonstrate the feasibility of enabling software defined radios to participate in a Prisoner's Dilemma exercise. In their study, two identical networks operating on different time slots used carrier sense multiple access (CSMA) , a probabilistic medium access control (MAC) protocol, to estimate each other's level of activity and arrive at ways to share channel resources (Silverman, 2006). This experiment confirmed that Nash Equilibrium theory could be applied using achievable radio technology.
- The author's own early simulation experiments confirmed that, under some conditions, three or more networks could apply non-identical measures of value to mitigate mutual interference and arrive at a feasible distribution of a common pool of spectrum (Jones, OSE Algorithm, 2002). The task of determining conditions for successful spectrum sharing constitutes much of the work of this thesis.
- A separate analysis of the potential effects of consumer-grade UWB devices on cable television services' satellite head-end stations, for which the author was principal investigator, confirmed the importance of power management

---

<sup>4</sup> OPNET is a trademark of OPNET Technologies, Inc., of Bethesda, Maryland.

in adjacent channels, even for sub-microwatt devices (Alion Science and Technology, 2004).

- Finally, several of the necessary technologies (interference sensing, policy logic, and coordinated re-tuning) for cognitive networks have been successfully demonstrated in small (4-6 nodes) field tests by Shared Spectrum Company for DARPA's XG program (Marshall, Martin, McHenry, & Kolodzy, 2006).

### **Chapter 3: Proposed Solution**

This research project originated as part of a Department of Defense response<sup>5</sup> to an FCC Notice of Inquiry regarding potential problems with the regulation of software defined radio. The primary concern, advanced primarily by telecommunications license holders (AT&T, 2000), was whether such opportunistic spectrum using devices could be governed at all. This paper examines a real-time spectrum distribution approach based on principles of economic utility and equilibrium among multiple competitors for limited goods in a bounded free market. The spectrum distribution problem may be viewed as a special case of multi-objective optimization of a constrained resource, a sort of “spectrum commons”.

Figure 2 illustrates an idealized spectrum commons problem faced by five land mobile radio (LMR) networks operating in close proximity to each other. If a consistent set of local spectrum usage restrictions applies to all non-license-holders within the area of regard and all nodes are equipped with software defined radios, it should be possible to program each network to sense and respond in a positive manner to the presence of the others.

---

<sup>5</sup> The author was employed during 2000-2006 as a contractor supporting the Defense Information Systems Agency (DISA).

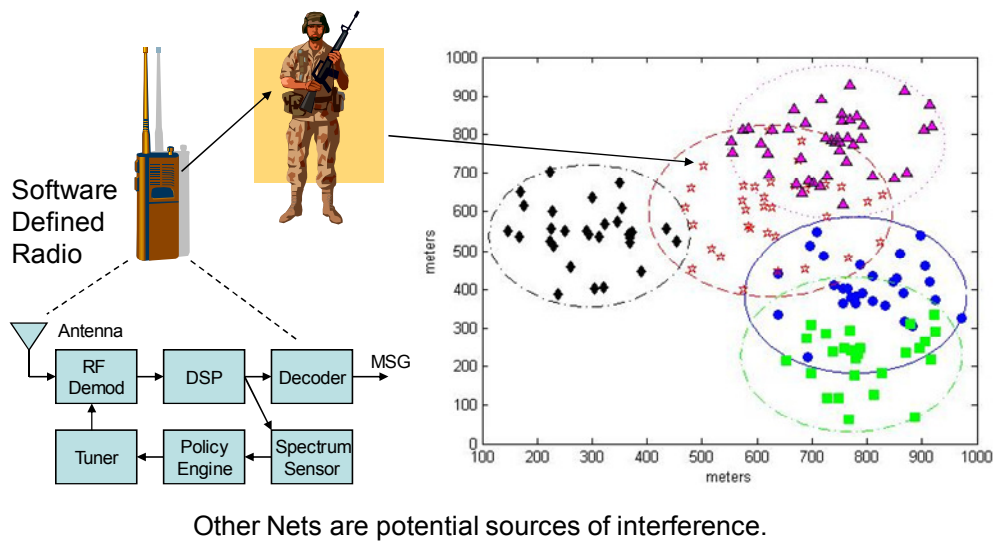


**Figure 2: Software defined radio can help negotiate “spectrum commons”**

For the purposes of this study a “tactical network” is considered to be a hierarchical aggregation of radio nodes running a common waveform, a common protocol (e.g., IP) for maintaining timing and connectivity, and at least one common application (voice, data, sensors, etc.) for a common operational goal. There is assumed to be at least one advantaged or “master” SDR node that is capable both in-network and out-of-network communication and usually associated with leadership at the company and battalion level<sup>6</sup>.

The analytical effort described here attempts to streamline the tasks of a spectrum manager for a hypothetical expeditionary infantry brigade. The immediate goal is to

---

<sup>6</sup> This distribution is consistent with U.S. Army deployment plans for the Joint Tactical Radio System (JTRS), a military version of software defined radio.

determine whether practical spectrum management rules for realizable networks can be derived through Monte Carlo simulation and statistical analysis.

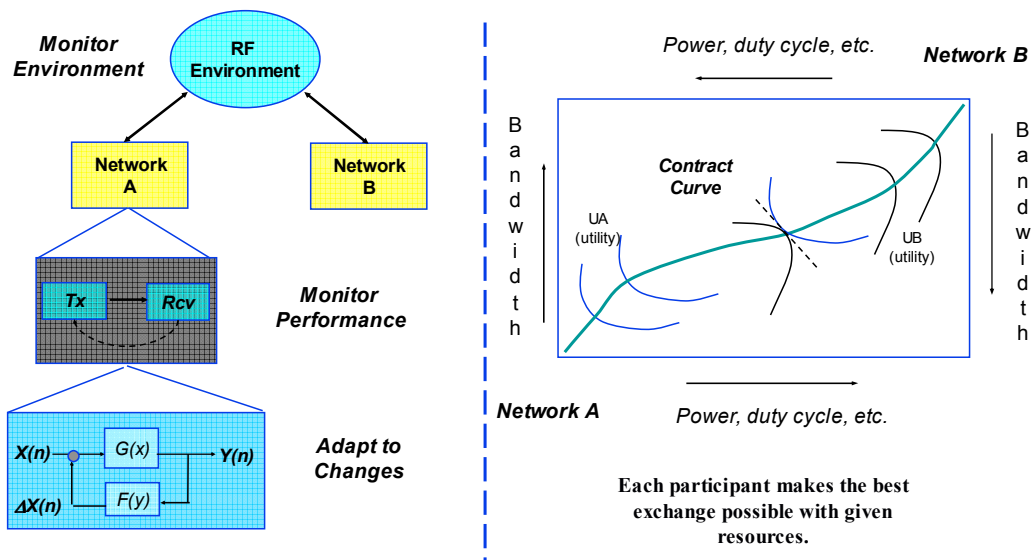


**Figure 3: Adaptive spectrum management as a microeconomics problem**

In the diagram on the left side of Figure 3, the nominal MANET is composed of SDR nodes that can sense local spectrum conditions and report link quality metrics back to a Master node. The Master node software monitors the various inputs, devises a tuning strategy to compensate for interference and transmits updates to the MANET. Each MANET contributes to the electromagnetic environment perceived by all MANET.

Cognitive radio systems like the DARPA-sponsored XG—that can sense, characterize, react, and adapt to actual spectrum usage—would enable significant increases in the effective spectrum available to support worldwide operations, and would



greatly reduce the time required to perform spectrum management tasks, but the prospect of thousands or millions of freely modulating, adaptive radios causes some understandable concern within both the Government and civilian radio regulatory authorities. Some of these concerns may be addressable by economics if we may assume that software defined radios can be designed to approximate extremely rational consumers of spectrum in a common market.

The diagram on the right side of Figure 3 is a microeconomics construct called an Edgeworth box<sup>7</sup>, a handy visual aid for analyzing simple economic systems. Here we have a two-agent pure exchange economy, where the quantities of all available goods are fixed. In such a system there is no production (e.g., no new spectrum added) and the only actions are exchange and consumption. Thus the only economic problem is allocation of resources. Each participant trades off some quantity (e.g., occupied frequency, bandwidth or transmit power) in order to better its situation, i.e., message quality of service (QoS). Classical economic theory says that trading will stop when each participant reaches a point of diminishing returns. Each agent only needs to know its wants, initial endowment of goods, and the current prices. Knowledge of the other party's needs or actions is not required, and equilibrium can be achieved without explicit cooperation (Katz & Rosen, 1998, pp. 375-378).

In theory, a large ensemble of adaptive radios should eventually distribute the available spectrum so as to approach an optimal state of "Nash equilibrium". In economic terms, energy consumption (transmit power) per unit of additional QoS achieved can be

---

<sup>7</sup> Named after the Irish economist and philosopher Francis Y. Edgeworth (1845-1926)

considered the equivalent of price, in that like a purchase on the open market, it represents an incremental commitment of resources that, after the exchange, cannot be reused by the original holder. Given a set of price-equivalent exchange ratios between resources expended and benefits received for all participants, and absent any new production (i.e., release of additional spectrum), an equilibrium distribution of assets should form in a constrained market (Starr, 1997). Predicting when such an equilibrium state will occur and what form it will take, so that spectrum resources can be constructively managed is a problem of multi-objective optimization, where closed form analysis rapidly becomes more complicated as the number of players increases.

### **Spectrum Utility**

Economic agents have to “want” something in order to drive adaptive behavior, so a Spectrum Utility Function was introduced into the model. A trial utility function of the form  $U_{OBJ} = \sum \alpha_n U_n$  was developed where the constants  $\alpha_n$  define system performance priorities and the components  $U_n$  include mission and application-related factors that would make sense to a communications engineer, and could feasibly be measured or calculated: channel capacity (bits/sec), area spectral efficiency (bits/sec/Hz/m<sup>2</sup>), and bit-error rate. The three component functions selected for the initial model are certainly not orthogonal, but strict orthogonality was not necessary at this stage. If we denote a MANET tuning state, which here consists of frequency  $f$ , bandwidth  $B$ , and transmit power  $P_t$ , by a state vector  $X$  such that  $X = \{f, B, P_t\}^T$  and denote the ambient electromagnetic environment by  $Q$ , the spectrum utility function takes the form:

$$U_{OBJ}(X, Q) = \alpha_1 \cdot U_{CAP} + \alpha_2 \cdot U_{ASE} + \alpha_3 \cdot U_{BER} \quad (1)$$

where the weighting constants  $\alpha_n$  define mission or application-dependent system performance priorities. The component “U functions” on the right-hand side of the equation are implicit functions of the tuning state and the local environment, and represent the efficacy of the MANET with regard to management of channel capacity ( $U_{CAP}$ ), power or geographical coverage ( $U_{ASE}$ ), and bit error rate ( $U_{BER}$ ).

Shannon’s channel capacity theorem (Shannon, 1948) is the basis for the first component,  $U_{CAP}$ . Gupta and Kumar discovered that the theoretical limit for per-link throughput for a MANET supplied with a given bandwidth and signal-to-noise ratio varies as  $1/\sqrt{N}$  where  $N$  is the number of nodes (Gupta & Kumar, 2000). For the purposes of this study the individual MANETs in each case were considered to be of equal status (e.g., company or platoon) in the hierarchy, and of comparable size, so the  $1/\sqrt{N}$  factor can be safely ignored. The channel capacity component of our spectrum utility objective function becomes:

$$U_{CAP} = B \cdot \log_2(1 + \gamma) \quad (2)$$

Here  $B$  represents the RF bandwidth currently occupied by a MANET and the Greek letter *gamma* ( $\gamma$ ) represents the minimum signal-to-interference-plus-noise ratio (SINR) experienced by the nodes. SINR accounts for interference due to external sources (e.g., other networks) as well as the “self-noise” generated by all electronic systems, and can be affected by changes in the tuning state. Thus  $U_{CAP}$  is a measure of minimum link capacity among all the nodes of a MANET. To keep  $U_{CAP}$  dimensionless we define  $B$  in

terms of some reference bandwidth, such as the 22 MHz used by the IEEE 802.11b wireless LAN waveform:

$$B = \frac{BW(MHz)}{BW_{ref}} \quad (3)$$

The second component,  $U_{ASE}$  or area spectral efficiency (Alouini & Goldsmith, 1997) is a measure the degree to which detectable MANET signals are confined to some geographic footprint  $A_{eff}$ .

$$U_{ASE} = \log_2(1 + \gamma)/A_{eff} \quad (4)$$

The third component,  $U_{BER}$ , is a function of the theoretical bit-error rate (BER) and exhibits diminishing-returns asymptotic behavior as BER approaches some practically useful limit  $p_{min}$  determined by the application.

$$U_{BER} = -\log(BER + p_{min}) \quad (5)$$

$$BER = Pe_{BPSK} = \frac{1}{2} \exp(-\gamma) \quad (6)$$

If the BER utility component is strongly weighted it can discourage greedy spectrum behavior, since any additional transmit power or occupied bandwidth used to reduce BER below  $p_{min}$  would be wasted. This self-policing capability makes the whole scheme very different from the *laissez faire* market behavior originally feared by regulators.  $U_{OBJ}$  may be thought of as a priority-weighted combination of all concerns for all players in the local spectrum arena. The value of  $U_{OBJ}$  and its components should

increase in a nonlinear fashion with greater signal-to-interference ratios, as illustrated in Figure 4.

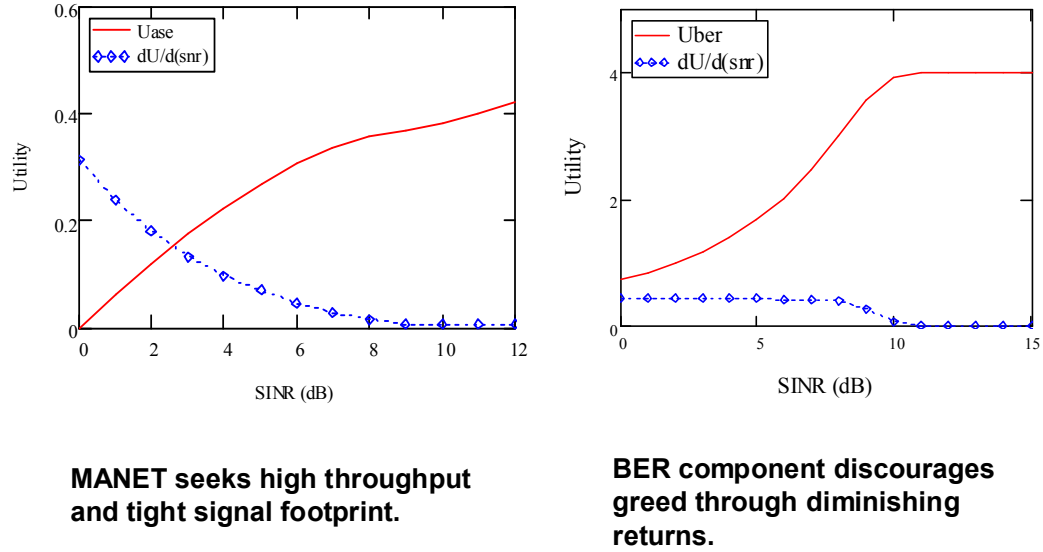


**Figure 4: Components of a nominal spectrum utility objective function**

For our purpose, it is sufficient to define the local RF environment vector  $Q$  in terms of the frequency, bandwidth, and interference-to-noise ratio (INR) of each interference source, as measured at the target receiver. (In the models used for this study there is an implicit assumption that the required interference parameters can be detected and estimated within a reasonable integration period. A tuning state vector  $X_A$  comprising the transmit power, frequency and bandwidth used by all local MANET is considered to be a better solution than another vector  $X_B$  if it results in a superior utility:

$$U_{OBJ}(X_A, Q_A) > U_{OBJ}(X_B, Q_B) \quad (7)$$

Here the environmental variables  $Q_A$  and  $Q_B$  denote the influence of all significant RF emitters in the area of regard, including other adaptive systems with the capability to respond to changes in the MANET of interest.

### **Local Spectrum Constraints**

The point of adaptive spectrum management is to take advantage of local inefficiencies in spectrum occupancy. Any opportunistic “listen before transmit” system will usually attract the attention of primary license holders and their attorneys and lobbyists well before certification and deployment. For this study the problem has been somewhat simplified by the assumption that pools of locally available frequencies have been identified well in advance of operations, following the location-based spectrum rights method proposed by Stine. In the simulation, a particular band is considered available to any government approved mobile networks operating within a specified geographic region.

For example, during a Marine combined arms exercise at Twentynine Palms in California, a frequency band normally allocated to cellular telephones (e.g., 930-970 MHz) might be available within a 30 km square on the vast and largely empty military base. In an urban emergency (e.g., a five-alarm fire or hazardous chemical spill), adaptive spectrum reuse could allow a similar frequency band to be quickly made available to police and firefighters over an area of 20 city blocks<sup>8</sup>. Such situational spectrum sharing

---

<sup>8</sup> This may require coordinating with the cellular company.

agreements could become attractive to holders of legacy spectrum licenses as demand for advanced digital “third generation” (3G) services draws cellular technology toward higher frequencies<sup>9</sup>.

In this simulation study, the essential constraints of the spectrum management problem for a particular case are represented by a priori limits on spatial distribution, frequency, bandwidth and transmit power, included in the case input data structure. For the sample input case listed in Appendix B, the applicable constraints are:

- Spatial limits (XY<sub>max</sub>): All the action takes place in a region represented by square 1.2 km on a side.
- Frequency limits (Freq<sub>lim</sub>): All land mobile networks entering this area must confine their transmissions to 590-635 MHz.
- Bandwidth limits (BW<sub>max</sub>): The maximum bandwidth allowed per network is 22.65 MHz
- Power limits (PT<sub>max</sub>): Mobile radios in this case are limited to a maximum equivalent isotropic radiated power (EIRP) of 15 dBm, or 70 milliwatts.

### **Previous Research on Spectrum Management for SDR**

The author’s initial investigations into automated spectrum management occurred in the course efforts to help DISA draft a response to an FCC Notice of Inquiry regarding

---

<sup>9</sup> Wideband code division multiple access (WCDMA) networks often operate near or above 1900 MHz.

the prospect of allowing software defined radio to leave the laboratory. Rather than seeing SDR as a merely a threat to the established regulatory order (AT&T, 2000), our position was that this technology could enable the creation of adaptive self-managed networks that could be programmed to “play well with others”, including so-called legacy radios.

To realize the promised gains in efficiency, a large measure of the positive control of such networks must reside in the embedded software of the radios. It is taken as given that SDR, like any other military or public safety equipment, can be trusted only to the extent that its hardware and software components can satisfy a rigorous certification process, including independent validation and verification (IV&V). Once it has been established that an agent will obey the imposed rules, the rules themselves become the proper subject of inquiry. This leads one to ask whether regulators would be able to anticipate the behavior of large numbers of SDR-enabled networks under yet-to-be developed spectrum rules of engagement. In an attempt to address that question, a simulation (Figure 5) of closely spaced, technically identical SDR nets was developed using MATLAB and its SIMULINK<sup>10</sup> graphical system modeling utility (Jones, OSE Algorithm, 2002).

---

<sup>10</sup> MATLAB and SIMULINK are products of The Mathworks, Inc., Natick, MA.



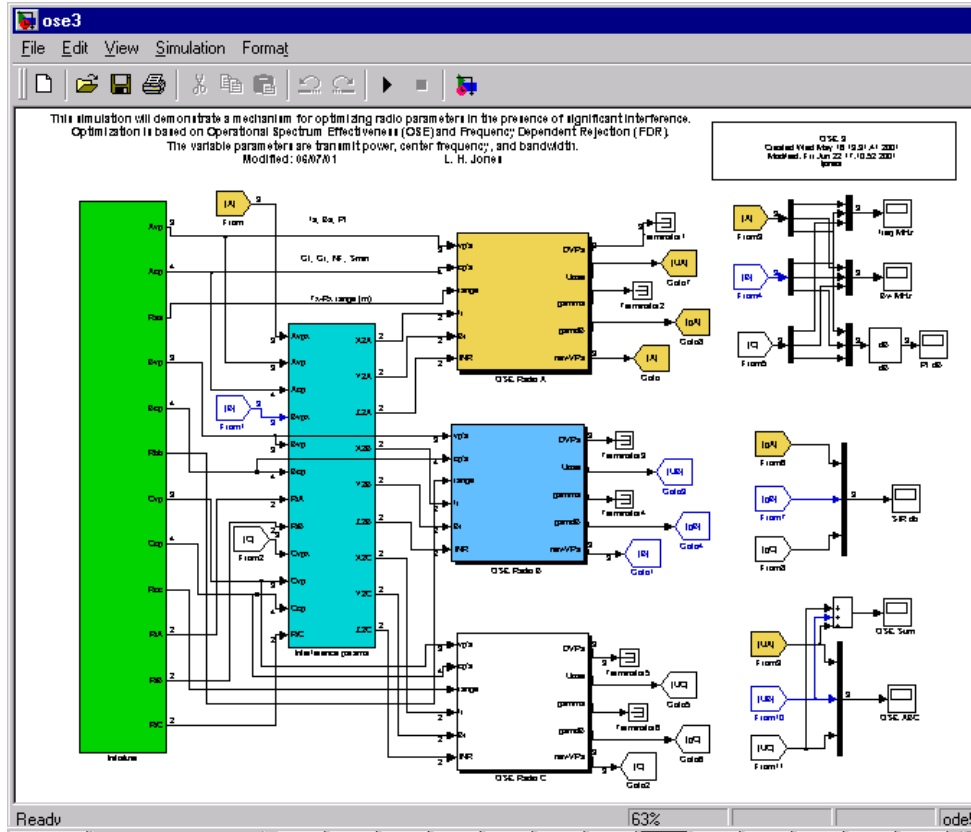
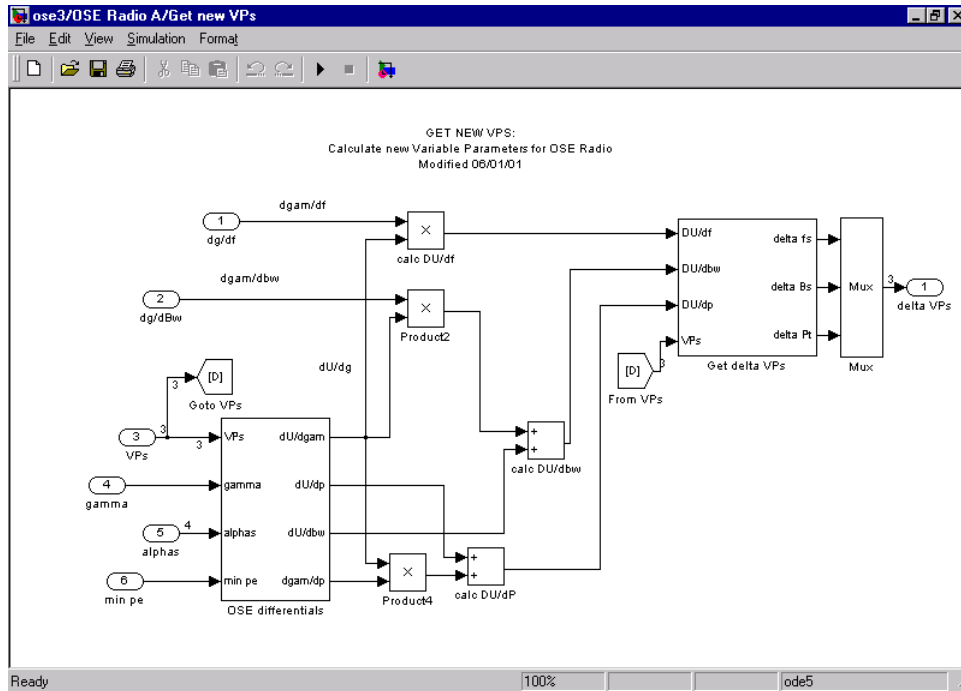


Figure 5: SIMULINK model of interactions between three adjacent SDR nets

Figure 6 represents the SIMULINK version of a cognitive radio tuning algorithm that takes into account perceived interference in adjacent bands to chart a course toward higher spectrum utility (then termed operational spectrum effectiveness or OSE) using the variable parameters power, frequency and bandwidth.



**Figure 6: SIMULINK model of cognitive radio tuning**

Figures 7 through 10 illustrate the evolution of three networks in terms of frequency, bandwidth, transmitter power, and spectrum utility, the latter scaled differently than in the current study. In this example, there is no communication between the simulated networks. Equipped with only interference sensing and a set of utility functions and their derivatives, based largely on SINR, the nets respond to the initial spectrum conflict by shifting frequencies (Figure 7), compressing bandwidths (Figure 8), and gradually increasing transmit power (Figure 9) to achieve a mutually beneficial outcome in terms of utility (Figure 10).

In each plot, the horizontal axis represents simulated time in seconds. This time scale represents the default settings of the early simulation effort rather than a detailed estimate of feasible timing for implementation, as in Appendix D.

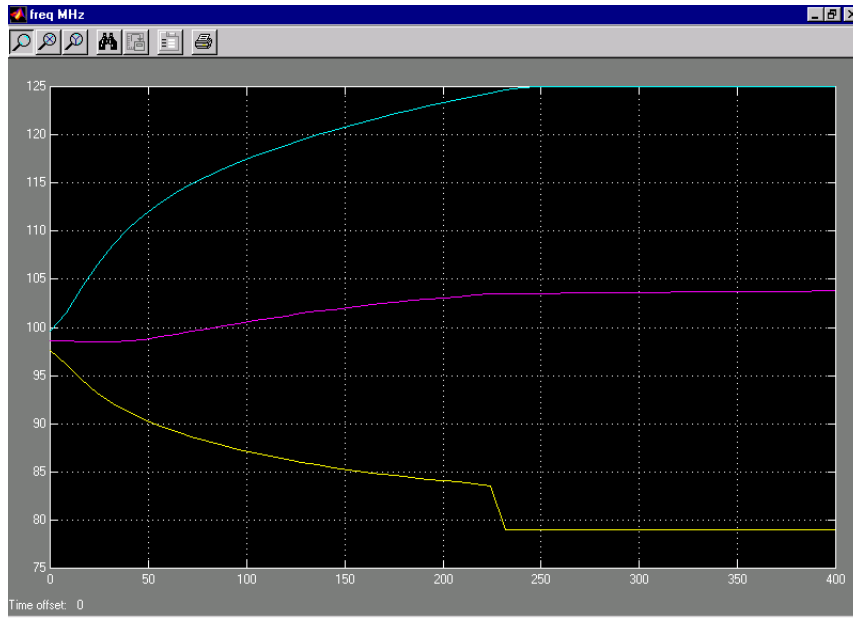


Figure 7: OSE-driven frequency (MHz) evolution (Jones, 2001)

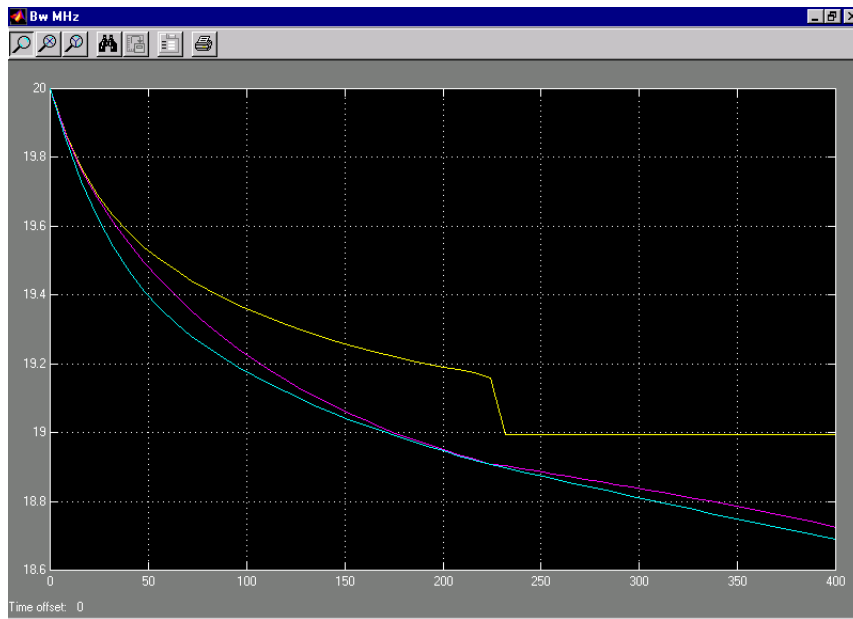
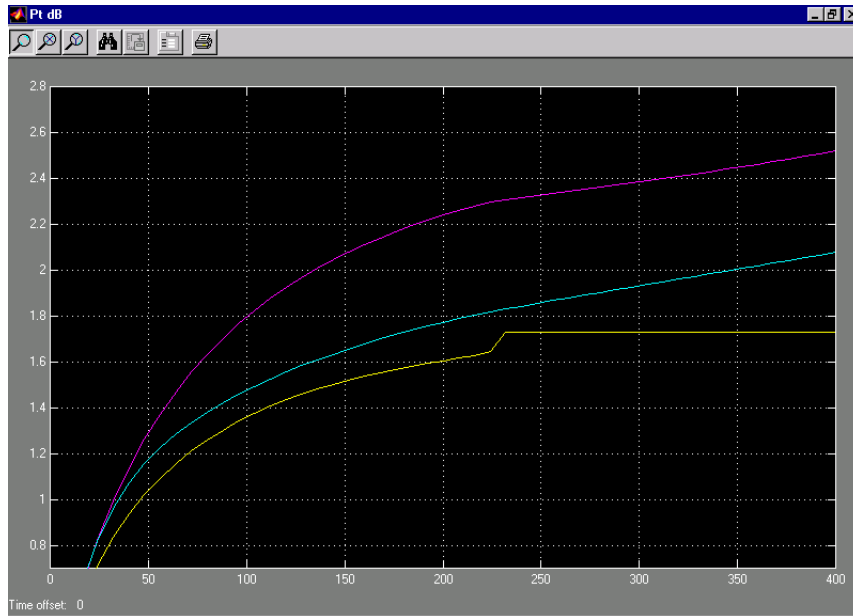
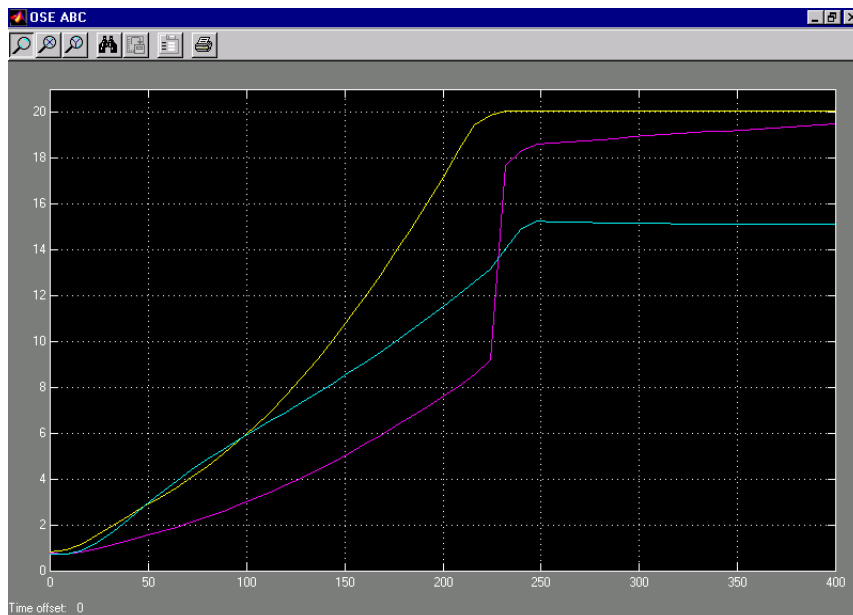


Figure 8: OSE-driven bandwidth (MHz) evolution (Jones, 2001)



**Figure 9: OSE-constrained power (dBW) evolution (Jones, 2001)**



**Figure 10: Each network tries to optimize its utility function (Jones, 2001)**

These early models used explicit algebraic formulas for continuous differentials of the objective function with respect to power, frequency, bandwidth and SINR. The

convenience of the graphical user interface was offset by the need to create a new model with many explicit connections to examine the effect of changes in the network distribution. This approach thus became unwieldy as the number of nets increased, but the essential point, that properly programmed cognitive radio networks could in some instances find their own way to a useful spectrum distribution, had been demonstrated.

Despite that early success, some questions remained. Cases of apparently chaotic behavior were sometimes encountered, where the SINR and OSE metric for one or more nets would rise, then abruptly fall. This phenomenon was attributed to some distributions being either “spectrum rich” (Figure 11) or “spectrum starved” (Figure 12), but a complete analysis of conditions leading to the two outcomes was missing (Jones, OSE Mgt, 2002). That question, with its potential significance for spectrum management, languished for several years until taken up again during the author’s doctoral studies.

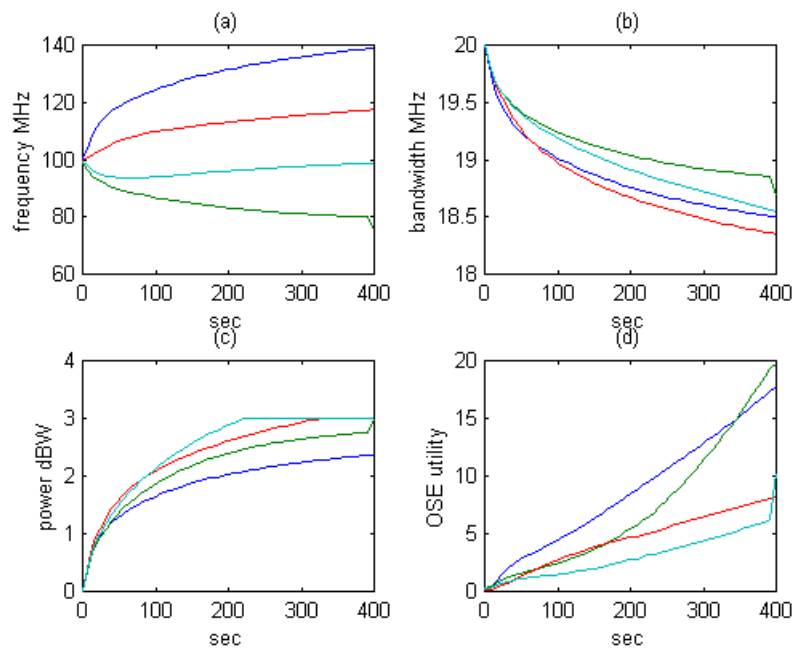
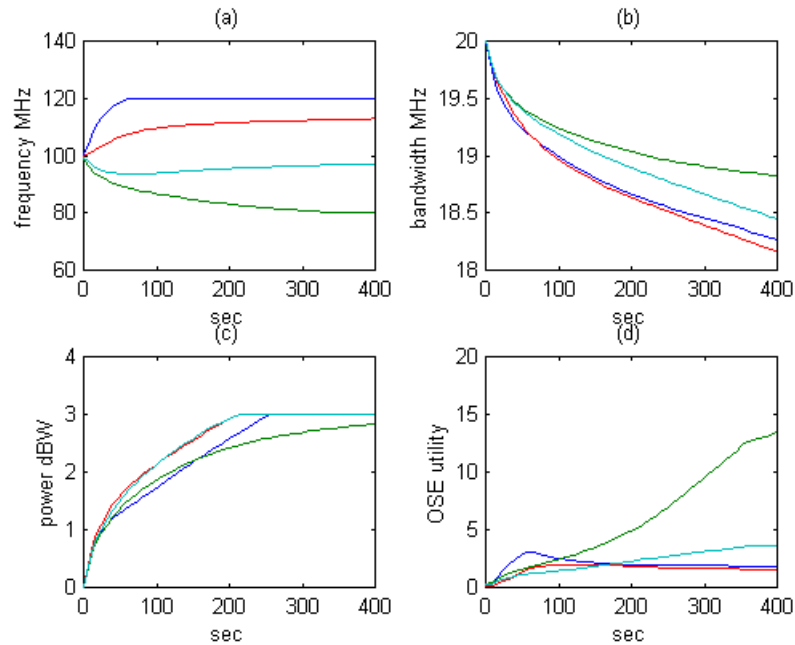


Figure 11: Evolution of a "spectrum rich" (100 MHz) four-net OSE distribution



**Figure 12: Evolution of a "spectrum-starved" (40 MHz) four-net distribution**

### Basic Research Questions

The potential of SDR and CR as enabling technologies for adaptive spectrum utilization has already been established by the defense community. In field tests conducted at Fort A.P. Hill in Virginia during the summer of 2006, the DARPA-sponsored XG radio demonstrated the capability to send and receive data on frequencies used by other nearby radios without noticeable interference, thus harvesting the spectrum “white space” and increasing the effective spectrum availability (Defense News, 2007). However, the regulatory structures and network management processes necessary to take full advantage of cognitive radio seem to lag far behind the technology.

Since cognitive radios do not yet exist in sufficient numbers to conduct large scale field experiments with many competing networks, we must rely on theory and simulation

for guidance in developing practices for efficient management of these devices. The study described here is a modest attempt to increase confidence in the practical application of SDR-enabled autonomous spectrum management by addressing a few basic questions:

- Can a stable market-like spectrum distribution be achieved without explicit cooperation?
- How robust is the equilibrium? In this context the term “equilibrium” refers to a viable spectrum distribution where no network can tune to improve its value (QoS) without adversely affecting the QoS of another network. A robust equilibrium implies that some important QoS metric is relatively insensitive to minor changes in initial conditions, such as node placement.
- Are the predictions generated by a market equilibrium model useful for real-time spectrum management?

The research for this dissertation was focused on comparing the merits of two idealized implementations of local autonomous spectrum management for MANET:

- *Global or “top-down” adaptation* – This model (Figure 13) represents the concept of real-time spectrum management by an agent with regional authority. The local agent must consider the bandwidth needs of each network in its area of responsibility, as well as the constraints imposed by propagation conditions, regulations and incumbent spectrum users. When two or more mobile networks are present, the additional dynamics require a

remarkably robust management agent. A similar management challenge is faced by the Warfighter Internet-Tactical (WIN-T) program, and potentially by public-safety agencies in metropolitan regions with existing commercial spectrum infrastructures.

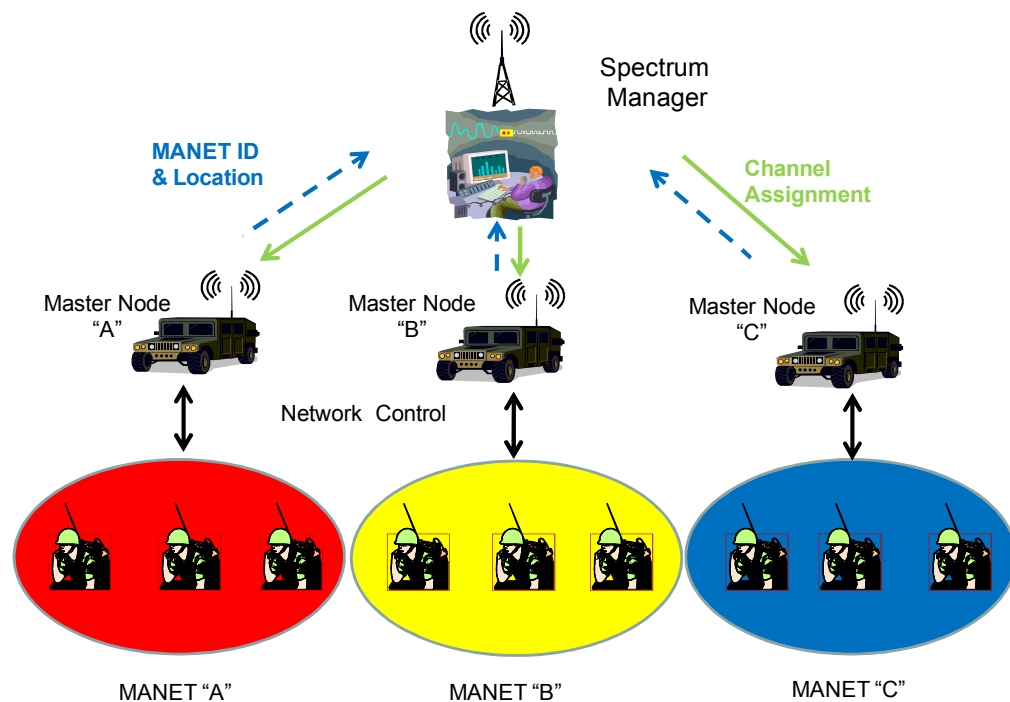


**Figure 13: Top-down model of automated spectrum management**

- Local or “bottom-up” adaptation* – This model (Figure 14) represents my proposed concept of distributed spectrum management. Here each SDR network is given a set of spectrum boundary conditions upon entry into a region, and is free to adapt to serve its best interests within those rules. The spectrum usage constraints can either be pre-loaded before deployment or broadcast by a regional authority, which would in either case be relieved of much of the “grunt-work” of real-time spectrum management.



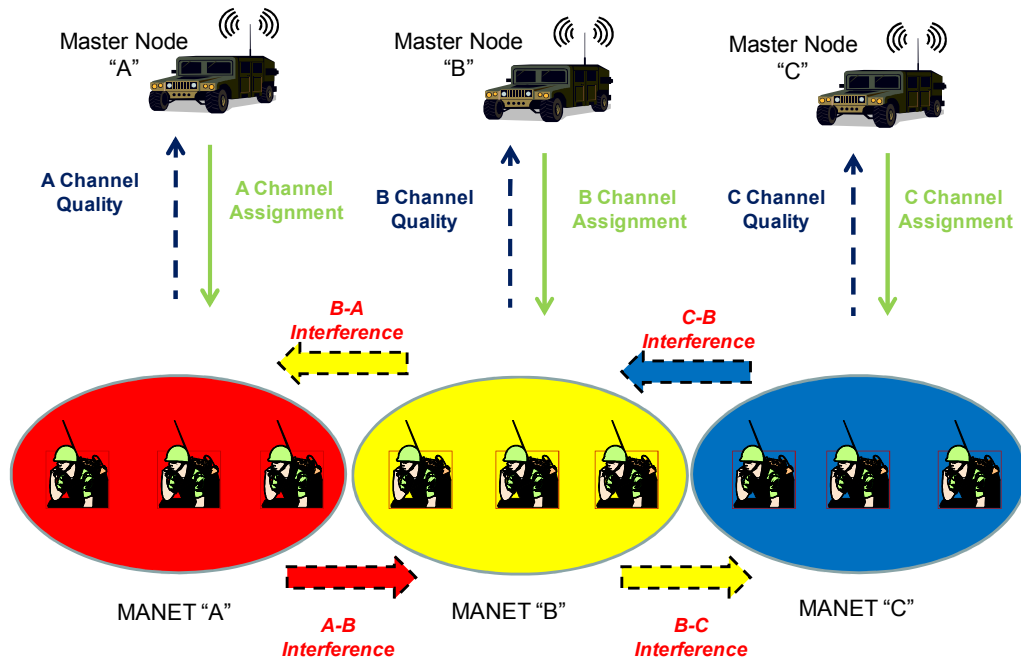


**Figure 14: Bottom-up model of automated spectrum management**

For the purpose of this study, global and local optimization agents were both modeled by using the SPSA algorithm. In the top-down case, the objective function was a weighted average SINR, based on circular-approximation estimates for effective interference distance. Individual bottom-up network optimization was driven by the MANET utility functions, where the tuning vectors represent the available dimensions of control - frequency, bandwidth and power.

To ensure representation of a feasible system, the exact node locations were assumed to be unavailable to the spectrum management algorithm, thus limiting the “chattiness” of a potential implementation.

*Geometric capacity approximation* – In principle it should be possible to determine some a priori limits on the useful spectrum “carrying capacity” within a region. In the simplified view of Figure 7, the area of regard, or “play-box”, is represented in two horizontal dimensions ( $x$  and  $y$ ), while the vertical dimension ( $z$ ) represents frequency. The signal footprint of a band-limited MANET is thus transformed into a sort of spectrum “pancake”, and the provisioning problem can be reduced to stacking the cakes within a box. The carrying capacity would thus be the number of networks ( $N_{cap}$ ) beyond which there is simply not enough contiguous space or bandwidth to place one additional MANET.

It is important to note that all of the schemes proposed here for improving the spectrum management process represent “best effort” attempts to distribute a finite supply of bandwidth among several friendly, or mutually supportive, groups (e.g., companies within a battalion, or police and firefighters on scene). Connectivity or quality of service cannot be guaranteed for any particular user by these methods. That purpose is better served by demand management, one example of which is “Betting for Bandwidth”, an investment-and-reward system devised by the author and several colleagues and implemented for the U. S. Army, whereby bandwidth is temporarily allocated for high priority intelligence-related traffic based on the perceived significance of the message (Jones, Johnson, Love, & Stegmann, 2009).

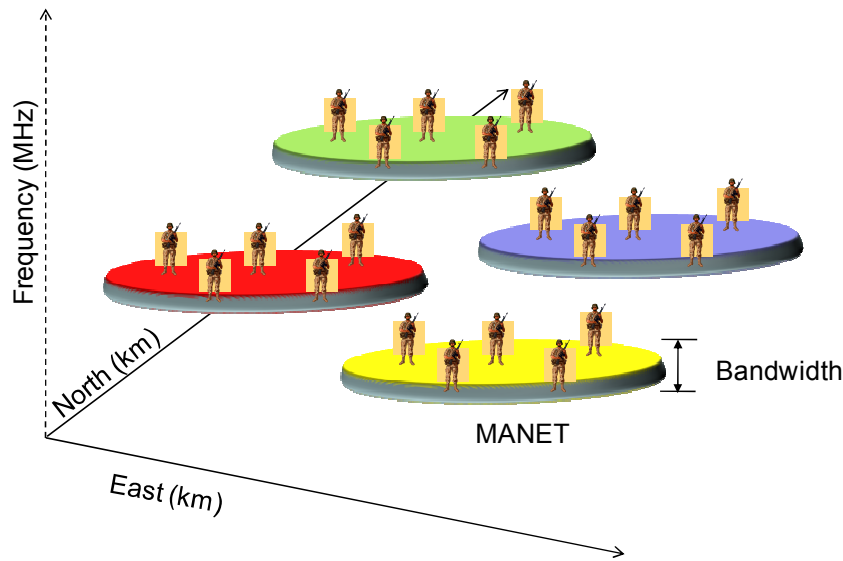


**Figure 15: Geometric “stacking” model for spectrum provisioning**

The centralized, or top-down, approach to spectrum management is applicable to military land mobile radio networks in general. The decentralized (bottom-up) approach, in contrast, requires the nets to react to changing conditions in order to maintain integrity, connectivity and functionality. In the reactive sense, the network must behave somewhat like an organism with a diffuse nervous system, or perhaps an ant colony. The power spectral density of interference sensed at the network periphery must be efficiently relayed to the master node, along with all other network housekeeping data, in a synchronized manner (via GPS or other common broadcast clock system) to prevent chaotic interaction with other friendly networks. These implied system requirements, along with the assumption of efficient power management (nearest-neighbor routing assumption) are highly suggestive of a MANET implementation.

This work applies only to land mobile radio network operating under conditions of bounded opportunistic spectrum availability. Stationary emitters, such as cell towers, are not participants but part of the electromagnetic environment. Ships at sea and aircraft are also excluded from this analysis.

### **Models of Physical Processes**

The elements of this simulation fall into two broad classes: emulation of physical processes and their OSI Layer 1 (physical layer) effects as perceived by the radio, such as bit error rate and signal-to-noise ratio; and emulation of the response of either of two spectrum management systems to the evolving electromagnetic environment. The model may be considered “complete” in the sense that all behavior is driven by elements internal to the model, as opposed to being externally scripted, and that all of the critical technologies either exist or are currently in development.

This section describes the governing equations for the physical layer models.

#### **Radio Node Model**

As shown in Figure 8, the radio component of each node in a MANET is modeled here as a simple transceiver with an omnidirectional antenna. The adaptive properties of the node are represented by a sensor module with spectrum analysis capabilities, a digital tuner module that contains the signal processing and adaptive (goal-seeking) algorithms, and the network coordination module that relays connectivity reports and tuning instruction among the member nodes. The adaptive tuner is assumed to be capable of

modifying the transmit power, center frequency and signal bandwidth in an attempt to maintain connectivity throughout the MANET and to improve the utility of the channel for a given set of applications. For simplicity of the model, it is assumed that all nodes within a given network are technically identical, but only one node at a time may serve as the “master” in terms of adaptive tuning. All others are assumed to have a “client” and “reporting” relationship to the master node.

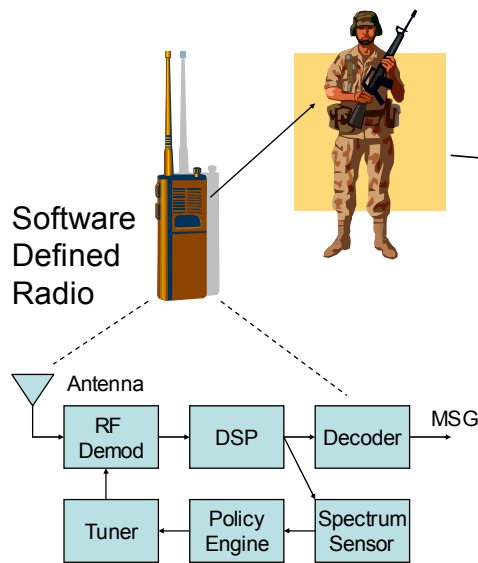


**Figure 16: Conceptual model for adaptive radio nodes**

### Network Connectivity

A network is assumed to be “connected” if each node can receive (detect and correctly demodulate) transmissions from two or more nodes within the network. The signal strength between two nodes is defined by:

$$S = Pt - L_p \quad (8)$$

where  $S$  = received signal strength (dBm),  $P_t$  = transmitted power in dBm and  $L_p$  = radio propagation loss (dB). Since propagation is independent of power levels, it may be eliminated from the calculation of signal margin. For this study, the minimum conditions for connectivity may be expressed as  $\Delta S \geq 0$ , where:

$$\Delta S = S - S_{min} = P_t - P_{t_{min}} \quad (9)$$

The quality of the connection is determined by the bit-error rate (BER), which in turn depends upon the *signal-to-interference plus noise ratio*,  $S/(I+N)$ . The radio connectivity and spectrum utility models each use the binary phase-shift keying (BPSK) formula for BER:

$$BER = \frac{1}{2} \exp(-\gamma) \quad (10)$$

where  $\gamma$  = the numerical value of  $S/(I+N)$ , so that:  $S/(I+N)_{dB} = 10 \log_{10}(\gamma)$ .

### Network Geometry and Motion

For the purposes of this study, the nodes within a MANET are randomly dispersed within a circle, the center ( $X_c, Y_c$ ) and radius ( $R_{max}$ ) of which are part of the network specification. Figure 9 illustrates an example MANET distribution.

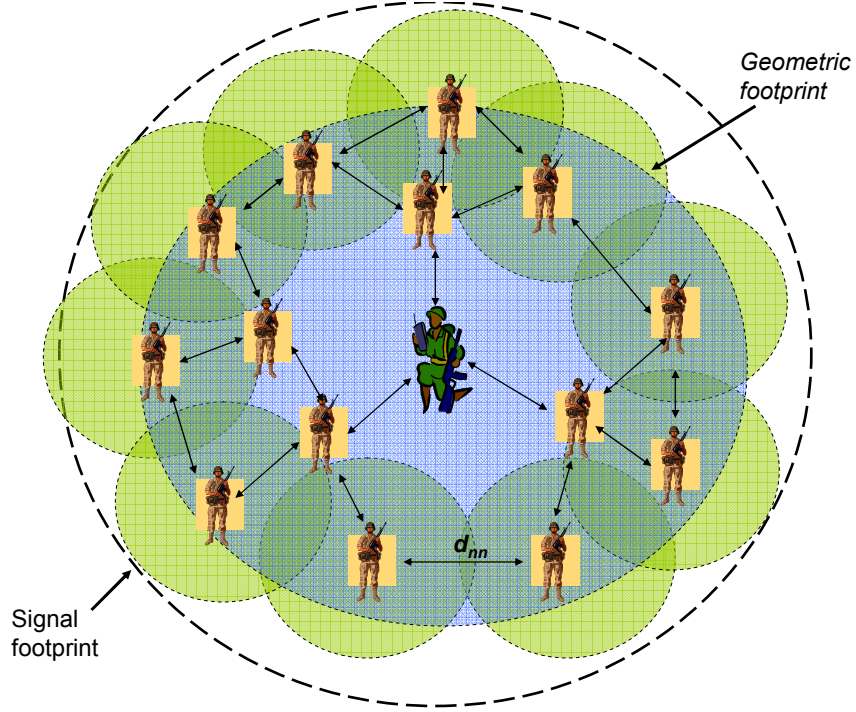


**Figure 17: Notional MANET Layout**

The intra-network nearest-neighbor distance ( $d_{nn}$ ) helps to determine the minimum transmit power ( $P_{t_{min}}$ ) to maintain connectivity within the network in the absence of external interference. This quantity also helps determine the effective signal footprint for a given network. This study uses two methods to determine  $d_{nn}$ , which tend to converge as the number of nodes,  $N$ , increases. A direct calculation can be performed with the omniscience available in a simulation:

$$\text{Direct calculation: } d_{nn} = \frac{1}{N} \sum_{j \neq i} \min(d_{ij}) \quad (11)$$

$$\text{where: } d_{ij} = \sqrt{(x_j - x_i)^2 + (y_j - y_i)^2} \quad (12)$$

To minimize the likelihood of “islands” forming within the MANET, the direct calculation of  $d_{nn}$  used in this study includes the average separation between a node and its three nearest neighbors. A “mean free path” approximation of  $d_{nn}$  can also be used as a variable for characterizing networks in statistical analysis.

$$\text{Mean free path approximation:} \quad \bar{d}_{nn} = R_{max} \left( \frac{\pi}{N} \right)^{1/2} \quad (13)$$

Regardless of any other power or propagation constraints, a minimum condition for successful MANET is to maintain connectivity with the “outer” nodes of the network. If we continue with the circular-boundary approximation, and assume the use of omnidirectional antennas, then at  $Pt_{min}$  the “signal footprint” ( $A_{sig}$ ) of the network, the region where its energy may be expected to impact comparable radio receivers, can be defined by:

$$A_{sig} \approx \pi R_{sig}^2 \leq \pi (R_{max} + \bar{d}_{nn})^2 \quad (14)$$

where  $R_{sig}$  represents the effective radius of the MANET electromagnetic footprint.

The expression for the signal footprint represents an ideal, interference-free, minimum effective power condition. In the course of this study, the transmit power must often be increased to compensate for interference from nearby sources transmitting on adjacent frequencies. In such cases the new signal footprint radius and area may be approximated by:

$$\tilde{R}_{sig} = R_{sig} \cdot 10^{\frac{\Delta S}{10v}} \quad (15)$$



$$\tilde{A}_{sig} = \pi \tilde{R}_{sig}^2 = A_{sig} \cdot 10^{\frac{\Delta S}{5\nu}} \quad (16)$$

Here  $\Delta S$  denotes the signal margin (the difference between the received and minimum discernible signal levels) in dB, while the general character of the radio propagation model is captured in the parameter  $\nu$ , where it is assumed that signal strength varies with distance as  $\sim 1/d^\nu$ . For terrestrial radio network analysis the value  $\nu = 2$  denotes free space propagation,  $\nu = 3$  approximates transmission through moderate foliage and  $\nu \geq 4$  roughly approximates urban conditions.

For a network in motion, such as a platoon or company on maneuver, it is assumed that the centroid of the group moves in some deliberate, straight-line course for the time of interest. Since this study is primarily concerned with spectrum distribution, no generality is lost by allowing the nodes to keep formation as the network moves. Thus, for a given group course ( $\theta_g$ ) and speed ( $V_g$ ):

$$X_n(t) = X_n(0) + V_g \cdot t \cos \theta_g \quad (17)$$

$$Y_n(t) = Y_n(0) + V_g \cdot t \sin \theta_g \quad (18)$$

### Radio Propagation Model

For the purposes of this study, terrain was considered to be homogenous over the play-box area. Consequently, radio propagation loss is modeled here as a simple “ $R^n$ ” loss function (Poisel, 2004) of the form:

$$L_p = \begin{cases} 20 \log \left( \frac{4\pi d}{\lambda} \right) : \text{for } d < d_{crit} \\ 20 \log \left( \frac{4\pi d_{crit}}{\lambda} \right) + 10n \log \left( \frac{d}{d_{crit}} \right) : \text{otherwise} \end{cases} \quad (19)$$

where,  $L_p$  = basic propagation loss in decibels (dB);  $f$  = frequency (MHz);  $d$  = path length (km);  $h_t$  = transmitting antenna height (m);  $h_r$  = receiving antenna height (m);  $\lambda$  = wavelength of the signal, and  $d_{crit}$  is a transition range for which the propagation loss is known:

$$d_{crit} = \frac{4\pi h_r h_t}{\lambda} \quad (20)$$

The constant  $n$  defines the propagation conditions. For example,  $n = 2$  corresponds to free-space conditions, while  $n \geq 4$  is a reasonable representation of urban propagation. The choice of propagation model determines the relationship between transmitted power and the MANET signal footprint.

### Signal Spectrum Model

The transmitted spectrum for a given MANET is considered to be bounded by a Gaussian function of the form:

$$H(f, f_c, B) = \exp \left[ \frac{-2.76(f - f_c)^2}{B^2} \right] \quad (21)$$

where  $f_c$  is the center frequency and  $B$  is the half-power (3 dB) bandwidth. This Gaussian spectrum model implies that most of the signal's power is contained within the nominal bandwidth. Figure 10 illustrates a case of interference between two signals of similar bandwidth that happen to overlap at their mutual half-power points.

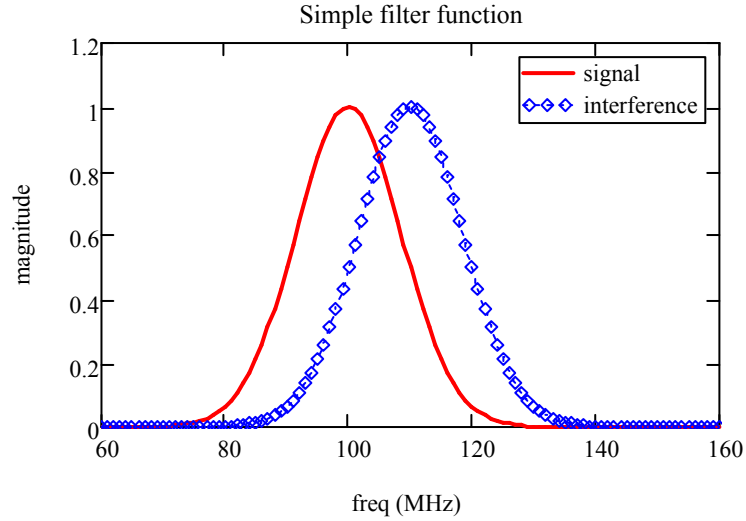


**Figure 18: Gaussian spectrum model for signals and interference**

Harmonics are also modeled by Gaussian functions, thus a signal from network  $k$ , transmitted on center frequency  $f_c$ , with bandwidth  $B$  and its first  $N_h$  harmonics would be received with a power spectral density (PSD) function defined by:

$$\rho_k(f) = \bar{p}_k \sum_{n=1}^{N_h} g_n H(f, n f_c, B) \quad (22)$$

The scale parameter  $p_k$  depends on the transmit power  $Pt_k$  in watts, the bandwidth  $B_k$ , and the propagation loss  $L_p$  in decibels:

$$\bar{p}_k = \left( \frac{Pt_k}{BS_k} \right) \cdot 10^{Lp/10} \quad (23)$$

For this simulation we assume that the power in each successive harmonic is 20 dB below that of its predecessor, so that the weighting factor  $g_n$  is given by:

$$g_n = 10^{-2(n-1)} \quad (24)$$

Strictly speaking,  $\sum g_n \simeq 1.01$  for  $N_h > 1$ . The practical impact of renormalization is an insignificant fraction of a decibel.

### Interference Model

Radio-frequency interference may come from a wide range of external sources, including the fixed relay infrastructure of incumbent spectrum users or other MANET operating in adjacent bands. Contention management within the MANET is assumed to work sufficiently well that “self-interference” is not a significant consideration. From the perspective of the master node, the interference spectrum is determined by the sum of the strongest interference signals received by the client nodes from all sources.

The strength of the interference between two networks is determined by the interference distance  $d_{AB}$ , defined here as the closest approach between any two nodes in the respective networks. In Figure 11 networks A and B are represented by two adjacent MANET distributions, where vectors  $\mathbf{X}_{A,j}$ , and  $\mathbf{X}_{B,k}$  represent individual node positions. The interference distance is then:

$$d_{AB} = \min_{j,k} \{ |\vec{X}_{A,j} - \vec{X}_{B,k}| \} \quad (25)$$

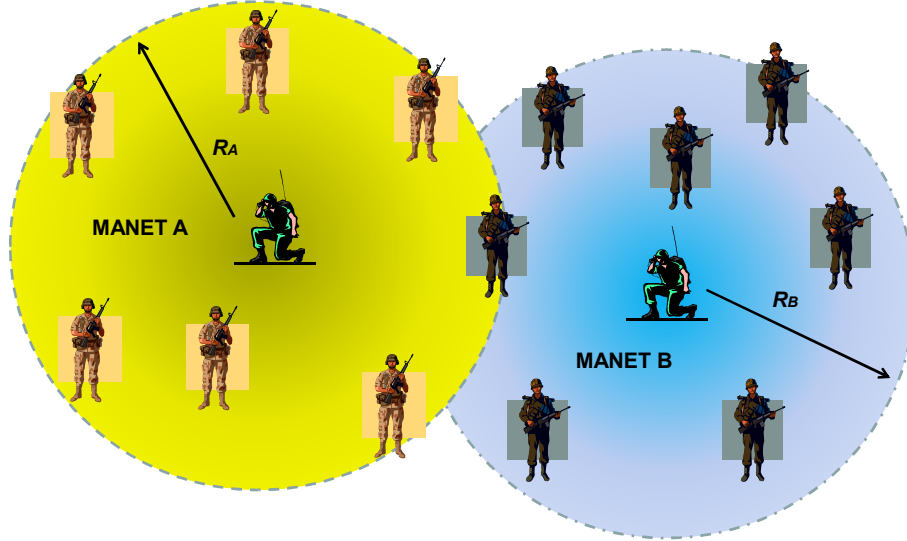


**Figure 19: Two adjacent MANET must deal with mutual interference**

The interference distance may also be approximated by using the circular-distribution limits for the individual MANET. When there is an overlap between two MANET regions, the interference distance should approach the smaller of the two networks' respective nearest-neighbor intervals:

$$d_{AB} \approx \max \left\{ (D_{AB} - R_A - R_B); \sqrt{\pi} \cdot \min \left( \frac{R_A}{\sqrt{N_A}}, \frac{R_B}{\sqrt{N_B}} \right) \right\} \quad (26)$$

Here  $D_{AB}$  is the distance between MANET centroids,  $R_A$  and  $R_B$  are the MANET radii, and  $N_A$  and  $N_B$  are the node populations. The maximum-level mask for the PSD of the combined interference received at network  $k$  from all adjacent sources is defined by:

$$\rho_{i_k}(f) = \sum_{j \neq k} \rho_j(f) \quad (27)$$

The received power spectral density  $\rho_j(f)$  is modified by the propagation loss  $L_p$  calculated for the interference distance to any external source, which in this case means all other networks.

### Receiver Noise Power

The power of the noise generated within a receiver's own circuitry can be approximated by the formula:

$$P_{Noise} = k_B T_0 B F_N \quad (28)$$

where  $k_B$  = Boltzmann's constant ( $1.38 \times 10^{-23}$  J/K),  $T_0$  = reference temperature (290 K),  $B$  = receiver 3dB bandwidth, and  $F_N$  = receiver noise figure. This self-noise level may be expressed in decibel-milliwatt (dBm) by:

$$N_{dBm} = 10 \log(B(MHz)) + F_N(dB) - 144 \quad (29)$$

### Frequency Dependent Rejection (FDR)

FDR and its converse, frequency dependent integration (FDI), are measures of the fraction of energy from an interference signal that would be rejected or admitted by the

receiver front end. FDR is commonly used in analysis of spectrum compatibility for new RF systems and applications, and is related to FDI by:

$$FDR = 1 - FDI \quad (30)$$

FDI is thus equivalent to a measure of the overlap between the power spectrum of the interference and that of the desired signal, defined in this simulation by:

$$\eta_{FDI} = \frac{\int_0^{f^{max}} H_s(f, f_s, B_s) H_i(f) df}{\int_0^{f^{max}} H_i(f) df} \quad (31)$$

Here the function  $H_s(f, f_s, B_s)$  defines the receiver passband, with center frequency  $f_s$  and bandwidth  $B_s$ , while  $H_i(f)$  defines the normalized spectral mask of the interference signal from a source of nominal bandwidth  $B_i$ . Here it is assumed that the PSD of all participants conforms to regulatory, e.g., NTIA spectrum-mask limits. This formulation will also apply when  $H_s(f)$  represents an aggregation of interference sources, providing there is one dominant mode. Strictly speaking, the upper integration limit  $f^{max}$  should approach infinity, but as a practical matter covering highest relevant harmonics by the following definition is more than sufficient:

$$f^{max} = \max(f_s, f_i) + 10 \max(B_s, B_i) \quad (32)$$

Here  $f_i$  and  $B_i$  represent the center frequency and half-power bandwidth of the interference. The use of Gaussian passbands in the simulation allows for a relatively simple approximation to FDI:

$$\eta_{FDI} \cong a_{FDI} \left\{ \operatorname{erf} \left( \frac{b_{FDI}}{B_i} \left( f_i - f_s + \frac{B_s}{2} \right) \right) - \operatorname{erf} \left( \frac{b_{FDI}}{B_i} \left( f_i - f_s - \frac{B_s}{2} \right) \right) \right\} \quad (33)$$

The constants  $a_{fdi}$  and  $b_{fdi}$  are determined by the shape of the nominal receiver passband.

For the Gaussian band models used in this investigation,  $a_{fdi} = 0.533$  and  $b_{fdi} = 1.667$ .

The relative distortion attributed to this approximation is less than one decibel.

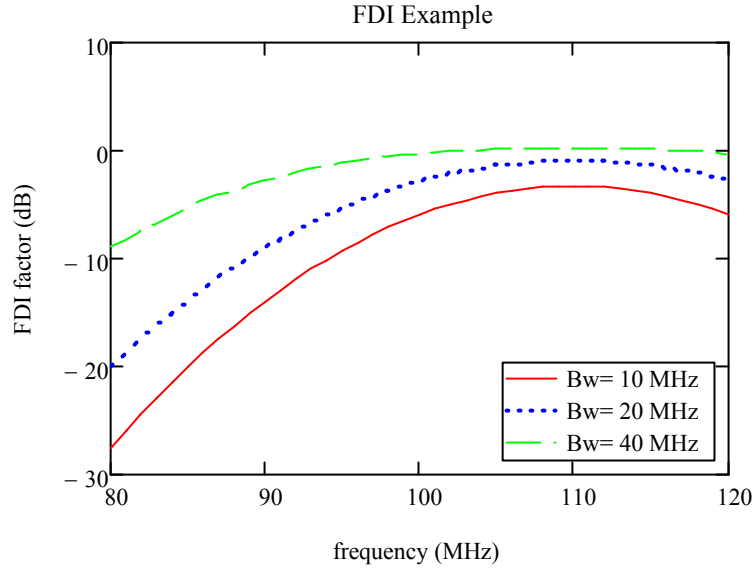


Figure 20: Example of FDI for Gaussian passband model

### SINR Calculation

The total effective interference power  $I_k$  at the most vulnerable nodes of MANET  $k$  is defined by:

$$I_k = \sum_{j \neq k} \eta_{FDI(j,k)} \cdot 10^{P_t_j - L_p(f_j, d_{jk})} \quad (34)$$

where  $\eta_{FDI(j, k)}$  = frequency dependent integration for interference source  $j$  upon signal  $k$ ,

$P_{t_j}$  = transmitter power in dBm for nodes in network  $j$ , and



$L_p(f_j, d_{jk})$  = propagation loss in dB at frequency  $f_j$  and interference distance  $d_{jk}$ .

The SINR at network  $k$  is thus:

$$SINR_k(dB) = 10 \log \left( \frac{S_k}{I_k + P_{Noise(k)}} \right) \quad (35)$$

Here the power levels of the intended signal  $S_k$ , interference  $I_k$  and noise  $P_{Noise(k)}$  are expressed in absolute units (mW or  $\mu$ W).

### **Application of SPSA to Spectrum Adjudication**

The top-down and bottom-up approaches to automated spectrum management both rest on the assumption that a goal-seeking algorithm exists that will render channel assignments in some “optimal” way, depending upon the definition of the goal or objective function. The optimization method was not meant to be an essential feature of the implementation, but an abstraction of the logical response of the spectrum management architecture to the stimuli presented by the physical layer models. This is the second, higher class of model components. For the purposes of this feasibility study it was sufficient to determine when a viable solution could be found, and to assume that in each such case an optimal solution exists.

The appeal of simultaneous perturbation stochastic approximation (SPSA) for this study lies in its inherent scalability to problems that involve many networks, each operating with several degrees of freedom (Spall, 1998). The SPSA algorithm also

eliminates the need to explicitly define a gradient for the objective function, a step that can quickly become rather unwieldy when one considers the complex interaction between actual radio propagation effects and realizable digital filter passbands. This section describes how the basic SPSA algorithm was adapted to the problem of automated spectrum management.

- Each MANET in a playbox operates at a certain frequency  $f$  (MHz), bandwidth  $B$  (MHz) and node transmit power  $P$  (dBm), resulting in a time dependent tuning state vector  $\mathbf{S}$ :

$$S_n = \begin{bmatrix} f_n \\ B_n \\ P_n \end{bmatrix} \quad (36)$$

- Ensembles of  $N_{\text{sys}}$  networks are assumed to have an equivalent state vector  $\Theta$  with dimensionality  $p = 3N_{\text{sys}}$ . In this simulation we allow  $3 \leq N_{\text{sys}} \leq 10$ , and thus a problem of dimension  $9 \leq p \leq 30$ , the solution of which would quickly become unwieldy by explicit gradient methods. SPSA requires no explicit knowledge of the functional form of the gradients, only the presumption that a gradient exists, i.e., the objective function is differentiable in all  $p$  dimensions.
- For convenience in working with MATLAB,  $\Theta$  can be folded into an equivalent  $3 \times N$  matrix:

$$\Theta = [S_1 \quad \dots \quad S_N] = \begin{bmatrix} f_1 & \dots & f_N \\ B_1 & \dots & B_N \\ P_1 & \dots & P_N \end{bmatrix} \quad (37)$$

- Hard constraints in the spectrum solution space are denoted by  $\Theta_{\min}$  and  $\Theta_{\max}$ :

$$\Theta_{\min} = \begin{bmatrix} f_i = f_{\min} \\ B_i = B_{\min} \\ P_i = P_{\min} \end{bmatrix}, \quad \Theta_{\max} = \begin{bmatrix} f_i = f_{\max} \\ B_i = B_{\max} \\ P_i = P_{\max} \end{bmatrix}, \quad \forall i(1 \leq i \leq N) \quad (38)$$

Here the frequency, bandwidth and power limits are determined by a combination of MANET spatial distribution, equipment capabilities and local spectrum policy.

- The SPSA algorithm requires an initial guess at a solution  $\Theta_1$ , which may be derived either from the initial MANET state vectors (bottom-up method), or by equipartition of the total available spectrum with minimum power settings (top-down, or referee method). Successive iterations take the form:

$$\hat{\Theta}_{k+1} = \hat{\Theta}_k - a_k \hat{g}_k(\hat{\Theta}_k) \quad (39)$$

Here  $g_k(\Theta_k)$  is an estimate of the p-dimensional gradient of the objective function at state vector  $\Theta_k$  and  $a_k$  is an iterated gain parameter. The gradient is estimated by applying a p-dimensional Bernoulli random perturbation  $\Delta_k$  to the current state vector, so that:

$$\hat{g}_k(\hat{\Theta}_k) = \frac{y(\hat{\Theta}_k + c_k \Delta_k) - y(\hat{\Theta}_k - c_k \Delta_k)}{2c_k} \begin{bmatrix} \Delta_{k1}^{-1} \\ \vdots \\ \Delta_{kp}^{-1} \end{bmatrix}$$

(40)

The function  $y(\Theta)$  is the value of the objective function at state  $\Theta$ . The step size  $a_k$  and gain  $c_k$  at each iteration  $k$  were determined by:

$$a_k = \frac{a}{(k + A)^{\alpha_s}} \quad (41)$$

$$c_k = \frac{c}{k^{\gamma_s}} \quad (42)$$

- In the top-down method the objective function was derived from a weighted sum of the minimum and average SINR (in decibels) among all MANET in the playbox. For the bottom-up method a spectrum utility function was evaluated for each individual MANET, and used to drive the next iteration.
- For both the top-down and bottom-up SPSA models, market equilibrium was determined by satisfying one of two conditions: convergence of the objective function:

$$|y(\Theta_{n+1}) - y(\Theta_n)| < \delta_{th} \quad (43)$$

where  $\delta_{th}$  is an arbitrary convergence threshold, or timeout as determined by reaching the maximum number of iterations,  $K_{max}$ :

$$K_{max} = 600 \times N_{sys} \quad (44)$$

- The selectable parameters  $a$ ,  $c$ ,  $A$ ,  $\alpha_s$  and  $\gamma_s$  were held constant for all cases examined in this simulation study. Consequently the SPSA algorithm was not optimally tuned, but for this feasibility study it was deemed sufficient to be able to find a viable spectrum solution with reasonable probability, providing that one exists.

## Chapter 4: Design of Simulation Experiment

Once the component algorithms for simulating locally autonomous spectrum management had been developed and successfully tested and integrated, the next task was to devise a meaningful experiment. To limit the scope of this inherently complex problem, the study began with an a priori assessment of the most relevant input variables and then determined reasonable boundaries and resolution for each identified variable. Considering what information would be available to an autonomous spectrum management device, the following list was settled upon as a plausible minimum set.

A certain subset of information denoted here as “master” data, would be either permanently associated with a given location, or unlikely to change significantly within a time scale on the order of hours to days:

- *Local area of regard* – In the simulation this factor is represented by the dimensions of the play-box ( $m^2$ ).
- *Available pool of frequencies* – Band limits (MHz)
- *Local RF emission constraints* – Maximum allowed transmit power (dBm)
- *Topology and weather* – Local RF propagation conditions; propagation constants

The remaining input variables, denoted as “client” data are considered to be much more volatile within a given scenario. These factors would need to be updated and their potential impact evaluated within minutes or seconds.

- *Number of MANET operating in area of regard* – Input variable  $N_{sys}$

- *Approximate location and range of action for each MANET* -- Centroid and radius in meters
- *Number of active nodes in each MANET* – Input variable *Nodes*
- *Radio technical parameters* – Noise figure and utility constants
- *Initial of default tuning states* – Frequency, bandwidth and transmit power for each MANET

In a nominal “top down” spectrum management architecture the master data set would reside within the regional spectrum management infrastructure, which would also house the spectrum distribution and assignment algorithms. The remaining data items would be supplied to the regional authority by each client MANET as part of the registration process required for permission to operate within its geographical and spectrum area of regard. The input data structure for a sample case is shown in Table 1.

In the “bottom up” architecture, each MANET has its own master node to which the master data set may be distributed prior to the mission. One reasonable SDR implementation would be periodic over-the-air database downloads of local spectrum constraints, keyed to GPS or some other estimate of location and time. With this architecture the client data represent only the self-knowledge of an individual MANET.

Such information would not need to be shared between the networks, which would potentially reduce the traffic overhead associated with spectrum management. While a bottom-up arrangement eliminates the need for a permanent physical spectrum management infrastructure, the potential drawbacks include longer average convergence

time for a local spectrum distribution, as well as somewhat lower confidence that a viable solution will be found at all.

Four sets of simulated MANET spectrum conflict were generated in an effort to determine whether statistical regression could find predictors of success. The number of cases in each data set varied with an *a priori* assessment of the number of potential significant variables. The data sets generated and analyzed were designated as follows:

- H0: Identical equipment for all MANET (700 cases)
- H1: Heterogeneous MANET (300 cases)
- H2: Low Geometric Loading (400 cases)
- H3: Equal Mixture of H0 & H1-type cases (1,000 cases)

**Table 1: Inputs for MANET simulation**

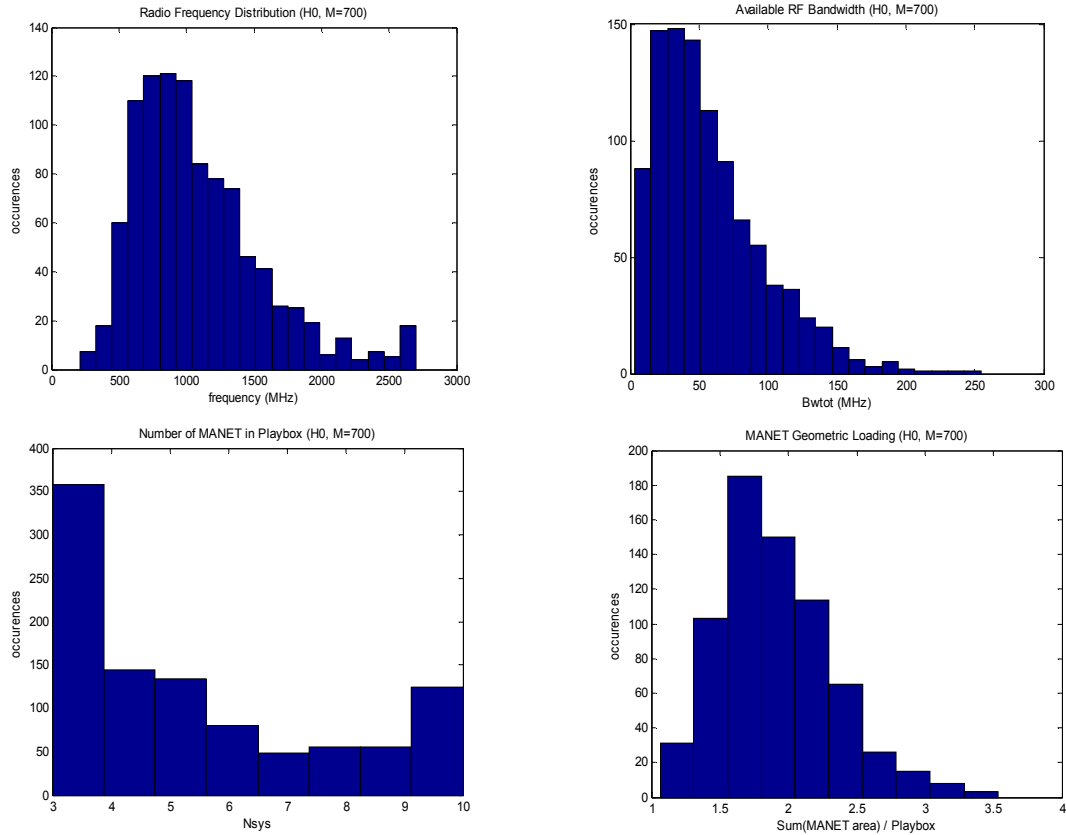
<b>Input</b>	<b>Name</b>	<b>Example</b>
Case number	Case_id	23
Heterogeneous MANET	Case_typ	0
Playbox limits (m)	XYmax	[1300 1300]
Frequency limits (MHz)	Freq_lim	[595.900 649.372]
Number of MANET	Nsys	6
Nodes per MANET	Nodes	[27 42 33 42 35 31]
MANET radius (m)	Radius	[337 352 461 478 363 401]
Maximum bandwidth per MANET (MHz)	BW_max	17.8238
Maximum transmit power (dBm)	PT_max	10
Propagation constant	npx	5
Receiver noise figure (dB)	NF	6
Spectrum utility constants	Alphas	[0.4659 0.3903 0.1439]
Centroid X-coordinate (m)	Xcnt	
Centroid Y-coordinate (m)	Ycnt	
Initial Frequency (MHz)	Freqi	
Initial Bandwidth (MHz)	Bwi	[10.5283 15.3895 12.8875 16.7280 11.9501 12.2017]
Initial Transmit Power (dBm)	Pti	[6.8695 6.1498 7.5565 6.8578 8.4054 5.2893]



## Distribution of Input Variables

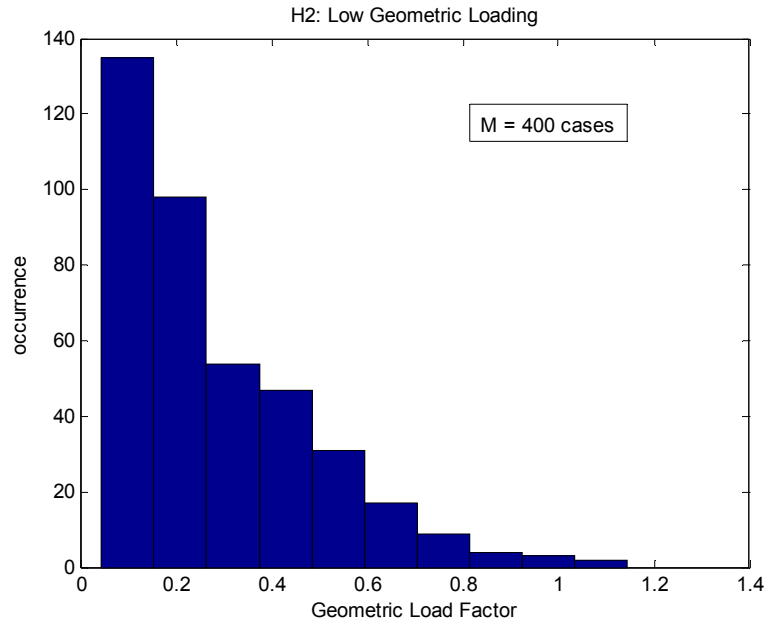
The histograms shown in Figure 13 depict the distribution of some key input variables for the spectrum-trading simulation:

- Frequency range (upper left): 300 MHz – 3 GHz; assumes a log-normal distribution with respect to radio frequency, with a peak near 1 GHz
- Bandwidth (upper right): Variable fraction of frequency (lower bound); ranges from 1 MHz – 250 MHz
- The number of MANET present (lower left) ranges from 2 to 10; this variable was intended to be a pseudo-uniform distribution. Each MANET may contain between 10 and 40 nodes. It should be pointed out here that these node populations are consistent with current field test procedures for JTRS, and do not exceed the Gupta-Kumar limits for MANET feasibility. For example, at the lowest extreme, distribution of 1 MHz bandwidth among 10 MANET of 40 nodes each yields an effective shared capacity of approximately 16 kHz per link, enough to support digital voice traffic if a suitable SINR is achieved.
- The lower right plot shows the occurrence of spatial overcrowding among MANETs. The play-boxes in data sets H0, H1 and H3 were always overloaded in terms of both geometry and minimum bandwidth needs. Contention for spectrum was thus virtually guaranteed.



**Figure 21: Distributions of selected input parameters for simulation**

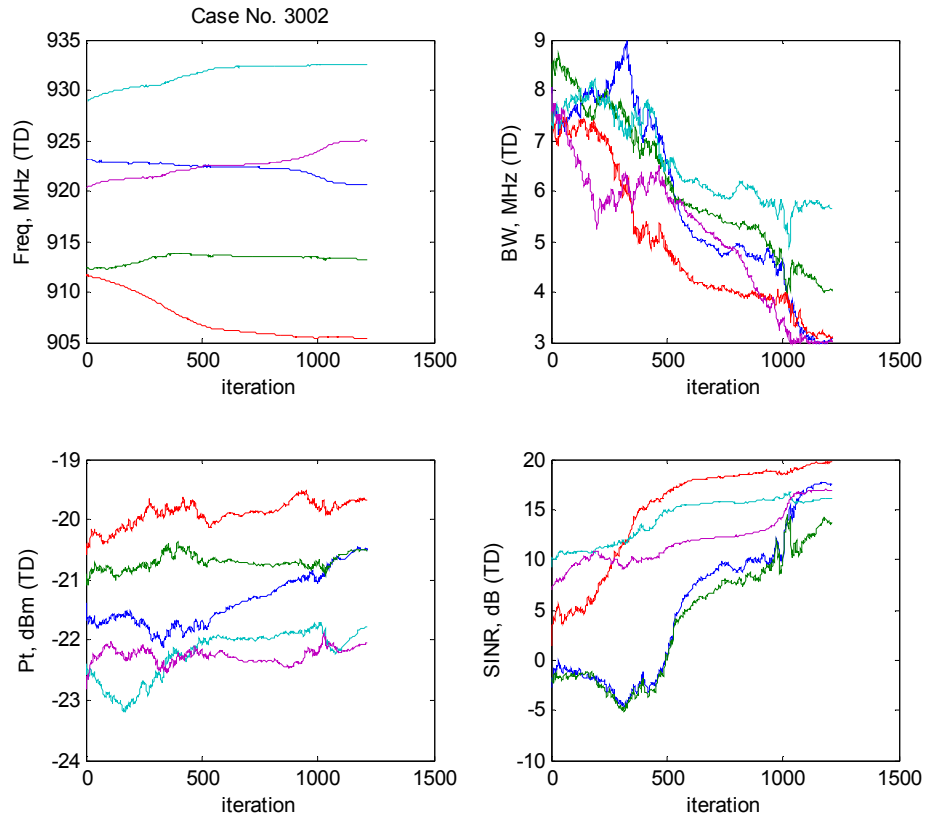
The majority of cases concentrated on intentionally stressful, densely packed MANET play-boxes. For the sake of completeness 400 additional random cases were generated (Data set H2), in which the networks were loosely packed geometrically. This means that the total area covered by all the MANET was usually much less than the play-box area. Figure 22 illustrates the distribution of geometric loading for this specially created data set.



**Figure 22: Histogram of cases for low geometric loading**

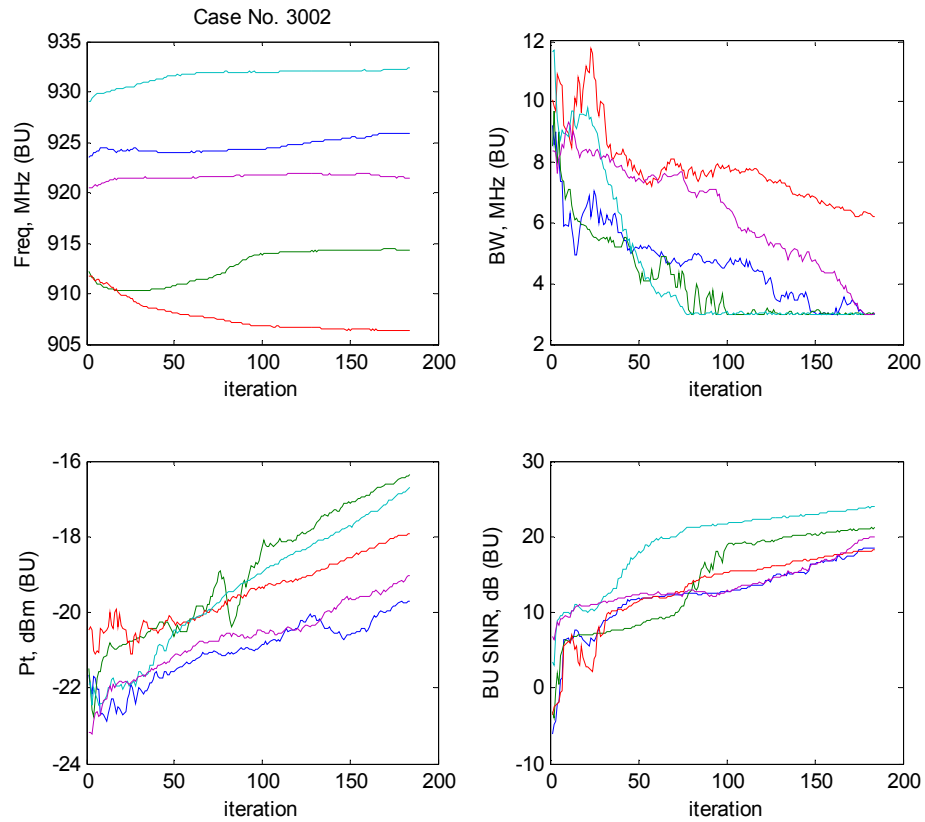
### **Time-Series Output**

The output for each case consists of a set of time series values that represent the evolution of an autonomous spectrum management solution in terms of the center frequency, occupied bandwidth, node transmit power and SINR for each MANET in the playbox. In each case the top-down and bottom-up spectrum models were run using the same initial state. Figure 23 illustrates the evolution of a top-down spectrum solution for the five-MANET setup shown in Figure 2. Note that the individual MANETs are directed to tune away from the strongest interference sources, while reducing bandwidth so as to occupy nearly all the available band. The resulting solution achieves a significant improvement in SINR for all five MANET with negligible changes in transmit power.



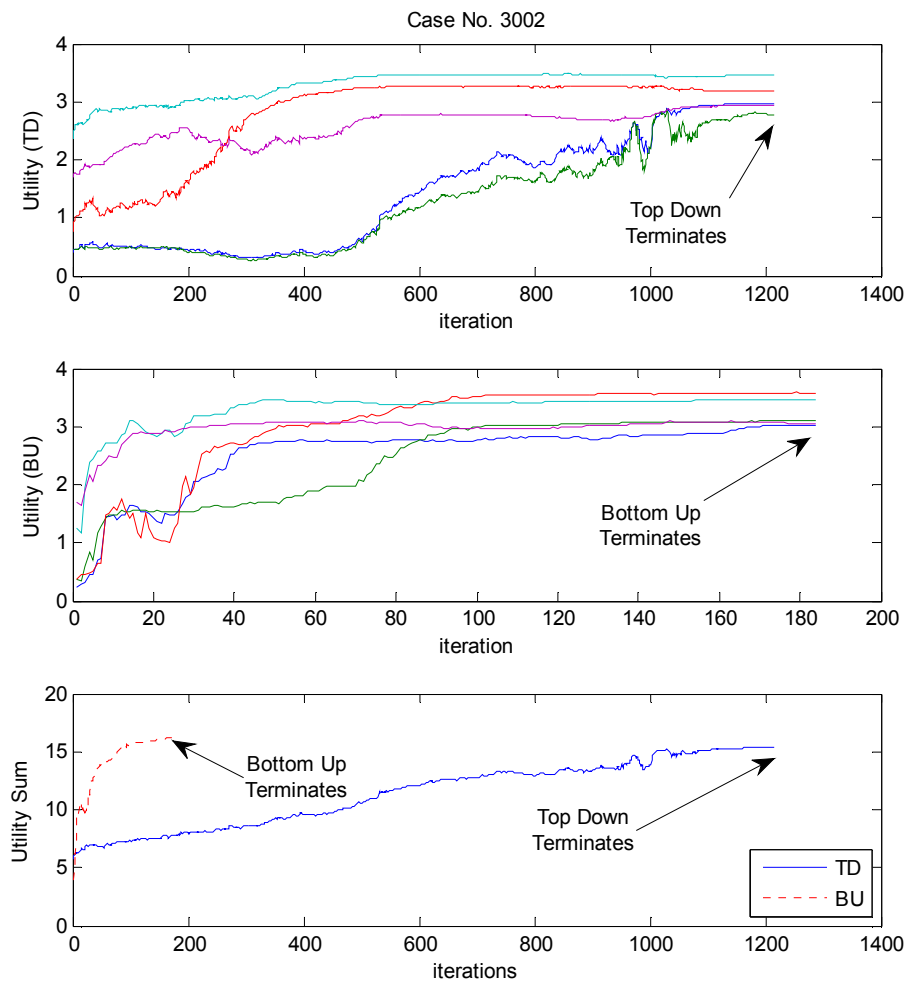
**Figure 23: A nominal “top-down” spectrum solution**

Figure 24 illustrates the evolution of a bottom-up solution for the same initial conditions. As in the top-down example, each network attempts to tune away from the perceived interference and to constrain its RF bandwidth when necessary to improve network utility. Again SINR improves significantly with only a modest increase in transmit power, but the solution is reached without any explicit cooperation among the MANET or communication with an external referee. Each MANET uses its own spectrum utility function to drive the tuning algorithm.



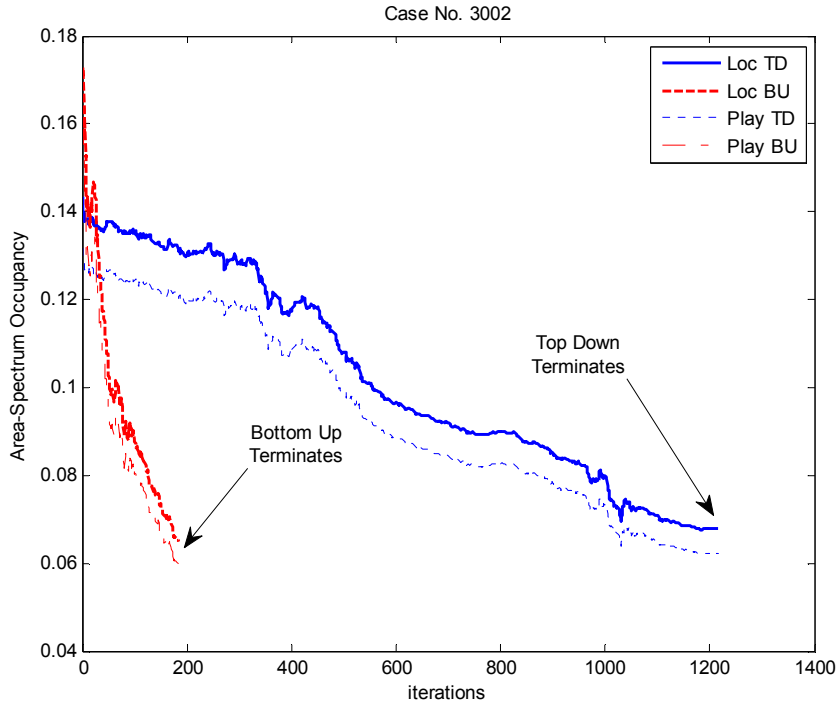
**Figure 24: A nominal “bottom-up” spectrum solution**

Figure 25 shows the evolution of the individual and aggregate utility metrics for both the top-down and bottom-up solutions. In the case of top-down spectrum management the regional referee neither knows nor cares about the MANET utility functions and has only an approximation of the MANET laydown to work with. Its objective function is based solely on the average and minimum SINR achieved among the networks. Although the number of iterations needed to reach equilibrium varies greatly between the top-down and bottom-up solutions, the time scales are not comparable for purposes of implementation.



**Figure 25: Spectrum utility for top-down and bottom-up solutions**

Figure 26 shows the overall product of area and spectrum occupied by the MANET with each solution. When the placement and extent of the MANETs are held constant, the only available course of action is to shift and flatten the spectrum “pancakes” that represent each network.



**Figure 26: Networks attempt to minimize overall spectrum occupancy**

One of the principal research questions was whether, without explicit cooperation, a collection of utility-driven MANET could arrive at a “bottom-up” spectrum distribution that was good enough to dispense with the infrastructure and communications overhead inherent in the proctored or “top-down” approach. In the case illustrated here, the answer was yes.

## Chapter 5: Analysis of Simulation Results

Analysis of over 2,000 simulated cases indicates that, given a suitable goal algorithm, a collection of SDR-enabled MANET can often, without explicit cooperation, arrive at a “bottom-up” spectrum distribution that provides sufficient quality of service, in terms of SINR or utility, to dispense with the infrastructure and communications overhead inherent in the proctored or “top-down” approach. Through multivariate least squares (MLS) analysis it was also discovered that SINR and the resulting spectrum utility could be reasonably predicted by means of a set of algebraic functions. After many variations only a few input variables proved significant for a simple polynomial fit:

- Number of MANET present:  $N_{sys}$
- Average MANET radius in meters:  $R_{avg}$
- Total available bandwidth in MHz:  $Bw_{tot}$
- Two spectrum utility coefficients:  $\alpha_2$  and  $\alpha_3$ 
  - Since  $\alpha_1 + \alpha_2 + \alpha_3 = 1$ , only two coefficients are needed to completely specify the utility function for an individual MANET

In the following discussion “observations” ( $y_{obs}$ ) are the raw output of a complex Monte Carlo simulation with many layered interactions and thus are not readily represented by a simple equation. By contrast “predictions” ( $y_{pred}$ ) are algebraic representations of the multivariate linear regression results for QoS related quantities such as minimum SINR or utility. The simulation residuals ( $\epsilon_{sim}$ ) are the differences



between the predictions and observations, and represent effects that are not completely explained by the regression model:

$$y_{obs} = y_{pred} + \varepsilon_{sim} \quad (45)$$

The general form of the resulting predictor functions for SINR and spectrum utility  $U_{OBJ}$  was:

$$y_{pred} = \sum_k a_k x_k \quad (46)$$

Here  $a_k$  is the regression coefficient associated with some function of the a priori input, denoted by  $x_k$ . The SINR generated by bottom-up optimization (*SNBU*) was the exception to this rule and required an additional quadratic fit of the form:

$$SNBU_{pred} = \sum_k b_k (y_{pred,SNBU})^k \quad (47)$$

This relatively simple regression may be attributed to the data sets being dominated by intentionally stressful cases, with dense packing for geometry and spectrum. When considering potential applications for a priori spectrum adjudication, the need for an assured minimum QoS in terms of either SINR or utility make the state of least favored MANET in a given ensemble a very useful criterion for spectrum supportability. Table 2 shows the relevant predictor coefficients for the worst-off among a set of technically identical MANET.

**Table 2: MLS Coefficients for Minimum SINR, Homogeneous MANET**

<b>k</b>	<b>x<sub>k</sub></b>	<b>a<sub>min_SNTD</sub></b>	<b>a<sub>min_SNBU</sub></b>	<b>b<sub>min_SNBU</sub></b>
0	1	2.2917	-8.9556	-0.5829
1	N <sub>sys</sub>	-2.0031	1.2792	1.4742
2	R <sub>avg</sub>	-0.0126	-0.0195	0.020
3	Bw <sub>tot</sub> /N <sub>sys</sub>	13.9153	8.8786	--
4	(Bw <sub>tot</sub> /N <sub>sys</sub> ) <sup>2</sup>	-2.1304	-1.6419	--
5	(Bw <sub>tot</sub> /N <sub>sys</sub> ) <sup>3</sup>	0.1183	0.1039	--
6	(Bw <sub>tot</sub> /N <sub>sys</sub> ) <sup>4</sup>	-0.0031	-0.003	--
7	(Bw <sub>tot</sub> /N <sub>sys</sub> ) <sup>5</sup>	3.803E-5	3.946E-5	--
8	(Bw <sub>tot</sub> /N <sub>sys</sub> ) <sup>6</sup>	-1.789E-7	-1.971E-7	--
9	α <sub>2</sub>	--	-3.8509	--
10	α <sub>3</sub>	--	-11.786	--

The results of MLS analysis for the three high-density data sets are summarized in Tables 3 through 5. Prior predictions for data set H3 were generated with regression coefficients developed from data sets H0 and H1 in advance of the simulation runs.

**Table 3: Multivariate Least Squares: Case H0 (Homogeneous Nets)**

	Minimum	Maximum	R-squared	Std Dev
Min SNTD (dB)	-34.42	26.14	0.7446	8.32
Max SNTD (dB)	-26.70	35.86	0.8094	6.52
Min SNBU (dB)	-47.74	39.71	0.5396	12.39
Max SNBU (dB)	-38.57	62.02	0.6829	13.34
Min UTD	0.0010	5.640	0.6008	0.8681
Max UTD	0.0082	5.678	0.7539	0.7814
Min UBU	0.0006	5.642	0.3362	0.9557
Max UBU	0.0044	5.678	0.6237	1.0722

**Table 4: MLS Analysis: Case H1 (Heterogeneous Nets)**

	Minimum	Maximum	R-squared	Std Dev
Min SNTD (dB)	-32.08	24.45	0.7890	7.55
Max SNTD (dB)	-26.82	35.11	0.8197	6.65
Min SNBU (dB)	-45.45	31.41	0.5911	11.64
Max SNBU (dB)	-31.15	47.51	0.6959	12.81
Min UTD	0.0012	5.774	0.6117	0.9636
Max UTD	0.0014	7.378	0.7204	1.0082
Min UBU	0.0004	5.842	0.3641	0.9692
Max UBU	0.0005	7.371	0.5711	1.3086

The mixed data set H3 was created to check the validity of predictions based on regression from H0 and H1. The regression results, shown in Table 5, indicate that knowledge of the homogeneity or heterogeneity between the contending networks is sufficient to preserve high correlation (R-squared) between prediction and observation.

**Table 5: Statistics for MANET Prior Prediction Fit: Case H3 (Mixed)**

	Minimum	Maximum	R-squared	Std Dev
Min SNTD (dB)	-42.6	28.0	0.7398	8.64
Max SNTD (dB)	-33.6	40.8	0.7715	7.30
Min SNBU (dB)	-59.0	34.8	0.4904	13.02
Max SNBU (dB)	-51.6	57.1	0.6711	13.35
Min UTD	0.0009	6.843	0.4213	1.232
Max UTD	0.0010	7.758	0.7447	0.925
Min UBU	0.0005	6.154	0.4277	0.926
Max UBU	0.0007	7.821	0.2677	2.084

Figure 27 illustrates the strong correlation between the minimum SINR achieved in the top-down simulation and the values derived from the MLS curve fit. On the upper plot the horizontal axis represents the minimum SINR as estimated by the curve fit, while

the vertical axis represents the minimum SINR output from the top-down simulation. The lower plot shows how far the simulation results deviate from the curve-fit values. In this plot the curve fit SINR is again on the horizontal axis, but the height of the vertical bars represents the deviation for individual cases. Both plots indicate a high level of agreement at the high and low extremes for SINR, and greater variation in the central region. In other words, the curve fit is very good at predicting either a very high SINR or a very low SINR outcome, with much greater potential for disagreement in moderate cases.

Figure 28 shows similar data, with a somewhat weaker correlation, for the minimum SINR in the bottom-up simulation. For both models the residuals appeared to be entirely random, with no obvious trend. Further investigation revealed that this assumption was not valid.

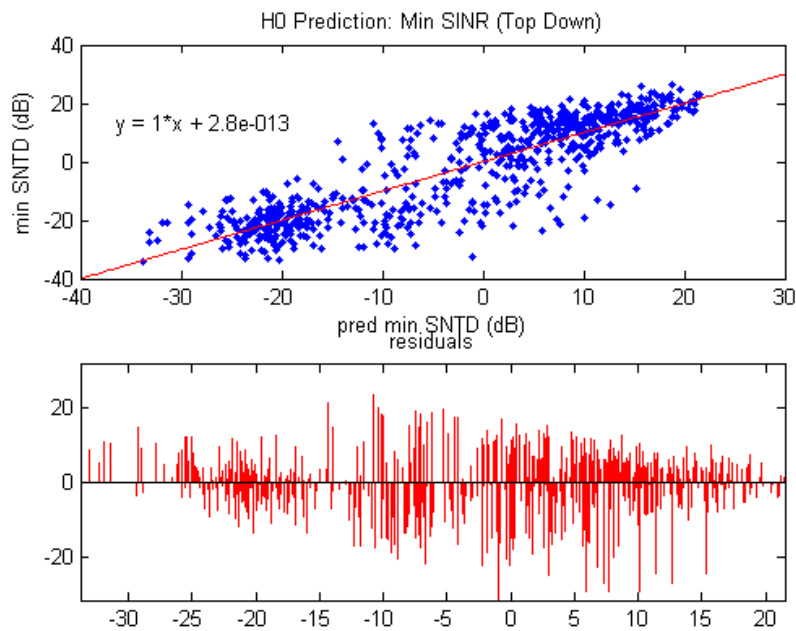


**Figure 27: MLS curve fit for top-down spectrum adaptation**

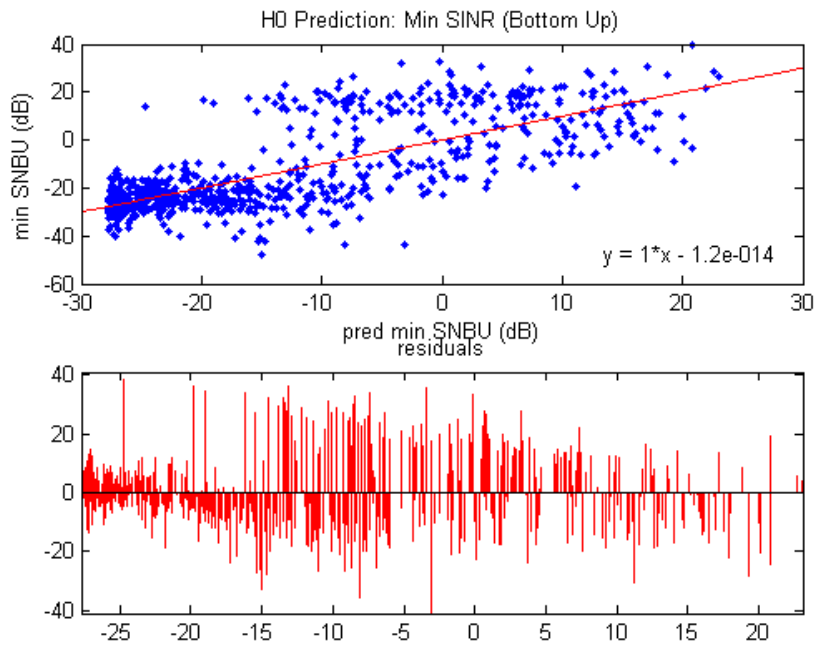


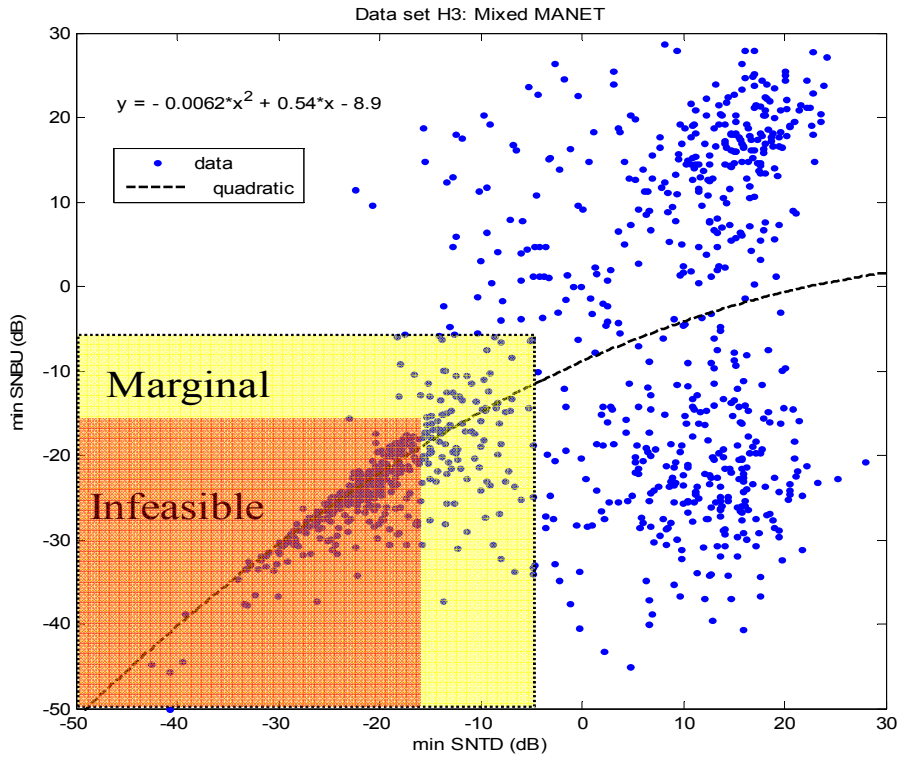
**Figure 28: MLS curve fit for bottom-up spectrum adaptation**

Some general observations can be made from the preliminary analysis of the simulation data:

- The top-down MLS model is a better predictor of the simulation outcomes than the bottom-up model, for both SINR and spectrum utility.
- The significant fraction of successful bottom-up cases (where minimum SINR is greater than 0 dB), indicates that under certain conditions, effective spectrum distribution can be achieved without explicit cooperation or negotiation between networks.

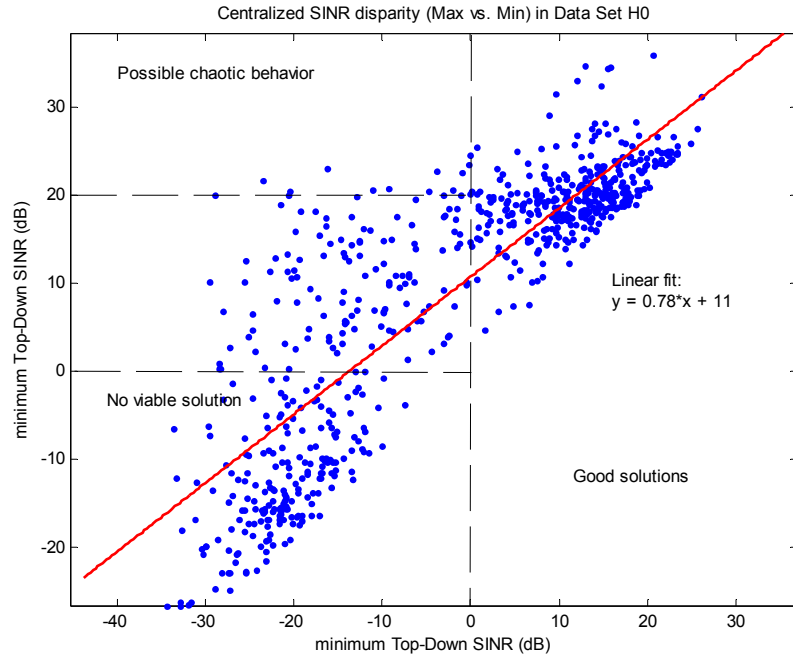
- Bottom-up and top-down solutions for minimum SINR are effectively uncorrelated once either value exceeds -15 dB, as illustrated in Figure 29. Radio communication is assumed to be infeasible below this threshold and only feasible in the “marginal” region for waveforms with high levels of redundancy, or processing gain.
- The top-down solution tends weakly toward higher SINR, as shown by the quadratic trend line in Figure 29, but this should not lead to the interpretation that the centralized approach is always better. There remain a significant number of cases where the bottom-up solution provides higher minimum SINR. Technical and operational tradeoffs, such as the opportunity cost of establishing a centralized infrastructure and its potential vulnerability, would be involved in such a selection.
- Because the utility function was constructed such that  $\sum\alpha = 1$ , only two of the three spectrum utility coefficients ( $\alpha$ ) are needed to predict  $U_{OBJ}$ .
- While the spectrum utility function appears to be useful for driving MANET behavior, the resulting bottom-up utility estimate seems to be a very weak predictor, and is probably useless for any practical threshold criteria.
- Both architectures allowed the possibility of potentially “chaotic” behavior, defined provisionally as solutions where the minimum SINR is less than 0 dB, while the maximum SINR is greater than 20 dB. These cases appear much less often in the top-down model. (See Figures 30 and 31.)
- The relatively high values for standard deviation observed in the regression data imply that multiple Bayesian-type entry criteria might be appropriate.

Figure 32 illustrates one such arrangement, in which the status of currently supported networks is used to refine prior estimates of the QoS impact of each new MANET that requests permission to operate within the local area. The revised estimates of the mean and variability of the minimum SINR, for example, can be used to estimate the probability that the least-favored network will fall below some critical performance threshold. Based on the revised QoS estimates for all MANETs, the new entry will be either rejected due to insufficiency of spectrum resources to ensure safe operation, or accepted and new channel assignments distributed. In theory one could devise confidence limits for SNTD, SNBU and UTD to be used as feasibility criteria for autonomous spectrum management. Any remaining exceptions or more subtle policy decisions could be left for human adjudication. Data set H3, composed roughly equally of homogeneous and heterogeneous cases, was generated to help test this proposition.



**Figure 29: Divergence of Top-Down and Bottom-Up minimum SINR**





**Figure 30: Potential for chaotic top-down SINR behavior**

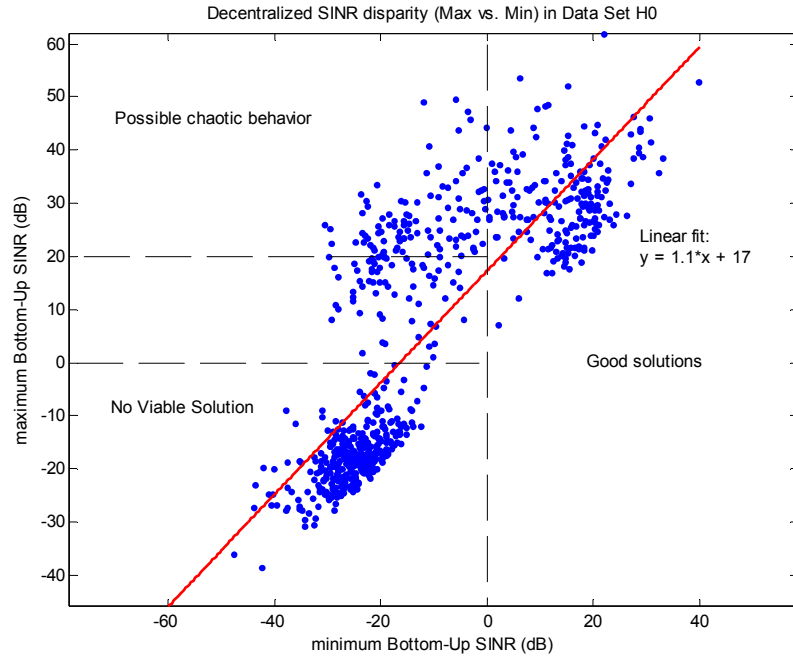


Figure 31: Potential for chaotic bottom-up SINR behavior

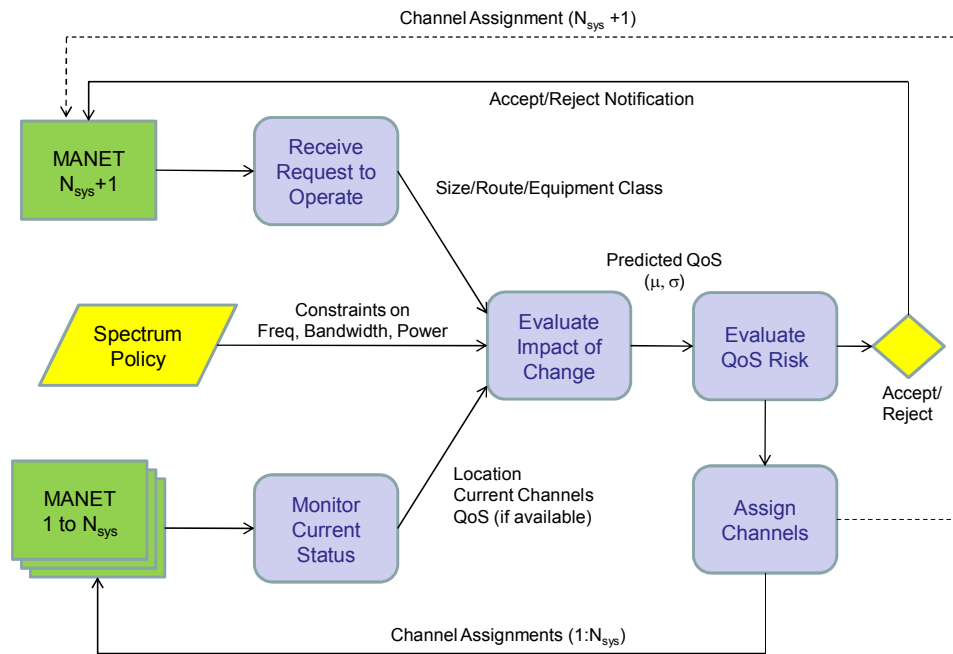


Figure 32: Risk-based spectrum access architecture (nominal)

One unexpected and potentially useful observation was that the prediction errors from the multiple linear regression models showed the surprisingly similar patterns illustrated in Figures 33 and 34. Attempts to compensate for this heteroskedasticity<sup>11</sup> through weighted least squares analysis did not produce a significant improvement in the quality of the predictions, relative to the computational effort expended. However, it was possible to derive a good prior estimate of the accuracy of any prediction of minimum or maximum SINR for both the top-down and bottom-up architectures by using a very simple exponential form:

$$\hat{\sigma}_e(SINR) = A \exp\left(-\frac{x_3}{B}\right) \quad (49)$$

Here  $x_3 = BW_{tot}/N_{sys}$  is the average available bandwidth per MANET. This is also one of the terms common to all of the multiple linear regressions described above, and so should be readily available to any local spectrum management algorithm. Coefficients for bounding the residuals were derived directly from the simulation results and are listed in Table 6.

---

<sup>11</sup> This is a statistical measure that refers to the variance of the errors over the sample. Time series data with similar error variance throughout are termed homoskedastic, while series with dissimilar error variances are termed heteroskedastic.

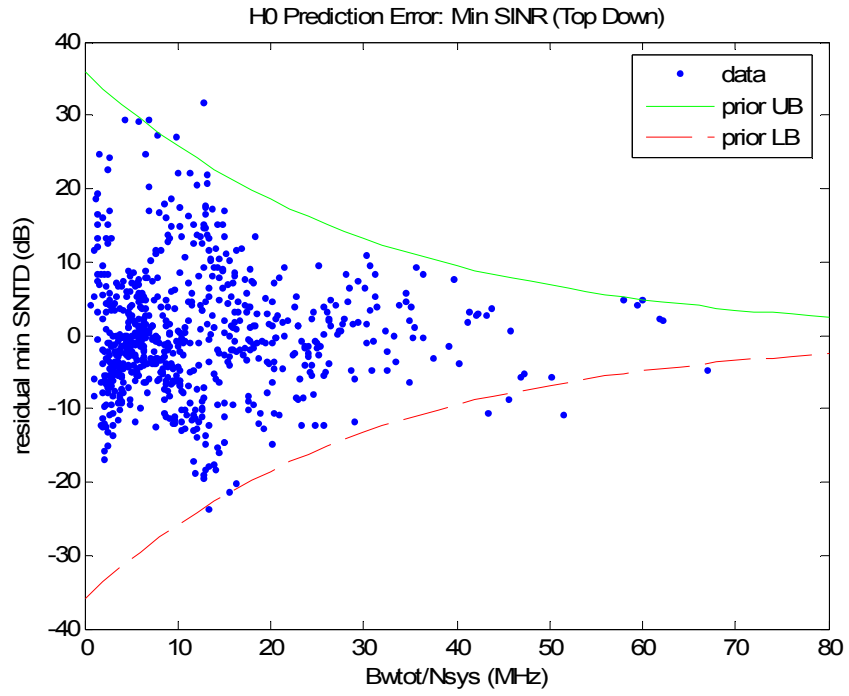


**Figure 33: Exponential bound for Top-down SINR residuals**

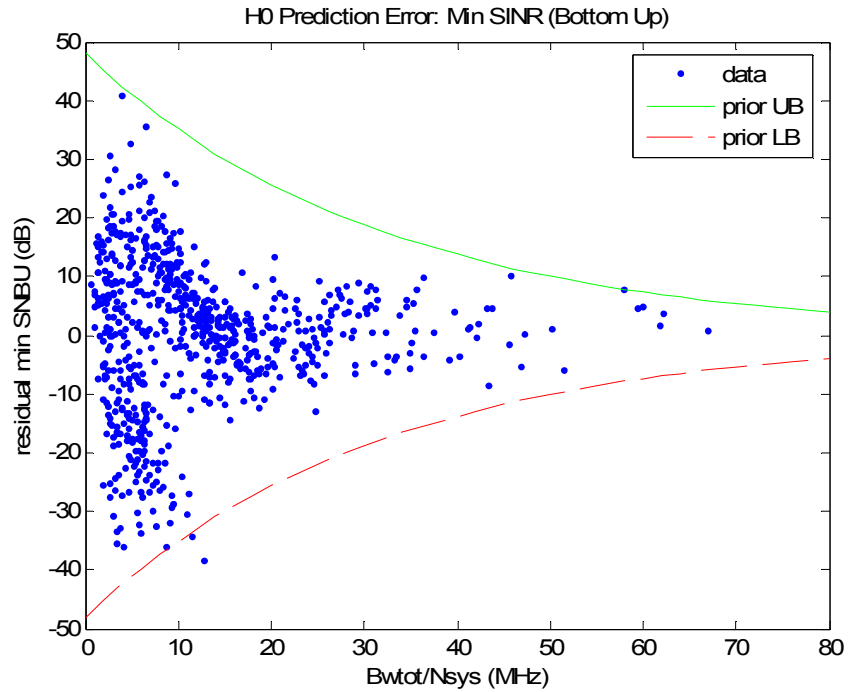


**Figure 34: Exponential bound for Bottom-up SINR residuals**

**Table 6: Coefficients for Prior Estimate of SINR Standard Error**

	$A_{H0}$	$B_{H0}$	$A_{H1}$	$B_{H1}$
Min SNTD	12	30	13.6	25
Max SNTD	12	30	13.2	25
Min SNBU	16	32	18	25
Max SNBU	18	32	21	25

When the low-density H2 data set was analyzed by the same method, no such helpful heteroskedasticity was observed. While a MLS model for low geometric loading shows decent predictive quality (Figure 35), a geometric optimization algorithm (e.g., stacking pancakes), with fixed locations and frequency as the 3rd dimension, might be simpler and faster.

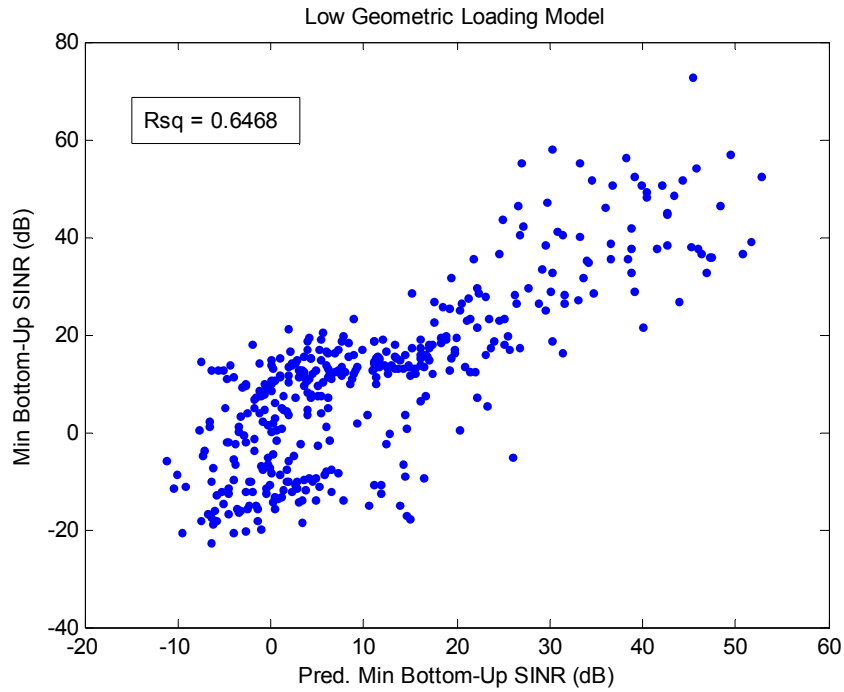


**Figure 35: MLS regression model results for low density of MANET**

The assumption that the standard deviation of the residuals was bounded by an exponential function in terms of the ratio of available bandwidth per MANET in the region warranted further examination. In the histograms shown below, the “normalized error” was based on the prior estimate parameters of Table 6. Both the top-down (Figure 36) and bottom-up model results (Figure 37) exhibited a bell-curve shape similar to a classical Gaussian “normal” distribution.

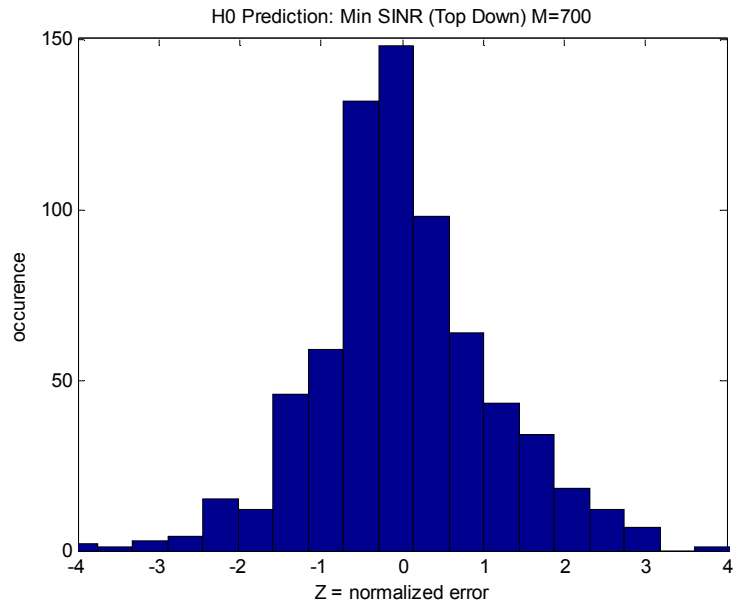


**Figure 36: Histogram of top-down prediction residuals**

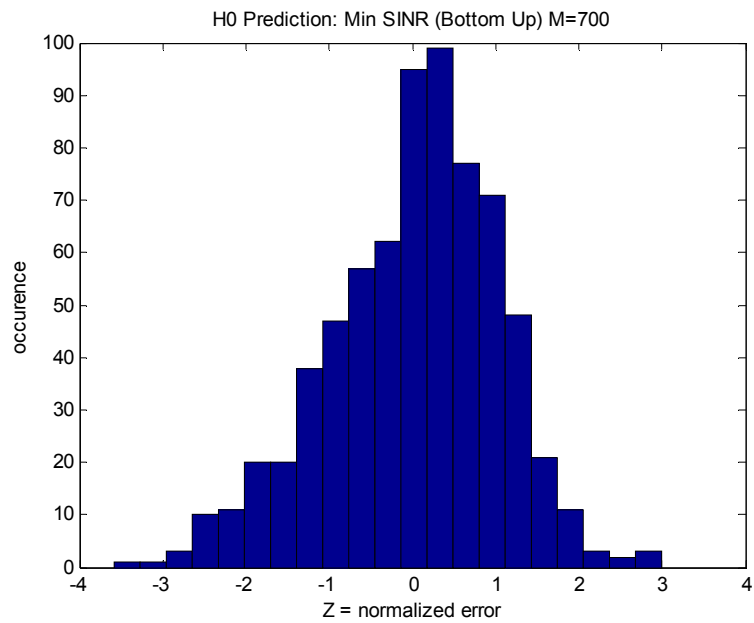


**Figure 37: Histogram of bottom-up prediction residuals**

When the cumulative probability distributions (CDF) for the simulated SINR outcomes were plotted, the four major predictors lined up very well with a theoretical Gaussian distribution, as shown in Figure 38. At this stage the assumption of normally distributed prediction errors required further examination but appeared to be sufficiently useful to begin developing heuristic performance models for market-driven spectrum management.

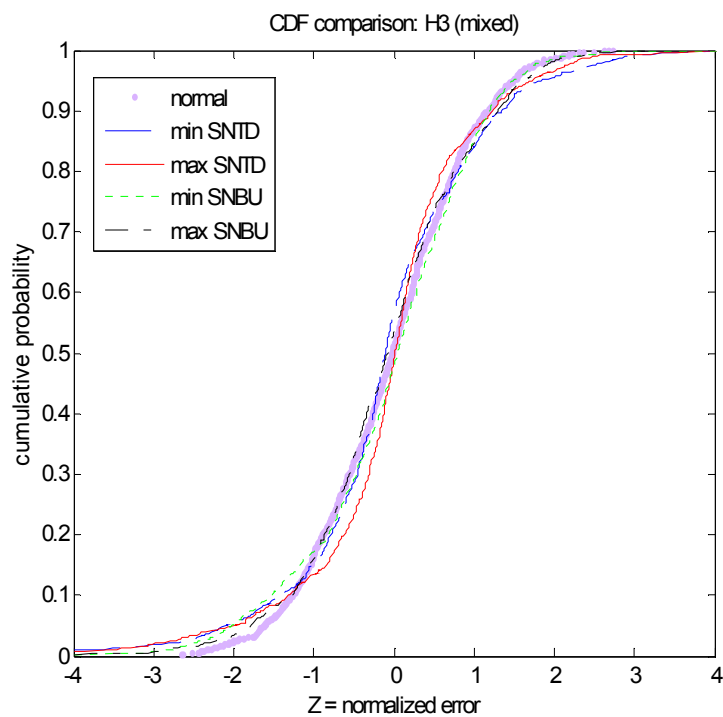


Figure 38: Cumulative distribution functions for simulated residuals

### Kolmogorov-Smirnov Test of SINR Residuals

Prior estimates for the accuracy of MLS prediction of minimum or maximum SINR for both the top-down and bottom-up architectures were observed to be bounded by a simple exponential function of the average available bandwidth per MANET. Although



assuming a normal distribution in the residuals helped to derive a first estimate of the confidence levels of SINR prediction, the *Kolmogorov-Smirnov* test indicated that the distributions were not strictly normal. The essential elements of this statistical test (CRC, 1996, p. 623) are:

- **Null hypothesis:** That the sample (residuals) with empirical cumulative distribution function  $F(x)$  is drawn from a population with an intrinsic CDF of  $G(x)$ , or more simply, that there are no significant differences between the sample and the assumed population.
- **K-S statistic:** For sample size  $n$ :  $D_n = \max |F(x)-G(x)|$
- **Criterion:** Reject the null hypothesis with confidence  $P=1-2\alpha$  if  $D_n > D_\alpha = \varepsilon$ , where the threshold  $\varepsilon$  may be determined by the series (Miller, 1956):

$$\alpha = \varepsilon \sum_{j=0}^{n-n\varepsilon} \binom{n}{j} \left(1 - \varepsilon - \frac{j}{n}\right)^{n-j} \left(\varepsilon + \frac{j}{n}\right)^{j-1} \quad (50)$$

Or asymptotically by:

$$\varepsilon \approx \sqrt{\frac{\ln\left(\frac{1}{\alpha}\right)}{2n}} \quad (51)$$

This test was applied to the residuals from data set H3, a mixture of homogeneous and heterogeneous MANET cases, where  $n=1000$ . For the 95% confidence level ( $\alpha = 0.025$ ) we have  $\varepsilon = 0.04295$  and the K-S test results listed in Table 7:

**Table 7: Results of K-S Test for Normally Distributed Residuals**

<b>Residual</b>	<b><math>D_n</math></b>	<b>Reject Null Hypothesis</b>
Min SNTD	0.0756	Yes
Max SNTD	0.0825	Yes
Min SNBU	0.0398	No
Max SNBU	0.0502	Yes

## Investigation of Heteroskedasticity in SINR Prediction Errors

If, as proposed here, it is feasible to trust autonomous tuning algorithms for real-time spectrum distribution among competing mobile ad hoc networks, then the minimum expected signal-to-noise-plus-interference ratio (SINR) among a group of MANET would be a very useful metric for evaluating a spectrum solution.

The random MANET layouts and spectrum playboxes created for this study were constrained in such a way that conflict in the form of inter-network interference would be inevitable. Given an initial spectrum “endowment” and some individual utility functions, the simulated MANETs were allowed to seek the best available spectrum distribution in either a refereed (top-down) or self-directed (bottom-up) tuning mode. Multivariate least squares (MLS) regression of the simulation output produced a set of predictor functions for the final minimum SINR with regression coefficient  $r^2$  approaching 0.75.

After many trials only a few input variables proved significant for a simple polynomial fit:

- Number of MANET present:  $N_{sys}$
- Average MANET radius in meters:  $R_{avg}$
- Total available bandwidth in MHz:  $BW_{tot}$
- Two spectrum utility coefficients:  $\alpha_2$  and  $\alpha_3$

Prediction errors (residuals) from the multiple linear regression models showed a surprisingly regular pattern when plotted against some of the input variables. It was possible to derive a good prior estimate of the accuracy of any prediction of minimum or maximum SINR for both the top-down and bottom-up architectures by using a very simple exponential form.

One obvious question is whether the exponentially bounded residuals observed in this study are simply artifacts of the particular simulation models used or do they represent some fundamental insights about the potential for autonomous spectrum management? Some clues may be found in the Gaussian passband model for frequency dependent rejection (FDR) and its complement frequency dependent integration (FDI).

### Gaussian Frequency Dependent Integration

In the MANET simulation the frequency dependent integration (FDI) factor was modeled as the difference between two Gaussian error functions. Neglecting a couple of scaling constants, we have the form:

$$\eta_g \approx \operatorname{erf}\left(x + \frac{\delta}{2}\right) - \operatorname{erf}\left(x - \frac{\delta}{2}\right) \quad (52)$$

Here  $x = c \Delta f / B_i$  and  $\delta = c B_s / B_i$ . As the number of nets increases, the average channel separation will approach equipartition of the total available bandwidth:  $\Delta f \rightarrow B_{w_{\text{tot}}} / N_{\text{sys}}$ . Also  $\eta_{\text{FDI}} = k \eta_g$ , where  $k = 0.533$  and  $c = 1.66$ . There will only be significant interference if  $x < 2$ .

We can safely assume that for the least favored (minimum SINR) MANET in the playbox, the interference power will dominate the internal receiver noise, so that:

$$SINR_{min,dB} = 10 \log \left[ \left( \frac{P_{ts}}{P_{ti}} \right) \left( \frac{d_i}{d_s} \right)^n \frac{1}{\eta} \right] \quad (53)$$

Here  $P_{ts}$  is the transmit power for the least favored MANET and  $d_s$  is the average inter-nodal distance. Likewise  $P_{ti}$  and  $d_i$  are the transmit power and node separation for the nearest interfering neighbor MANET, while  $n$  is the RF propagation constant within the playbox. The inter-nodal distances do not vary within the simulation and can be approximated by  $R/N^{1/2}$  where  $N$  is the number of nodes and  $R$  is the MANET radius.

The variance of the minimum SINR in dB is thus:

$$\sigma^2(SINR) = \sigma^2 \left( \left( \frac{P_{ts}}{P_{ti}} \right)_{dB} \right) + n\sigma^2 \left( \left( \frac{d_i}{d_s} \right)_{dB} \right) + \sigma^2(\eta_{FDI}) \quad (54)$$

The variance of the final minimum SINR in a spectrum-contention scenario will be dominated by the variance of the strongest contributing factor, FDI. The first two terms are largely determined by the initial setup geometry, and should be adequately accounted for by MLS regression. The error estimate for the residuals after MLS curve fitting will thus be:

$$s_e(SINR) \approx \sqrt{O(1) + \sigma^2(\eta_{FDI})} \quad (55)$$

Evaluating a couple of derivatives may shed some light on the heteroskedasticity mentioned above. The analytical derivative for the Gaussian approximation for FDI is given by:

$$\frac{d\eta(x,\delta)}{dx} = \frac{2}{\sqrt{\pi}} \left[ \exp \left( - \left\{ x + \frac{\delta}{2} \right\} \right) - \exp \left( - \left\{ x - \frac{\delta}{2} \right\} \right) \right] \quad (56)$$

The derivative of the natural logarithm of FDI should also be a significant factor in determining the variance of any effective adjacent-channel interference.

$$\frac{d}{dx} \ln\{\eta(x, \delta)\} = \frac{\exp\left(-\left\{x + \frac{\delta}{2}\right\}\right) - \exp\left(-\left\{x - \frac{\delta}{2}\right\}\right)}{\frac{\sqrt{\pi}}{2} \left( \operatorname{erf}\left(\frac{\delta}{2} + x\right) + \operatorname{erf}\left(\frac{\delta}{2} - x\right) \right)}$$

(57)

As illustrated in Figure 39, this version of the FDI function is very close to a log-linear relationship with respect to a normalized frequency offset.

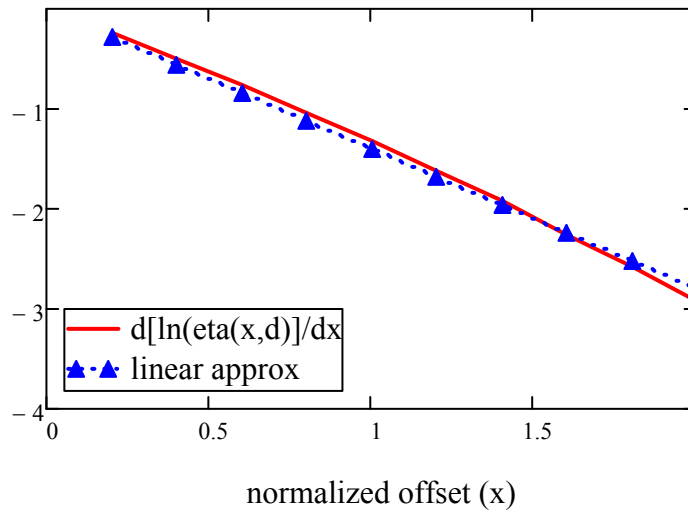


**Figure 39: Log-linear behavior of FDI derivative**

As a check to see whether, as suspected, the form of the FDI function was a strong driver in the smooth heteroskedasticity phenomenon, some simple but mathematically distinct passband functions were created, along with their associated FDI functions. Figure 40 illustrates ideal versions of circular, rectangular and triangular

passbands. For a normalized frequency offset  $z = \Delta f/B_s$ , the passbands are described by the following equations:

$$\text{Circular:} \quad \text{circ}(z) = \sqrt{1 - z^2} \text{ for } |z| < 1 \quad (58)$$

$$\text{Rectangular:} \quad \text{rect}(z) = 1 \text{ for } |z| < \frac{1}{2} \quad (59)$$

$$\text{Triangular:} \quad \text{tri}(z) = 1 - |z| \text{ for } |z| < 1 \quad (60)$$

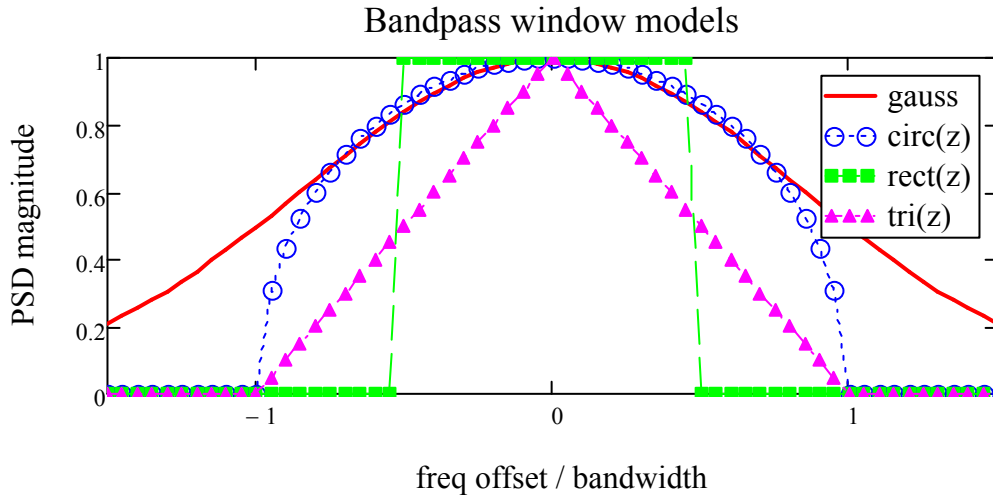


**Figure 40: Idealized alternative passband functions**

For each ideal passband function, the corresponding FDI integral becomes a scaled autocorrelation function. Nominal FDI in decibels is plotted in Figure 41, where the zero-crossing problem of potentially infinite negative dB was addressed by inserting a 10 dB per bandwidth linear degradation at appropriate asymptotes.

*Circular-passband FDI:*

$$\eta_{circ}(u, \delta) = \frac{2}{0.849\pi\delta} \int_{-\infty}^{\infty} circ\left(\frac{y-\frac{u}{2}}{\delta}\right) circ\left(\frac{y+\frac{u}{2}}{\delta}\right) dy \quad (61)$$

*Rectangular-passband FDI:*

$$\eta_{rect}(u, \delta) = \frac{1}{\delta} \int_{-\infty}^{\infty} rect\left(\frac{y-\frac{u}{2}}{\delta}\right) rect\left(\frac{y+\frac{u}{2}}{\delta}\right) dy \quad (62)$$

*Triangular-passband FDI:*

$$\eta_{tri}(u, \delta) = \frac{1.5}{\delta} \int_{-\infty}^{\infty} tri\left(\frac{y-\frac{u}{2}}{\delta}\right) tri\left(\frac{y+\frac{u}{2}}{\delta}\right) dy \quad (63)$$

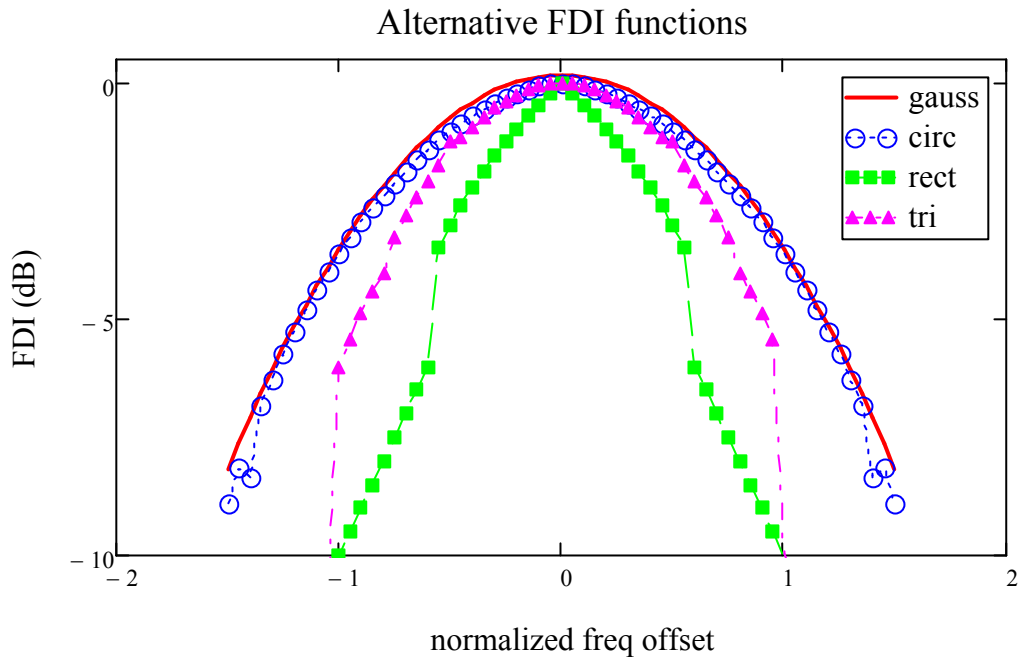


**Figure 41: Nominal FDI functions for idealized passbands**



Figure 42 compares numerical approximations to the derivative of FDI (in decibels) for the idealized passband functions. Only the Gaussian passband model shows an approximately log-linear pattern. Can this plot be interpreted to explain the apparent exponential decay in the simulation residuals as the average bandwidth per MANET increases? If so then the alternative passbands exhibit no such predictable decay.

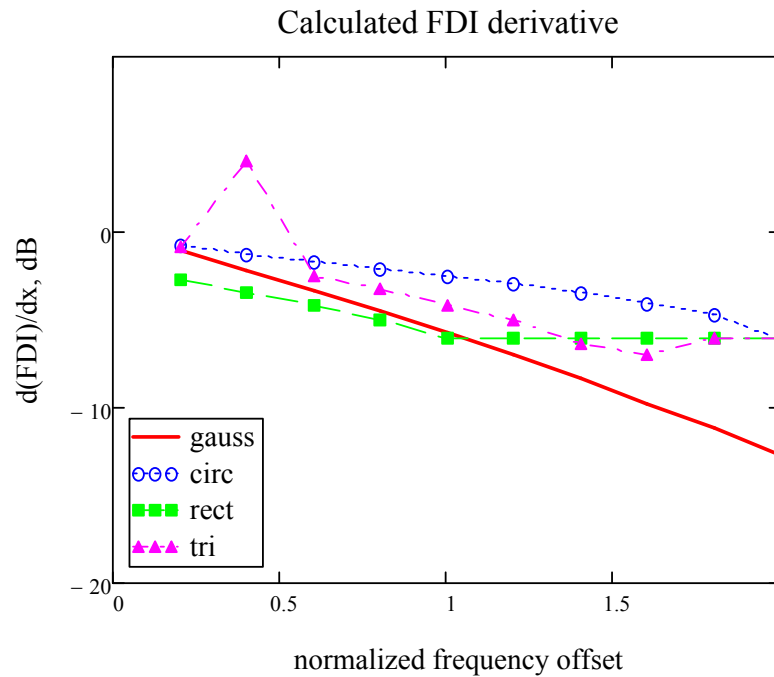


Figure 42: FDI derivative for several passband models

A Monte Carlo exercise was performed on the various FDI functions, which may partially explain the relative magnitude of the residuals. For 500 trials of  $\eta(x, \delta)$  where  $x$  is a normally distributed random variable with unit variance and a mean of 1.66 and  $\delta=1.66$  the following standard deviations resulted:

$$\text{Gaussian:} \quad \sigma(\eta_{\text{gauss}}) = 11.7 \text{ dB} \quad (64)$$

$$\text{Circular:} \quad \sigma(\eta_{circ}) = 6.5 \text{ dB} \quad (65)$$

$$\text{Rectangular:} \quad \sigma(\eta_{rect}) = 6.0 \text{ dB} \quad (66)$$

$$\text{Triangular:} \quad \sigma(\eta_{tri}) = 6.9 \text{ dB} \quad (67)$$

When the predictable heteroskedasticity of the Gaussian passband model is ignored, the overall residual for  $\text{SINR}_{\min}$  is approximately 8 dB. A case could be made that the Gaussian passband assumption represents a reasonable worst case for feasible autonomous spectrum management simulation. For example, the rectangular passband represents an ideal but impractical filter, while the Gaussian model relaxes assumptions about filter design.

To test this proposition, a sample set of 200 MANET cases was run with both the Gaussian and rectangular passband models for FDI, with the spectral response shown in Figure 43. The rectangular FDI function was scaled so that response curves would be comparable within the 3 dB bandwidth.

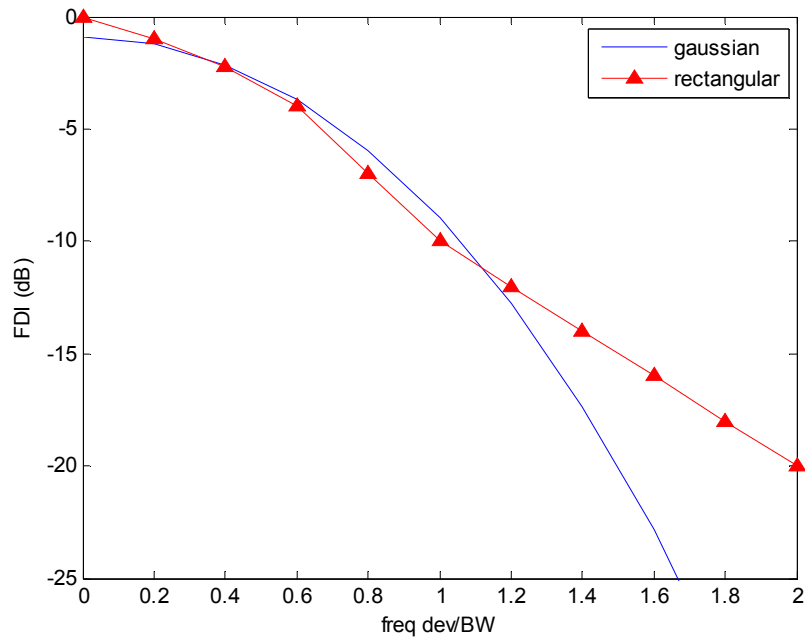


**Figure 43: FDI response for Gaussian and rectangular passbands**

After MLS regression was applied to the simulation output for minimum and maximum top-down SINR, the residuals compared between passband models. As shown in Figure 44, the estimation errors induced by the rectangular passband model typically fall well within the 3-sigma bounds previously calculated for the Gaussian model.

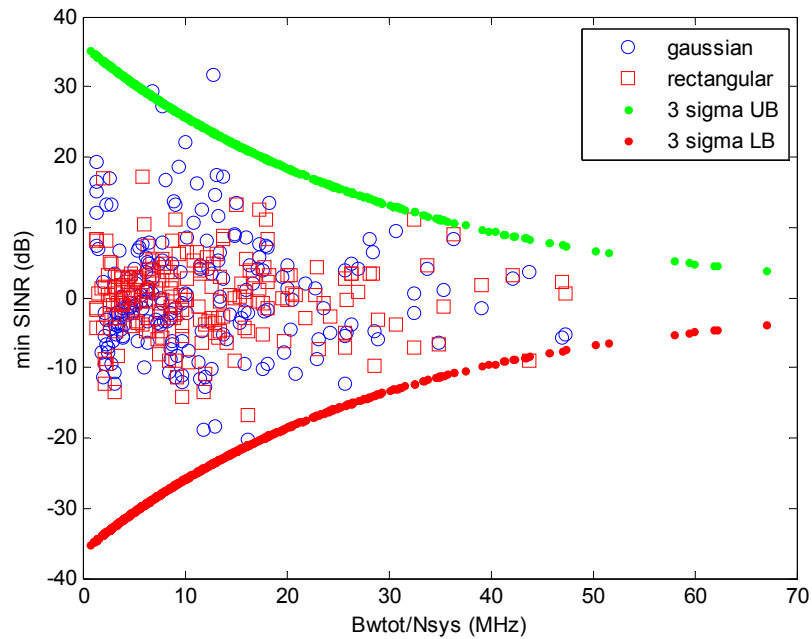


**Figure 44: Comparison of Residuals for Gaussian and Rectangular passbands**

The MANET simulations at the heart of this study contain many competing entities, along with the subtle interactions between several random variables. It would be impractical to analytically isolate one single cause for the well behaved bounding of the residuals. The preceding investigation indicates that the choice of the Gaussian passband model is both a major influence in the outcomes and a reasonable first order assumption for adaptive spectrum dependent systems.

The results of this simulation-based study demonstrate the feasibility of a limited class of solutions to a potential spectrum management problem.

## Chapter 6: Potential Applications

A good stochastic performance predictor can lend efficiency and speed to plans for future MANET deployment. A nominal MANET provisioning problem can be framed in the following manner: If a given number (N) of MANET can self-manage within a region defined by area and bandwidth, what will be the impact of adding the N+1st network? In Figure 45 the top-down homogenous predictor model (H0) was applied to sets of MANET with an average radius of 200 meters. If we assume that the nets will be running applications that require a minimum SINR of 8 dB, then a local spectrum allocation of 20 MHz will support at most seven MANET. To support 8 or 9 MANET would require more bandwidth, 25 to 30 MHz in this example. Based on the regression models developed for this study, a bottom-up model typically yields a mean SINR 11 dB lower than top-down. A given bandwidth could thus be expected to support fewer MANET in the bottom-up configuration, leading to more conservative spectrum budgeting.

Regarding application of this work to improve the spectrum management process, a distinction should be made between the technology required to implement either a centralized (top-down) or decentralized (bottom-up) architecture, and the a priori estimation of the likelihood of success in particular instance, in terms of SINR, spectrum utility, or some other QoS measure. This is akin to the distinction between whether a thing *can* be done and whether it *should* be done.

In the former case, the representations of physical phenomena and logical operations that constitute the simulation represent abstractions of well understood

engineering principles, along with technologies that exist or are in research and development today (e.g., location-based spectrum access, adjacent band sensing, and high-content in-band signaling via IPv6). In the latter case, the relatively few and readily available nature of the inputs needed for a high quality a priori estimate of minimum SINR and the variability of the observed outcome lend themselves to the development of a class of probabilistic decision aids. There is a practical point, yet to be determined, where the additional detail (plus the computational and network overhead) needed to drive the variation down to an arbitrary level ceases to be worthwhile.

If the operational goal is to get more value out of the available spectrum while avoiding spectrum “fratricide” due to friendly interference, then the likelihood and potential consequences of an unfavorable outcome (e.g., lack of connectivity due to low SINR), the essential elements of risk analysis, are intimately bound up in the decision to implement and rely upon any automated spectrum management method.

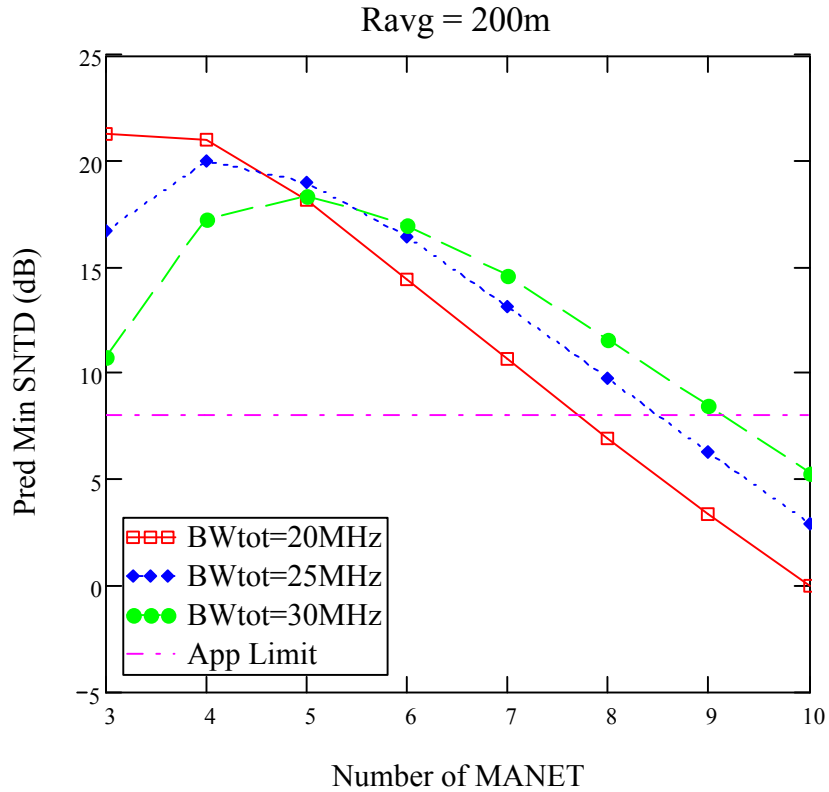


**Figure 45: Spectrum Provisioning for Top-Down Autonomous Management**

A mature model for the behavior of adaptive RF systems under various spectrum constraints could give spectrum managers rapid assessment of the impacts of deploying such devices. Several potential applications come to mind:

- **Spectrum management** – An adaptive MANET behavioral model could be incorporated into existing planning software to improve pre-operational spectrum planning.
- **System development and acquisition** – Models of the operational impacts of cognitive radio technologies can aid simulation based acquisition studies and interoperability analysis. Description of the electromagnetic

environment in terms of loss parameters will allow modeling of spectrum utility to aid deployment of new radio services while minimizing disruption of legacy services.

- **Autonomous network management** – Trusted spectrum-trading algorithms, designed to follow accepted spectrum “rules of engagement” can allow many routine spectrum control and sharing functions to reside within the wireless units themselves. Predictable behavior will ease regulatory and certification processes for SDR-based systems.

Although this study is primarily a feasibility analysis, some consideration should be given to timeliness of solutions. Conservative estimates of the time to solve a spectrum allocation solution using these preliminary algorithms range in tens of seconds for both the top-down and bottom-up models, as shown in Appendix D. These figures would be expected to significantly improve in any determined development and acquisition program.

If the concepts outlined in this preliminary study can be extended to cover a wide variety of physical-layer radio technologies, then it should be possible to develop a software application tool with which RF system designers and network developers may evaluate the impacts of aperture technologies in light of “top-down” requirements received from the spectrum management community. A nominal data flow for antenna (aperture) engineering is shown in Figure 46. The proposed tool would examine real-time spectrum distribution in mobile ad-hoc networks as a function of the aperture effects



model selected. The results would inform engineering changes and provide an analytical basis for policy recommendations regarding future adaptive networks. An important step in this effort is the development of a credible method for quickly assessing the so-called “operational impact” of a new technology. This will require the development of credible scenarios in which MANET and other radio systems are employed in relevant ways by military and public safety organizations.

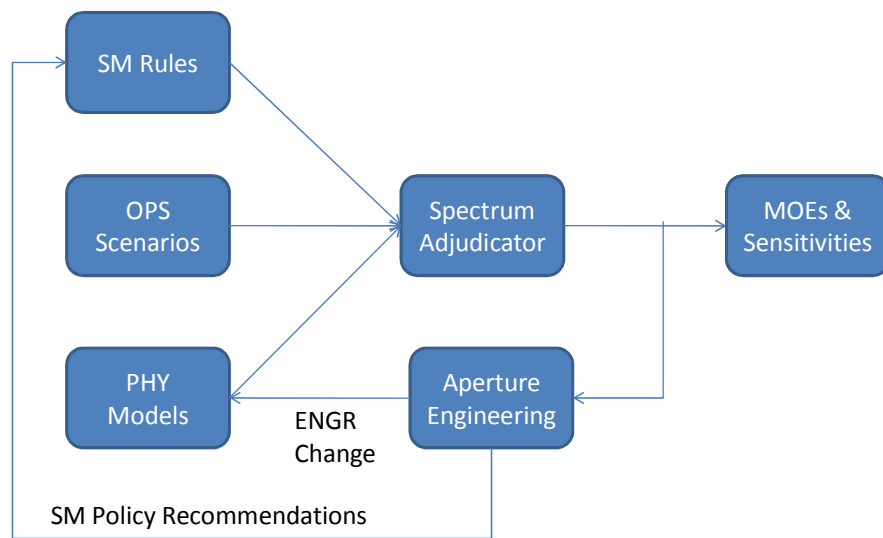


**Figure 46: Spectrum management model for engineering analysis**

All of the above applications depend in some way on the confidence level (CL) of SINR predictions. The plots below (Figs. 47 and 48) were derived from the homogeneous MANET (H0) data set, based on the assumption of normal variance in the prediction errors for top-down and bottom-up MANET loading. A minimum SINR criterion of zero decibels (i.e., signals are discernible through an equal amount of background noise) was assumed for a particular type of wideband tactical radio application. Each data point

represents an estimate of the likelihood that a simulated minimum SINR will exceed the designated operating criterion.

The threshold for an acceptable autonomous-SM solution can thus be correlated to the amount of risk that the spectrum manager is willing to tolerate. For example, if a link confidence level of 80% is desired for each MANET in a given area, then the decision to allow autonomous spectrum management requires a predicted minimum SINR of approximately 10 dB for both the Top-down and Bottom-up architectures.

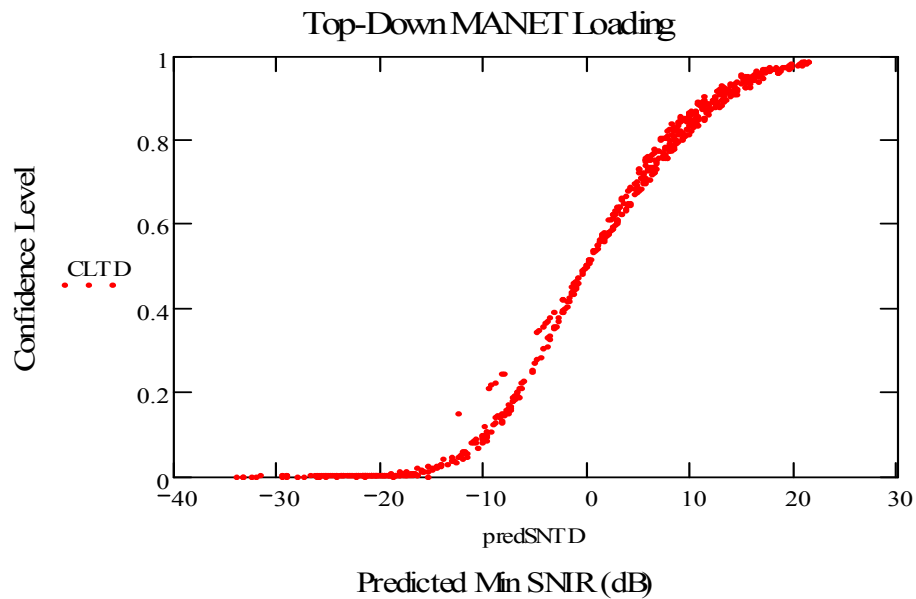


**Figure 47: Derived confidence metric for top-down minimum SINR**

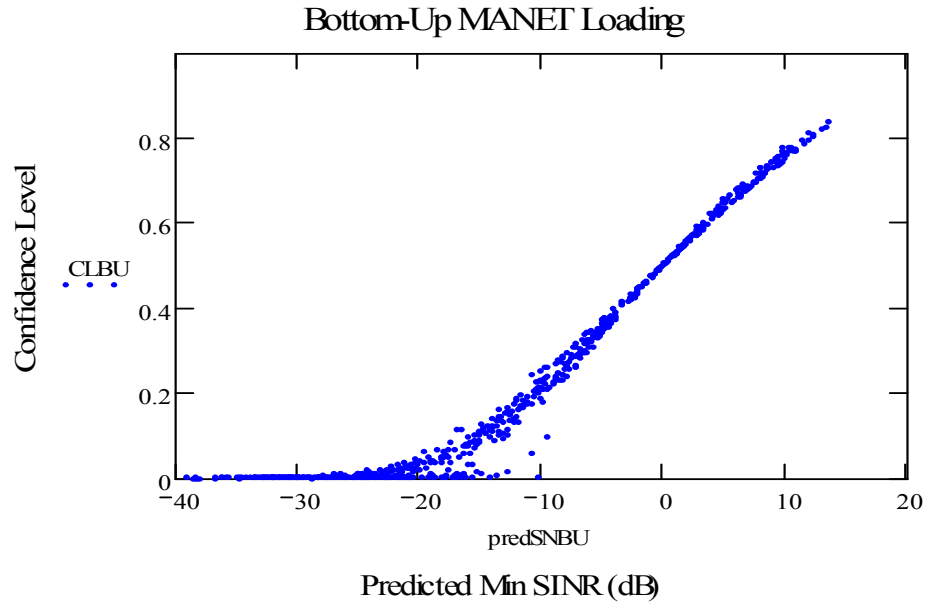


**Figure 48: Derived confidence metric for bottom-up minimum SINR**

## Chapter 7: Extensions of Interference Models

By extending the concept of frequency dependent integration to include several current methods of signal discrimination, one may devise measures of the degree to which reception of desired information is degraded by the presence of undesired signals in any format.

### Time Diversity Interference Model

The impacts of time division multiple access (TDMA) and interference from pulse modulated sensors such as radar can be modeled by considering the convolution of two generalized pulse trains,  $g_1(t)$  and  $g_2(t)$ , defined by:

$$g_1(t) = w_1(t/\tau_1) \otimes \sum_{k=0}^M \delta(t - kT_1) \quad (68)$$

$$g_2(t) = w_2(t/\tau_2) \otimes \sum_{k=0}^M \delta(t - kT_2) \quad (69)$$

In the above equations  $w(t)$  is a unit pulse function and  $\delta(t)$  is the Dirac delta function. The idealized sequences are defined by the pulse width  $\tau$ , the pulse interval  $T$ , and the phase-amplitude coefficients  $\alpha$ . The relative time-based interference upon pulse train  $g_1$  by pulse train  $g_2$  can be defined by:

$$\eta_{pulse(1,2)} = \frac{\int_0^{\infty} |g_1(t) \cdot g_2(t)| dt}{\int_0^{\infty} |g_1(t)|^2 dt}$$

Sharply rectangular pulses are very difficult to generate, and rarely survive channel phenomena without distortion. Consequently, simplifying approximations (such as Gaussian pulse shapes) may often prove useful here. Upper bound approximations for time-like interference could also be used to generate exclusionary operating rules for pulse-modulated systems. This nominal time-like interference measure is asymmetric, in the sense that  $\eta_{pulse(2,1)} \neq \eta_{pulse(1,2)}$ .

### **Code Diversity Interference Model**

*Wideband code division multiple access* (WCDMA) is a spectrum sharing technique used in certain types of “third generation” (3G) cellular telephone networks. Each bit of the original message is encoded and decoded by a special digital sequence, a *spreading code* that repeats the bit many times with pseudo-random phase changes, effectively spreading the bit energy over a wide bandwidth, typically 5 MHz. The resulting data redundancy enhances reception by coherent addition. The orthogonality of the spreading codes ensures that the interference signal will not have enough code chips in common with a legitimate signal to upset the bit-detection logic of the receiver, and will thus be treated as incoherent noise. The effective channel isolation factor is determined by the correlation between code sequences. If we consider two adjacent MANET that use direct sequence spread spectrum codes  $S_1$  and  $S_2$ , the additional isolation due to code diversity would be:

$$\eta_{code} = \max\{corr(S_1, S_2)\} \quad (71)$$

For the 128-chip Gold codes<sup>12</sup> used to discriminate between WCDMA base stations, the isolation factor approaches -20 dB.

### Spatial Diversity Interference Model

Advances in spectrum policy have been limited by a nearly exclusive focus on omnidirectional antennas. The introduction of advanced apertures with steerable beams will enable future physical layer (PHY) aware network protocols to perform angular discrimination of intended from unintended receivers. Such a capability would have a profound impact on spectrum management for mobile networks.

Figure 49 illustrates a gain pattern for a nominal steerable antenna array. In this example the main lobe has been steered 20 degrees to the left. All side lobes appear to be at least 25 dB below the main lobe gain, indicating a maximum integrated sidelobe level (ISL) of -25 dB. If we are primarily concerned with two-dimensional terrestrial links, then we can estimate an “angular isolation factor” for a given class of antennas that would be analogous to frequency dependent rejection:

$$\eta_{antenna} = \frac{\theta_{beam} + (2\pi - \theta_{beam}) \cdot 10^{\frac{ISL}{10n}}}{2\pi} \quad (72)$$

---

<sup>12</sup> Robert Gold (1967) showed that for certain well-chosen m-sequences, the cross correlation only takes on three possible values, namely -1, -t or t-2. Two such sequences are called preferred sequences. Here t depends solely on the length of the linear feedback shift register (LFSR) used.

where  $\theta_{beam}$  is the main lobe width in radians,  $n$  is the local radio propagation constant and  $ISL$  is the integrated sidelobe level in decibels. The principal effect of introducing this factor would be to shrink the electromagnetic footprint of each node equipped with a directional antenna, consequently rendering the entire MANET more spectrally permeable.

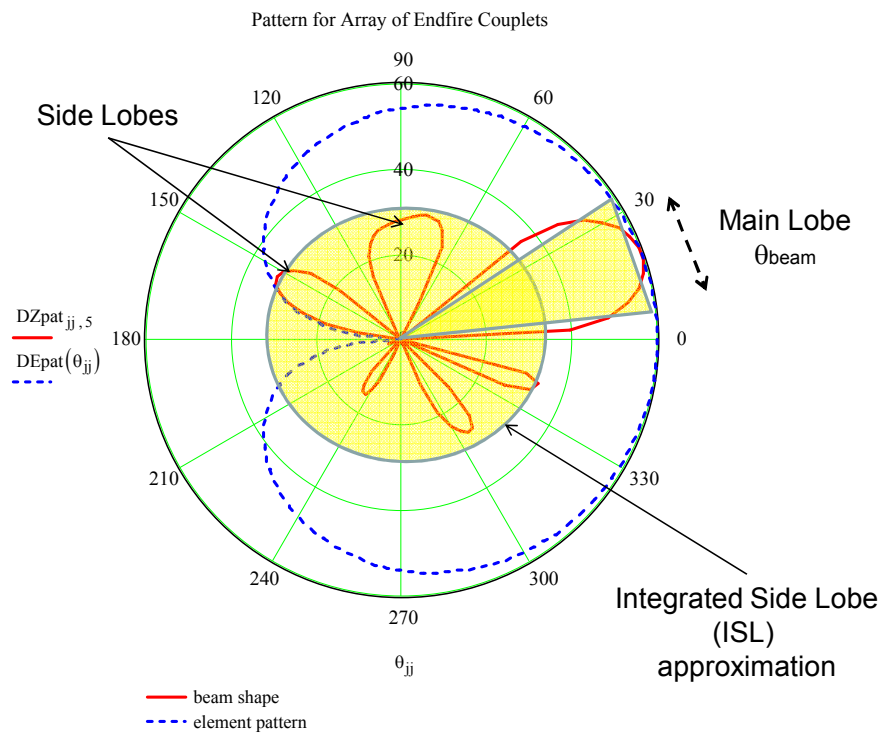


**Figure 49: Gain pattern for a nominal directional antenna array**

The antenna isolation factor can also be used to account for the probability that a potential interference source or victim (e.g., member of another network) may appear

within the antenna main lobe. One way to estimate this probability for two overlapping networks  $A$  and  $B$  is by:

$$F_{antenna}(A, B) \approx 1 - [1 - \eta_{antenna}(A)]^{\mu(A, B)} \quad (73)$$

where  $\eta_{antenna}(A)$  is the spatial diversity factor for directional antennas in network  $A$  and  $\mu(A, B)$  represents the average number of nodes from network  $B$  that will be within nearest-neighbor distance of a node from network  $A$ . This relationship is asymmetric when networks  $A$  and  $B$  use dissimilar antennas:

$$F_{antenna}(B, A) \neq F_{antenna}(A, B) \quad (74)$$

By assuming the uniform densities and circular MANET bounds of the top-down spectrum management model, one can apply the following approximation to overlapping networks of radii  $R_A$  and  $R_B$  with populations  $N_A$  and  $N_B$ :

$$\mu(A, B) \approx \pi \frac{N_B}{N_A} \left( \frac{R_A}{R_B} \right)^2 \quad (75)$$

Even a very wide-beam steerable antenna can confer significant advantages to a network if the MANET protocol is able to keep track of neighbor locations within its routing table. For a nominal example of two overlapping MANET of populations  $N_A = 30$  and  $N_B = 40$ ; radii  $R_A = 100\text{m}$  and  $R_B = 150\text{m}$ ; outfitted with steerable antennas of beamwidths  $\theta_A = 30$  deg and  $\theta_B = 45$  deg and assuming minimum  $ISL = -20$  dB, the nearest-neighbor density factors can be estimated by:

$$\mu(A, B) \approx 1.86 \quad (76)$$



$$\mu(B, A) \approx 5.3 \quad (77)$$

The resulting probabilities for inter-network beam interaction for this example are:

$$F_{antenna}(A, B) \cong 1 - \left(1 - \frac{1}{12}\right)^{1.86} \cong 0.15 \quad (78)$$

$$F_{antenna}(B, A) \cong 1 - \left(1 - \frac{1}{8}\right)^{5.3} \cong 0.51 \quad (79)$$

The probability of a beam from network  $A$  hitting a node from network  $B$  is approximately 15 percent while the converse probability ( $B$  sweeping  $A$ ) is about 51 percent. The expected long-term SINR improvement for each MANET would require much more detailed investigation, but a somewhat pessimistic lower bound can be estimated from the probability that neither of the directional antenna-equipped MANETs will significantly interfere with the other:

$$\Delta SINR \geq [1 - \Pr(\overline{A \rightarrow B}) \cdot \Pr(\overline{B \rightarrow A})]^{-1} \quad (80)$$

$$\Delta SINR_{dB} \geq 10 \log \left( \frac{1}{1 - [1 - F_{antenna}(A, B)] \cdot [1 - F_{antenna}(B, A)]} \right) \quad (81)$$

In the preceding example the estimated minimum improvement in SINR is approximately 2.4 dB, which is hardly dramatic, but may be sufficient to preserve connectivity in some marginal conditions. If a more detailed engineering model were to raise this simple estimate by as little as two decibels it might be sufficient to justify the investment in directional antennas. Future development of adaptive antenna technology and location-aware networking protocols will certainly require some assessment of the impact of directional antennas and spatial diversity. Monte Carlo simulation of inter-MANET interference is just one tool for such analysis.

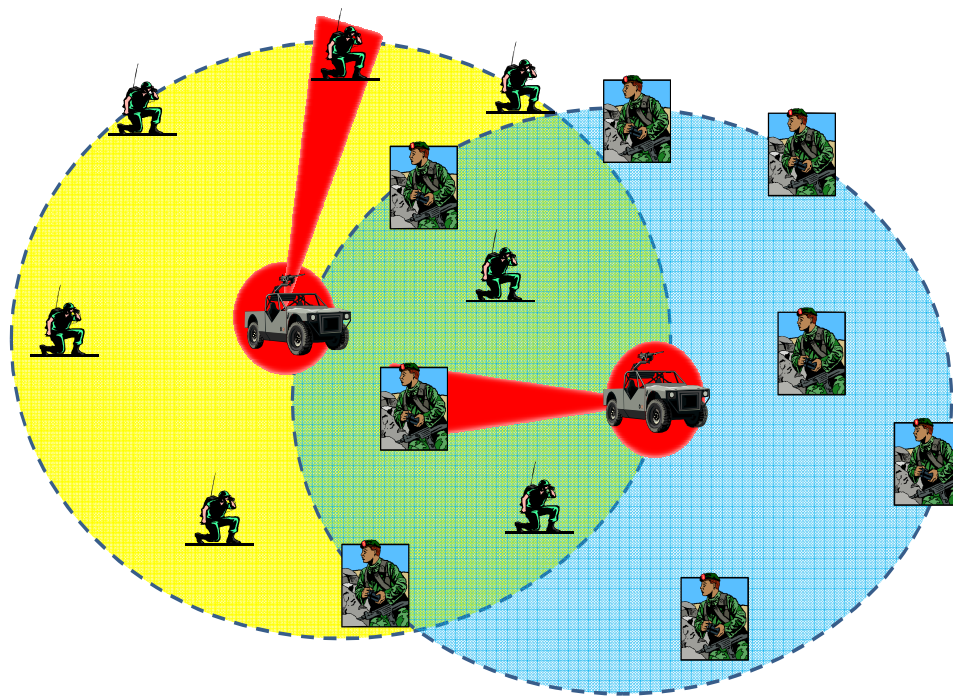


**Figure 50: Directional antennas can enable angular discrimination**

## Chapter 8: Conclusions

This study presented and examined via simulation two methods for automating the search for viable local spectrum distributions for land mobile radio networks.

Minimizing human participation in this critical time-consuming step would dramatically accelerate the spectrum management process by decreasing its overall cycle time. The simulations were used to develop heuristics that can tell a decision maker when self management will or will not work, and can quantify how much confidence one should place in that prediction.

With regard to the principal research questions proposed for this study, the following conclusions may be drawn:

- *Feasibility*: In both the continuous-gradient (Jones, OSE Algorithm, 2002) and the current SPSA-driven version of decentralized spectrum management it was shown that cognitive wireless networks are capable of solving spectrum contention issues on their own. This can be accomplished if there are:
  - Rules sets – Location based spectrum rights and restrictions
  - The ability to monitor network performance and detect interference
  - Goal-seeking algorithms to determine tuning changes
  - Signaling and synchronization of tuning changes across a network
- *Robustness*: The final distribution of SINR for both the centralized and decentralized approach is sensitive to the placement of the networks within the area of regard, and is thus likely to evolve as MANET migrate across

the area. The uncertainty in the solution is bounded by a decaying exponential function in terms of average available bandwidth per network, parameters that are usually known or estimated a priori. This observation allows one to estimate the probability that the minimum QoS among all networks will meet or exceed some threshold of usefulness. A prime example would be deciding whether or not to assign a newly arrived network into an already occupied band.

- *Useful applications:* Armed with QoS predictions based on a market equilibrium approach to spectrum, an automated spectrum adjudication algorithm can make useful decisions regarding whether to admit one more network into the local spectrum pool (Figure 32). Alternatively, human decision makers can devise engineering models to evaluate the risks and potential benefits of deploying emerging spectrum-related technologies (Figure 46), including the automated spectrum adjudication system itself.

### Technical Interpretation

The simulations developed for this study indicate that autonomous spectrum management is feasible for MANETs in either a refereed (“top down”) or a mutually negotiated (“bottom up”) configuration. The top-down model would be appropriate for urban public safety (e.g., police and firefighters) networks where emergency spectrum availability could be pre-negotiated or appropriated by state authority.

The bottom-up spectrum management model, with its lack of a vulnerable physical infrastructure, is better suited to the needs of an expeditionary military organization. The significant proportion of successful solutions, where the minimum SINR was greater than zero decibels, indicates that this method is indeed feasible. A conservative estimate of bottom-up settling time is 33 seconds, with the potential for order-of-magnitude improvement.

The objective function in each case was a reasonable surrogate for quality of service, while the SPSA optimization has been successfully used for many years in a wide range of system control applications.

Regression analysis of the simulation output also indicates that adaptive MANET spectrum management is a tractable problem. Not only were viable solutions (based on minimum SINR) achieved with algorithms of only mid-level complexity, but the quality and variability of these outcomes could be estimated by algebraic means using only presumably available state inputs. The smoothly varying bounds on the SINR prediction errors could for instance be used as the basis for additional spectrum supportability and risk management applications.

This study assumes the availability of location based spectrum rights, GPS-quality synchronization, and a signaling and control medium for large numbers of software defined radios. Internet Protocol Version 6 (IPv6) has the potential to enable the type of autonomous network management functions described here. Its extended address structure (128 bits versus 32 bits for IPv4) includes a “destination options” header and “flow labeling” features for exchanging control information in mobile networks. (OPNET

Technologies Inc., 2007) With  $2^{128}$  unique addresses available, IPv6 can afford to assign addresses to specific devices, which can, with the exchange of control information, enable the integration of signal diversity, smart directional antennas and MIMO processing into future networking protocols. Significant deviation from the strict OSI reference model (Tanenbaum, 1996) will be required to allow communication between the physical layer and the network layer if the goal is to make MANET signal envelopes more permeable and to extract more value from the available spectrum.

### *Economic Interpretation*

Although it was not the original intent of the study, the results for the utility-driven, bottom-up spectrum management model confirm the assertions of 2009 Nobel laureate economist Elinor Ostrom (Ostrom & Dietz, 2002) that locally autonomous groups and individuals are as capable of managing a common resource as any external authority, such as the government.

### *Future Work Needed*

As mentioned previously, what is presented here is not a new radio protocol, but a potential decision aid for the deployment of adaptive radio networks. More understanding of the subtle factors affecting the margin between success and failure (often just a few decibels for digital systems) is needed. Future tasks contemplated include characterizing the contributions of increased physical fidelity (e.g., mobility,

terrain and fading) and the impact of technical means for increasing signal diversity (e.g., TDMA, CDMA, and directional or polarization-switching antennas).

Agile, adaptive radio devices will soon begin to proliferate in the military services. The market for public safety communications equipment can be expected to follow suit. Only the means of managing these devices are in question. Autonomous spectrum management can transform adaptive systems from headache to asset. The utility-driven approach proposed in this study is viable solution to a limited class of spectrum problems, which will require the participation of government and industry in order to be realized. At the very least the methods used here can help to form the basis of procedures by which policy makers can quantify confidence in certain types of advanced wireless technologies.

## Appendix A: Spectrum Management Simulation

### Program Structure

Figure 51 depicts the executive (master) level structure implemented in MATLAB for a simulation study of utility-based spectrum allocation for mobile ad hoc networks (MANET).

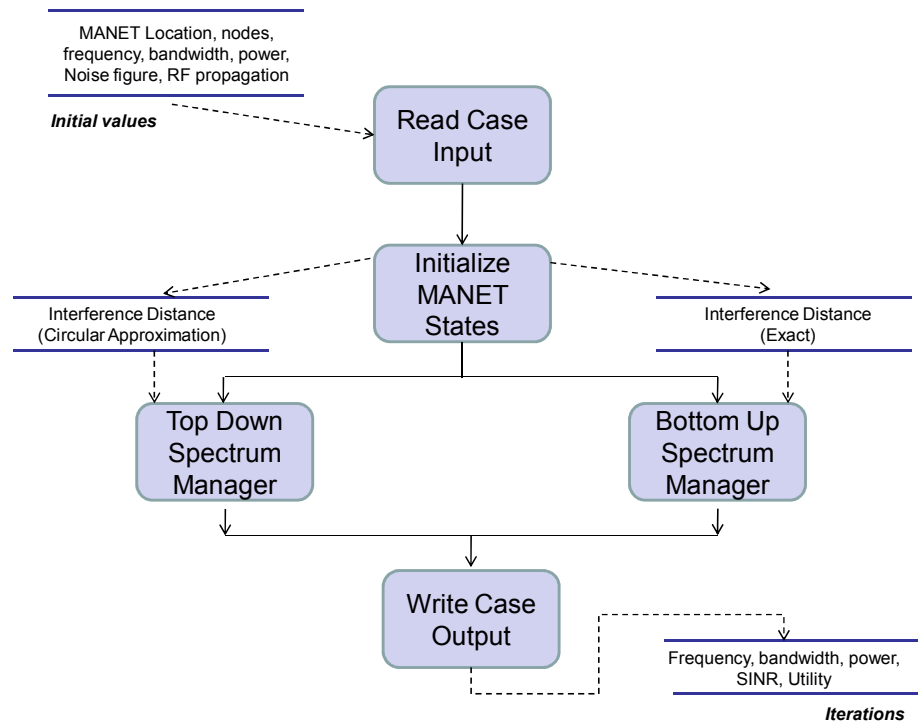


**Figure 51: Architecture diagram of spectrum management simulation**



Figure 52 depicts the application of the simultaneous perturbation simulated annealing (SPSA) method to autonomous spectrum management. The *top-down* spectrum management model uses a set of approximate inter-MANET and intra-MANET distances based on the location, radius and node population of each MANET. The propagation path losses between networks and within each network are calculated based on these distances, the current frequency set, node antenna heights, and local EM propagation constant. The top-down SPSA algorithm attempts to optimize a weighted sum of the mean and minimum *signal-to-interference-plus noise* ratio (SINR). The initial “guess” for a tuning state solution  $\Theta_1$ , is based on equally dividing the available spectrum.

For the first iteration (top-down) of MANET settings ( $n = 1 \dots N_{sys}$ ) for center frequency ( $f$ ) bandwidth ( $B$ ) and transmitter power ( $P$ ) are:

$$\Theta_1 = \begin{bmatrix} f_1 & \dots & f_{N_{sys}} \\ B_1 & \dots & B_{N_{sys}} \\ P_1 & \dots & P_{N_{sys}} \end{bmatrix} \quad (82)$$

The initial trial allocation of frequencies and bandwidth is defined by:

$$\Delta f = \frac{f_{max} - f_{min}}{N_{sys}} \quad (83)$$

$$f_n = f_{min} + (n - 1)\Delta f \quad (84)$$

$$B_n = \Delta f \quad (85)$$

The initial transmit power is set to ensure a link *signal-to-noise* ratio (SNR) of 10 dB in each MANET, in the absence of external interference:

$$P_n = N_{dBm} + L_p(\hat{d}_{nn}) + 10 \quad (86)$$

The *bottom-up* spectrum management model is based on each MANET sensing the interference caused by the others and re-tuning to avoid it. Each network attempts to improve its spectrum utility, which is a function of the SINR calculated from the “exact” link and interference distances (based on node locations), current frequencies and associated path losses. The initial state vector  $\Theta_1$  is taken directly from the initial frequencies, bandwidths and powers of the case input. The SPSA routine terminates when either the mean utility converges or the maximum iteration count ( $K_{max} = 600 \times N_{sys}$ ) is reached.

Although similar in concept and implementation, the top-down and bottom-up spectrum management models produce very different results.

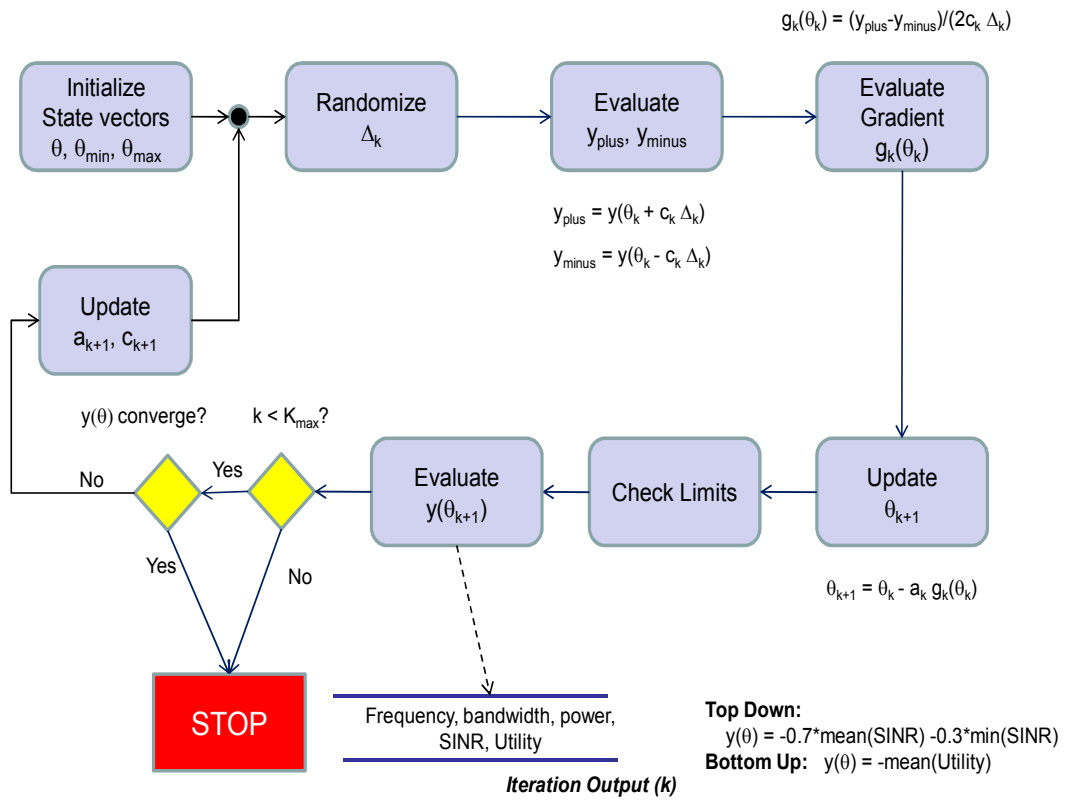


Figure 52: SPSA algorithm for spectrum management

## **MATLAB Source Code**

The following pages contain printouts of the MATLAB source code for several critical elements of the simulation used in this study. By no means does the author assert that these routines represent the only, or even the best way to approach the emulation of centralized and decentralized spectrum management, but merely that he was able to make them work.

Source code is included for the following routines:

1. Spectrum Management Executive
2. Process Initial States
3. Top-Down Spectrum Management (SPSA)
4. Bottom-Up Spectrum Management (SPSA)
5. Radio Propagation Loss
6. Frequency Dependent Integration
7. Spectrum Utility Function
8. Individual Loss Function
9. Group Loss Function

```

% ***** MANET Spectrum Executive Simulation *****
% This code is the executive (master) segment for a simulation study of
% utility based spectrum allocation for maneuverable ad hoc networks
% (MANET).
% Author: Leo H. Jones
% Created: 25 Sept 2006
% Last modified: 03 Sept 2008
% *****
% SECTION 1: INPUT
%global InitVals
%global CurrVals
% Open the input file and data structure "Caseinp".
%fid=0; fid2=0;
%while fid < 1
    %filename=input('Open input file: ', 's');
    %[fid, message] = fopen(filename, 'r');
    %if fid == -1
        %disp(message)
    %end
%end
%load(filename);
%caseout= caseinp;
%while fid2 < 1
    %f2name=input('Output file: ', 's');
    %[fid2,message2]= fopen(f2name, 'w');
    %if fid2 == -1
        % disp(message2)
    %end
%end
%InitVals = caseinp(1,1); %This is a kludge!
istart = input('Start with row number? ');
irx = 0;
% For each separate case:
[Irows, Jcols] = size(caseinp); ncas=0;
caseout(1:Irows-istart+1,:)=caseinp(istart:Irows,:);
for ir = istart:Irows
    irx = irx + 1;
    for jc = 1:Jcols % Jcols=1
        disp([ir,jc]);
        % Read the case input values.
        InitVals = caseinp(ir,jc);
        % Calculate derived inputs.
        proc_init_states;
        caseout(irx,jc).XY = CurrVals.XY;
    % SECTION 2: EXECUTION
    % Branch A: SPSA Top-Down Optimization
    Top_Down_Spectrum_Mgt2;
    % Branch B: SPSA Bottom-Up/Individual Goal-Seeking
    Bottom_Up_Spectrum_Mgt2;
    % Branch C: General Equilibrium Theory Solution
    %
% SECTION 3: OUTPUT
% Append results to data structure "Caseout".
caseout(irx,jc).FTD = fxa;
caseout(irx,jc).BTD = bxa;
caseout(irx,jc).PTD = pxa;

```

```

caseout(irx,jc).SNTD= sna;
caseout(irx,jc).UTD = una;
caseout(irx,jc).KTD = kfa;
caseout(irx,jc).FBU = fxu;
caseout(irx,jc).BBU = bxu;
caseout(irx,jc).PBU = pxu;
caseout(irx,jc).SNBU = snu;
caseout(irx,jc).UBU = unu;
caseout(irx,jc).KBU = kfu;
% SECTION 4: DATA COLLECTION & EXPORT
%
% End Case Loop
clear InitVals CurrVals;
    end
end
%
% Save Output Files
% First format: MATLAB structure (MAT-file)
save temp_out.mat caseout;
%count = fwrite(fid2, caseout);
% Close Input and Output Files
%fclose(fid);
%fclose(fid2);
%
% END PROGRAM

```

```

% ----- Initialize Network Interference States -----%
% Leo H. Jones, 08 Oct 2007
% Latest rev: 04 Feb 2008
% *****
% SECTION 1: INPUT
%global InitVals
%global CurrVals
Nsys = InitVals.Nsys;
clear CurrVals;
%ptype = InitVals.Ptype;
pmin = 1e-6; Bnom=InitVals.BW_max; alpha=InitVals.Alphas;
NF = InitVals.NF; npx=InitVals.npx;
% Initialize some needed arrays
DiMat = zeros(Nsys);
dnn = zeros(1,Nsys); D3nn = dnn;
%R=zeros(max(InitVals.Nodes),Nsys); Q=R; X=R; Y=R;
%
% 1. Get current geometry and location info for all (Nsys) networks in
play.
Np=InitVals.Nodes; Rmax=InitVals.Radius;
Xcn=InitVals.Xcnt; Ycn=InitVals.Ycnt;

% 2. Get initial tuning state (freq, bw, pt) for each network.
fmhz=InitVals.Freqi; Bmhz=InitVals.Bwi; PtdBm=InitVals.Pti;
%
% 3a. DiMat = Matrix of effective interference distances (circular
approx)
for i = 1:Nsys
    [R,Q,X,Y,D3nn(i)] =
setup_net_geometry(Np(i),Rmax(i),Xcn(i),Ycn(i));
    %Diagonal = intra-network (signal)
    dnn(i) = Rmax(i)*sqrt(pi/Np(i));
    DiMat(i,i) = dnn(i);
    %Off-diagonal = inter-network (i=Tx, j=Rx)
    if (i<Nsys)
        for j=i+1:Nsys
            Na = Np(i); Ra = Rmax(i); XYa= [Xcn(i),Ycn(i)];
            Nb = Np(j); Rb = Rmax(j); XYb= [Xcn(j),Ycn(j)];
            [DiMat(i,j),Ao,dna,dnb]=
circ_interf_approx2(Na,Ra,XYa,Nb,Rb,XYb);
            DiMat(j,i)=DiMat(i,j);
        end
    end
end
for k =1:Np(i)
    CurrVals.RTheta(i,k,1:2)=[R(k),Q(k)]; %#ok<AGROW>
    CurrVals.XY(i,k,1:2)=[X(k),Y(k)]; %#ok<AGROW>
end
end
% 3b. DxMat = Matrix of effective interference distances (exact)
for i =1:Nsys
    DxMat(i,i) = D3nn(i); Na = Np(i); %#ok<AGROW>
    XA = zeros(1,Na); YA = XA;
    for ii=1:Na
        XA(ii)=CurrVals.XY(i,ii,1); %#ok<AGROW>
        YA(ii)=CurrVals.XY(i,ii,2); %#ok<AGROW>
    end
end

```

```

end
if (i<Nsys)
    for j=i+1:Nsys
        Nb = Np(j); XB=zeros(1,Nb); YB=XB;
        for jj=1:Nb
            XB(jj)=CurrVals.XY(j,jj,1); %#ok<AGROW>
            YB(jj)=CurrVals.XY(j,jj,2); %#ok<AGROW>
        end
        [Dxx, Rcc] = interf_distance(XA,YA,XB,YB);
        DxMat(i,j) = max(Dxx, 5); %#ok<AGROW>
        DxMat(j,i)=DxMat(i,j); %#ok<AGROW>
    end
end
end
%
% Evaluate the spectrum utility function for this group
[SU,SINR]=grp_spec_util(fmhz,Bmhz,PtdBm,Rmax,Bnom,NF,DiMat,pmin,alpha,n
px);
[UX,SINX]=grp_spec_util(fmhz,Bmhz,PtdBm,Rmax,Bnom,NF,DxMat,pmin,alpha,n
px);
%
%Update current network states
CurrVals.Nsys = Nsys;
CurrVals.Nodes = Np;
CurrVals.fmhz = fmhz;
CurrVals.Bmhz = Bmhz;
CurrVals.PtdBm = PtdBm;
CurrVals.SU = SU;
CurrVals.SINR = SINR;
CurrVals.UX = UX;
CurrVals.SINX = SINX;
CurrVals.dnn = dnn;
CurrVals.DiMat = DiMat;
CurrVals.DxMat = DxMat;
CurrVals.Rmax = Rmax;
CurrVals.Xcn = Xcn;
CurrVals.Ycn = Ycn;
CurrVals.D3nn = D3nn;
CurrVals.npx = npx;

```

```

% ----- Top-Down Spectrum Management Optimization Model -----%
% This routine uses simultaneous-perturbation simulated annealing to
% approximate a global-optimum spectrum distribution. The relevant
inputs
% are network tuning states (freq, bw, pwr), inter- and intra-network
% distance matrix (DiMat) and RF propagation exponent (npx). Output is
% recommended tuning configuration: theta = <freq, bw, pwr>^Nsys. The
% objective function is based on the resulting network S/(I+N) values.
% Leo H. Jones, 12 Nov 2007
% Latest rev: 05 June 2008
% *****
%global InitVals
%global CurrVals
% Set SPSA starter parameters
a=0.5; alfa=0.55; c=0.5; gam=0.05; A=20;
%Step1: Get current network states and relevant distances
Nsys = InitVals.Nsys;
fmhz = CurrVals.fmhz;
Bmhz = CurrVals.Bmhz;
PtdBm = CurrVals.PtdBm;
alpha = InitVals.Alphas;
Rmax = CurrVals.Rmax;
npx = CurrVals.npx;
NdBm = InitVals.NF+10*log10(Bmhz)-114;
BWmin = InitVals.BW_max/4;
%Initialize current spectrum state vectors.
Lpx = zeros(1,Nsys); Ptx = zeros(1,Nsys); fguess = zeros(1,Nsys);
theta=zeros(Nsys,3);thetamax=theta;thetamin=theta;Vdelta=theta;
qdelta=theta;
%Start with enough power for S/N=10 dB.
%First guess: Divide the available spectrum equally.
Fmin = InitVals.Freq_lim(1); Fmax = InitVals.Freq_lim(2);
Fdiv = (Fmax-Fmin)/Nsys;
[F,IX]=sort(fmhz);
for i=1:Nsys
    Lpx(i) = Rn_Prop_Loss(fmhz(i),CurrVals.dnn(i),2,2,npx);
    Ptx(i) = NdBm(i)+Lpx(i)+10;
    theta(i,1:3)=[fmhz(i), Fdiv, Ptx(i)];
    thetamax(i,1:3) = [InitVals.Freq_lim(2)-
BWmin/2,InitVals.BW_max,InitVals.PT_max];
    thetamin(i,1:3) = [InitVals.Freq_lim(1)+BWmin/2,BWmin,-30];
    %Create a discrete difference vector for gradient estimation
    Vdelta(i,1:3)=[(thetamax(i,1)-thetamin(i,1))/20, (thetamax(i,2)-
thetamin(i,2))/20, 1];
    %Vdelta(i,1:3)= [1, 1, 1];
end
%Step2: Modify SPSA core to use current formulation
clear yta ya_trig;
clear fxa bxa pxa sna una yminus yplus ghat;
n=Nsys*600; ytrig = 1; k=0;
%for k=0:n-1
while lt(k,n)&& gt(ytrig,2e-4)
    ak=a/(k+1+A)^alfa;
    ck=c/(k+1)^gam;
    delta=2*round(rand(Nsys,3))-1;
    for i=1:Nsys

```



```

        for j=1:3
            qdelta(i,j)=delta(i,j)*Vdelta(i,j);
        end
    end
    thetaplus=theta+ck*qdelta;
    thetaminus=theta-ck*qdelta;
    %yplus=loss(thetaplus);
    yplus=grp_loss_fcn(thetaplus,Rmax,Bnom,NF,DiMat,pmin,alpha,npx);
    %yminus=loss(thetaminus);
    yminus=grp_loss_fcn(thetaminus,Rmax,Bnom,NF,DiMat,pmin,alpha,npx);
    ghat=(yplus-yminus)/(2*ck*qdelta);
    theta=theta-ak*ghat;
    theta=min(theta,thetamax);
    theta=max(theta,thetamin);
    yta(k+1)=grp_loss_fcn(theta,Rmax,Bnom,NF,DiMat,pmin,alpha,npx);
    if (k>1)
        ya_trig(k+1)=0.7*ya_trig(k)+0.3*abs((yta(k+1)-yta(k))/yta(k));
    else
        ya_trig(k+1)=abs((yta(k+1)-0.5*(yplus+yminus))/yta(k+1));
    end
    ytrig = ya_trig(k+1);
    if yta(k+1)>1
        ytrig = max(ytrig,1e-3);
    end
    k=k+1;
    fxa(k,1:Nsys)=theta(1:Nsys,1);
    bxa(k,1:Nsys)=theta(1:Nsys,2);
    pxa(k,1:Nsys)=theta(1:Nsys,3);

    [uu,ss]=grp_spec_util(fxa(k,1:Nsys),bxa(k,1:Nsys),pxa(k,1:Nsys),Rmax,Bn
om,NF,DxMat,pmin,alpha,npx);
    una(k,1:Nsys)=uu; sna(k,1:Nsys)=ss;
end
kfa=k;
theta;

```

```

% ----- Bottom-Up Spectrum Management Optimization Model -----%
% This routine uses simultaneous-perturbation simulated annealing to
% approximate local-optimum spectrum distribution. The relevant inputs
% are network tuning states (freq, bw, pwr), inter- and intra-network
% distance matrix (DiMat) and RF propagation exponent (npx). Output is
% recommended tuning configuration: theta = <freq, bw, pwr>^Nsys. The
% objective function is based on the resulting network S/(I+N) values.
% Leo H. Jones, 12 Nov 2007
% Latest rev: 5 June 2008
% *****
%global InitVals
%global CurrVals
% Set SPSA starter parameters
a=0.5; alfa=0.55; c=0.5; gam=0.05; A=20;
%Step1: Get current network states and relevant distances
Nsys = InitVals.Nsys;
fmhz = CurrVals.fmhz;
Bmhz = CurrVals.Bmhz;
PtdBm = CurrVals.PtdBm;
alpha = InitVals.Alphas;
Rmax = CurrVals.Rmax;
npx = CurrVals.npx;
NdBm = InitVals.NF+10*log10(Bmhz)-114;
BWmin = InitVals.BW_max/4;
%Initialize current spectrum state vector.
Lpx = zeros(1,Nsys); Ptx = zeros(1,Nsys); fguess = zeros(1,Nsys);
thetu=zeros(Nsys,3);thetamax=thetu;thetamin=thetu;Vdelta=thetu;
%Start with enough power for S/N=10 dB.
for i=1:Nsys
    Lpx(i) = Rn_Prop_Loss(fmhz(i),CurrVals.dnn(i),2,2,npx);
    Ptx(i) = NdBm(i)+Lpx(i)+10;
    thetu(i,1:3)=[fmhz(i), Bmhz(i), Ptx(i)];
    thetamax(i,1:3) = [InitVals.Freq_lim(2)-
BWmin/2,InitVals.BW_max,InitVals.PT_max];
    thetamin(i,1:3) = [InitVals.Freq_lim(1)+BWmin/2,BWmin,-30];
    %Create a discrete difference vector for gradient estimation
    Vdelta(i,1:3)=[(thetamax(i,1)-thetamin(i,1))/20, (thetamax(i,2)-
thetamin(i,2))/20, 1];
end
%Step2: Modify SPSA core to use current formulation
clear ytu yu_trig;
clear fxu bxu pxu snu unu uplus uminus ghu;
n=Nsys*1200; ytrig = 10; k=0;
%for k=0:n-1
while lt(k,n)&& gt(ytrig,1e-4) %#ok<AND2>
    ak=a/(k+1+A)^alfa;
    ck=c/(k+1)^gam;
    delta=2*round(rand(Nsys,3))-1;
    for i=1:Nsys
        for j=1:3
            qdelta(i,j)=delta(i,j)*Vdelta(i,j); %#ok<AGROW>
        end
    end
    thetaplus=thetu+ck*qdelta;
    thetaminus=thetu-ck*qdelta;
    %yplus=loss(thetaplus);

```

```

uplus=indv_loss_fcn(thetaplus,Rmax,Bnom,NF,DxMat,pmin,alpha,npx,0);
%yminus=loss(thetaminus);
uminus=indv_loss_fcn(thetaminus,Rmax,Bnom,NF,DxMat,pmin,alpha,npx,0);
for i=1:Nsys
    qdu = qdelta(i,1:3);
    ghu(i,1:3)=(uplus(i)-uminus(i))./(2*ck*qdu);
end
%ghat=(yplus-yminus)./(2*ck*qdelta);
thetu=thetu-ak*ghu;
thetu=min(thetu,thetamax);
thetu=max(thetu,thetamin);
%Goal-seek based on spectrum utility function
yuu = indv_loss_fcn(thetu,Rmax,Bnom,NF,DxMat,pmin,alpha,npx,1);
ytu(k+1)=-mean(yuu);
if (k>0)
    yu_trig(k+1)=0.3*yu_trig(k)+0.7*abs((ytu(k+1)-ytu(k))/ytu(k));
else
    %yu_trig(k+1)=abs((ytu(k+1)-0.5*mean(uplus+uminus))/ytu(k+1));
    yu_trig(k+1)=1;
end
ytrig = yu_trig(k+1);
k=k+1;
fxu(k,1:Nsys)=thetu(1:Nsys,1);
bxu(k,1:Nsys)=thetu(1:Nsys,2);
pxu(k,1:Nsys)=thetu(1:Nsys,3);

[uu,ss]=grp_spec_util(fxu(k,1:Nsys),bxu(k,1:Nsys),pxu(k,1:Nsys),Rmax,Bn
om,NF,DxMat,pmin,alpha,npx);
    unu(k,1:Nsys)=uu;
    snu(k,1:Nsys)=ss;
end
kfu=k;
thetu;

```

```

%----- Radio Propagation Loss Calculation -----
% This function calculates R^n radio propagation loss in decibels.
% Reference: R.A. Poisel, "Modern Communications Jamming Principles
% and Techniques", Artech House, Norwich MA (2004).
% Created 11/01/07 by Leo H. Jones
% Inputs: fMHz = Frequency (MHz)
%   dist = path length (m)
%   ht = Transmit antenna height (m)
%   hr = Receiver antenna height (m)
%   nx = Propagation exponent
%       2 = Free space; 3 = Rolling open terrain;
%       4+ = Urban (street); 5+ = Urban (indoors)
% Outputs: Lp = Basic transmission loss (dB)
%*****
function Lp = Rn_Prop_Loss(fMHz,dist,ht,hr,nx)
%Calculate critical distance (meters) for free-space region
dCrit = 4*pi*ht*hr*fMHz/300;
Lcrit = 20*log10(4*pi*dCrit*fMHz/300);
% Calculate transmission loss using coefficients
if (dist < dCrit)
    Lp = Lcrit + 20*log10(dist/dCrit);
else
    Lp = Lcrit + 10*nx*log10(dist/dCrit);
end
return

%-----Frequency Dependent Integration-----%
% This routine calculates the Frequency Dependent Integration (FDI)
factor
% between two band-limited signals, specified by center frequency and
% bandwidth. Uses Gaussian form to model passband.
% Leo H. Jones, 14 March 2006
% Modified 25 Jan 2008
% Inputs: fs = center frequency of desired signal
%   fi = center frequency of undesired (interference) signal
%   Bs = half-power (3 dB) bandwidth of desired signal
%   Bi = half-power (3 dB) bandwidth of interference signal
%*****
function eta = fd_integ(fs,fi,Bs,Bi)
u1 = real((fi-fs+0.5*Bs)/Bi);
u2 = real((fi-fs-0.5*Bs)/Bi);
fdi = 0.533*(erf(1.66*u1)-erf(1.66*u2));
eta = min(fdi+eps,1);
return

```

```

%----- Group Spectrum Utility Calculation -----%
% This function determines a composite measure of the value of a given
% network tuning state. The principal components are derived from:
% (1) Shannon channel capacity limit (bit/s)
% (2) Area spectral efficiency (bps/Hz/m^2)
% (3) Bit-error rate (dimensionless)
% Created by Leo Jones, 28 March 2006
% Modified: 25 Jan 2008
% Inputs:
%   Nets = Number of MANET to consider
%   fmhz = Center frequency (MHz) for individual MANETs
%   Bmhz = Signal bandwidth (MHz)
%   PtdBm = Average node transmit power (dBm)
%   NF = Receiver noise figure (dB)
%   DMat = Matrix of effective interference distances
%         diagonal = intra-network
%         off-diagonal = inter-network (i=Tx, j=Rx)
%   B0 = Nominal signal bandwidth
%   pmin = Lowest operationally significant BER (Anything less is
wasted)
%   alpha(1:3) = Weighting factors for significance of each component.
%   npx = RF propagation exponent (R^n model)
% Outputs:
%   Ueff(1:N) = Spectrum utility for each network
%   SINR = S/(I+N) ratio (dB)
%*****
function [Ueff, SINR] =
grp_spec_util(fmhz, Bmhz, PtdBm, Rmax, B0, NF, DMat, pmin, alpha, npx)
% Calculate Noise Floor (dBm)
NdBm = -114 + NF + 10*log10(Bmhz);
% Calculate Propagation Loss matrix LPMat; Initialize intermediates
Nets = length(fmhz);
LPMat = zeros(Nets); feta = zeros(Nets);
SdBm = -200*ones(1,Nets); SINR = SdBm; Ueff = SdBm;
for i=1:Nets
    for j=1:Nets
        LPMat(i,j)= Rn_Prop_Loss(fmhz(i), DMat(i,j), 2, 2, npx);
        if (j==i)
            % Intra-network (nearest neighbor) FDI factor
            feta(i,j)= 1;
        else
            % Inter-network (closest approach) FDI factor
            feta(i,j)=fd_integ(fmhz(j), fmhz(i), Bmhz(j), Bmhz(i));
        end
    end
    % Intra-network signal strength (dBm)
    SdBm(i)= PtdBm(i)-LPMat(i,i);
end
% Effective signal margin: Assumes min 6dB S/N for useful signal
Smarg = SdBm - NdBm - 6;
% Now get the interference power at each net
for j=1:Nets
    ImW = 0;
    for i=1:Nets
        if (i~=j)
            ImW = ImW + feta(j,i)*10^(0.1*(PtdBm(j)-LPMat(j,i)));
        end
    end
end

```

```

        end
    end
    % S/(I+N) ratio - decibels
    INdBm = 10*log10(ImW + 10^(0.1*NdBm(j)));
    SINR(j) = SdBm(j)-INdBm;
    % S/(I+N) ratio - numeric
    gamma = 10^(SINR(j)*0.1);
    % Common SINR factor for all elements
    gfac = log2(1+gamma);
    % Shannon channel capacity (bps) Capac = Bmhz*log2(1 + gamma)*1e6;
    Ucap = gfac*Bmhz(j)/B0;
    % Signal footprint (circular limit)
    A0 = pi*Rmax(j)^2;
    Asig = pi*(Rmax(j) + DMat(j,j)*10^(0.1*Smarg(j)/npx))^2;
    % Area spectral efficiency (bps/Hz/m^2) ASE = (Capac*1e-
6)/(Bmhz*Asig);
    Uase = gfac*A0/Asig;
    % Bit error rate (BPSK)
    Pbe = 0.5*exp(-gamma);
    Uber = -log10(Pbe+pmin);
    % Spectrum utility function
    % Ueff = alpha(1)*log10(Capac)+alpha(2)*log10(ASE)-log10(Pbe+pmin);
    Ueff(j) = alpha(1)*Ucap+alpha(2)*Uase+alpha(3)*Uber;
end
return

```

```

%***** Individual Loss Function for Bottom Up SPSA Method ****
%   Created 11/25/07
%   Latest mod: 12/05/07
%*****
function [Yeff] =
indv_loss_fcn(theta,Rmax,B0,NF,DiMat,pmin,alpha,npix,iout)
ir = size(theta,1); fx=zeros(1,ir);bx=fx;ptx=-60*ones(1,ir);
for i=1:ir
    fx(i)=theta(i,1);bx(i)=theta(i,2);ptx(i)=theta(i,3);
end
[SU,SINR]=grp_spec_util(fx,bx,ptx,Rmax,B0,NF,DiMat,pmin,alpha,npix);
switch iout %Output type
    case 0 %Use S/(I+N) ratio in dB
        Yeff = -SINR;
    case 1 %Use ad hoc spectrum utility function
        Yeff = -SU;
end
return

%***** Group Loss Function for Top Down SPSA Method ****
%   Created 11/25/07
%   Latest mod: 11/30/07
%*****
function [Yeff] = grp_loss_fcn(theta,Rmax,B0,NF,DiMat,pmin,alpha,npix)
ir = size(theta,1);
for i=1:ir
    fx(i)=theta(i,1);bx(i)=theta(i,2);ptx(i)=theta(i,3);
end
[SU,SINR]=grp_spec_util(fx,bx,ptx,Rmax,B0,NF,DiMat,pmin,alpha,npix);
%Yeff = -sum(SU);
%Yeff = -mean(SINR);
Yeff =-0.3*mean(SINR)-0.7*min(SINR);
return

```

## **Appendix B: Sample Case Input**

The MATLAB simulation developed for this study runs in batch mode and operates on a two-dimensional data structure matrix. Each entry in this input matrix, e.g., *caseinp(10, 30)* is a data structure that describes the starting conditions for a particular case, as described in Table 8. This case examines the spectrum conflict and potential resolution when four MANET are together in a region represented by a 1.2 km x 1.2 km square. All nodes are identically equipped and run similar applications, consequently the utility functions are also identical.

The node populations and radio propagation constant are suggestive of teams of police and firefighters responding to an urban emergency. The response squads have arrived on the scene with their radios nets in an initial state of mutual interference and are probably much too busy to resolve this problem manually.



**Table 8: Simulation Inputs for Sample Case**

<b>Input</b>	<b>Name</b>	<b>Example</b>
Case number	Case_id	104
MANET mix: <i>0=homogeneous,</i> <i>1=heterogeneous</i>	Case_typ	0
Playbox limits (m)	XYmax	[1200 1200]
Frequency limits (MHz)	Freq_lim	[589.8013 635.1012]
Number of MANET	Nsys	4
Nodes per MANET	Nodes	[11 11 9 10]
MANET radius (m)	Radius	[282 239 295 256]
Maximum bandwidth per MANET (MHz)	BW_max	22.6500
Maximum transmit power (dBm)	PT_max	15
Propagation constant	npx	4
Receiver noise figure (dB)	NF	9
Spectrum utility constants $\alpha_n$	Alphas	[0.0120 0.8602 0.1278]
Centroid X-coordinate (m)	Xcnt	[838.0214 802.2270 343.4400 369.1579]
Centroid Y-coordinate (m)	Ycnt	[818.4263 563.6132 566.0221 698.4720]
Initial Frequency (MHz)	Freqi	[605.4943 620.1504 605.4270 623.0794]
Initial Bandwidth (MHz)	Bwi	[19.4448 17.2566 20.3721 17.4806]
Initial Transmit Power (dBm)	Pti	[6.8695 6.1498 7.5565 6.8578 8.4054 5.2893]

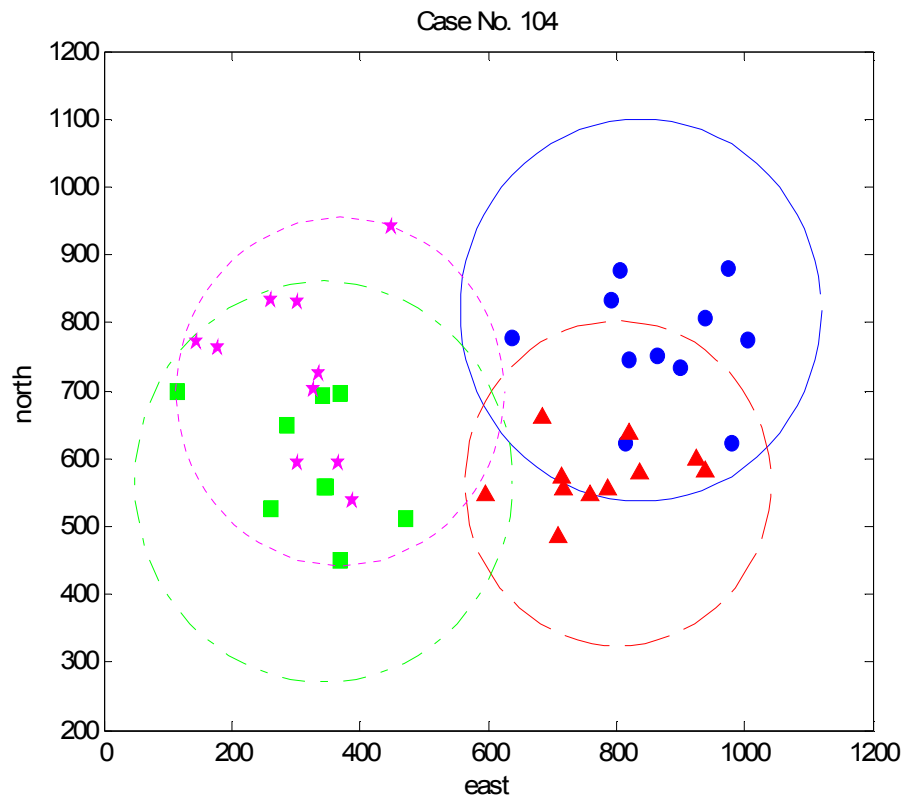
## Appendix C: Sample Case Output

In the MATLAB simulation used in this study, the case output was appended to the input data structure for convenient post-processing. The elements of the case output are listed in Table 9.

**Table 9: Simulation Case Output**

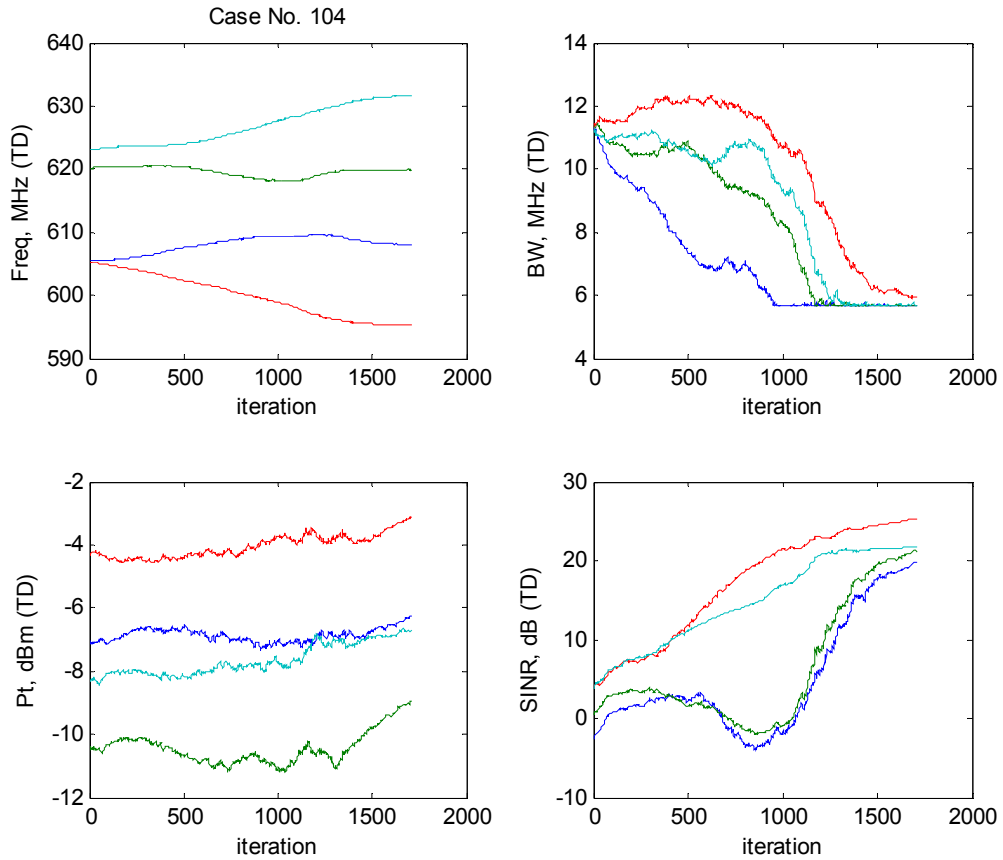
<b>Output</b>	<b>Name</b>	<b>Units</b>
Initial node locations (east, north)	XY	m
Frequency sequence (top-down)	FTD	MHz
Bandwidth sequence (top-down)	BTD	MHz
Power sequence (top-down)	PTD	dBm
SINR sequence (top-down)	SNTD	dB
Utility sequence (top-down)	UTD	---
Number of iterations (top-down)	KTD	---
Frequency sequence (bottom-up)	FBU	MHz
Bandwidth sequence (bottom-up)	BBU	MHz
Power sequence (bottom-up)	PBU	dBm
SINR sequence (bottom-up)	SNBU	dB
Utility sequence (bottom-up)	UBU	---
Number of iterations (bottom-up)	KBU	---

Figure 53 depicts a random distribution of radio nodes generated from the initial input listed in Table 8. Nodes associated with emergency response teams are assumed to be free to move anywhere within the current boundary for their particular MANET. The centroid locations, boundaries and individual node locations are inputs to the approximate (top-down) and exact (bottom-up) models for inter- and intra-MANET link distances.



**Figure 53: MANET node distribution generated for Sample Case**

Figure 54 depicts the sequences of frequency, bandwidth, node power and SINR for the top-down solution of the sample case. Figure 55 shows the corresponding sequences for the bottom-up solution of the same case.



**Figure 54: Top-Down Spectrum Solution for Sample Case 104**

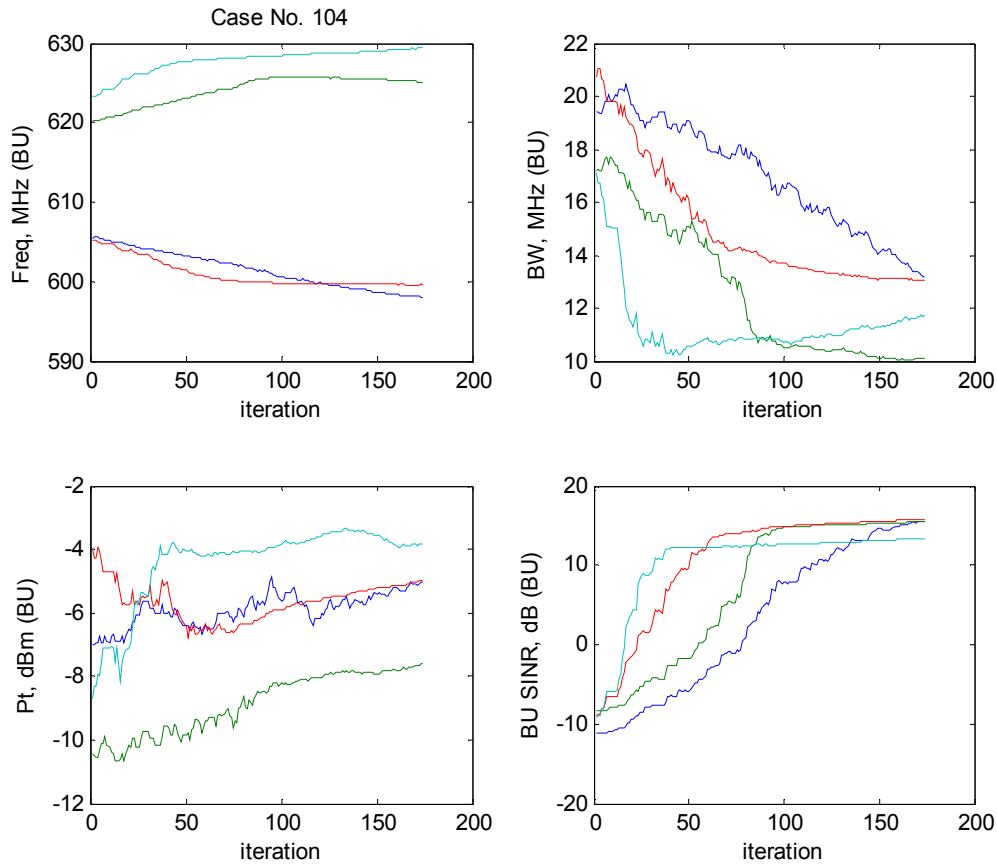


**Figure 55: Bottom-Up Spectrum Solution for Sample Case 104**

It is important to remember that although in this instance the top-down solution takes nearly ten times as many iterations as the bottom-up (1709 steps versus 174), the time scales are not comparable for purposes of implementation. The top-down solution speed is limited only by the efficiency of the algorithm and the computational power of one central device. As estimated in Appendix D, the time to reach bottom-up equilibrium is determined by the number of hops needed to promulgate incremental tuning commands throughout the nets, a number bounded by the logarithm of the number of nodes.

Figure 56 depicts the evolution of the individual MANET utility functions for both the top-down and bottom-up models. The bottom plot in this figure shows the sum of utility for all four networks.

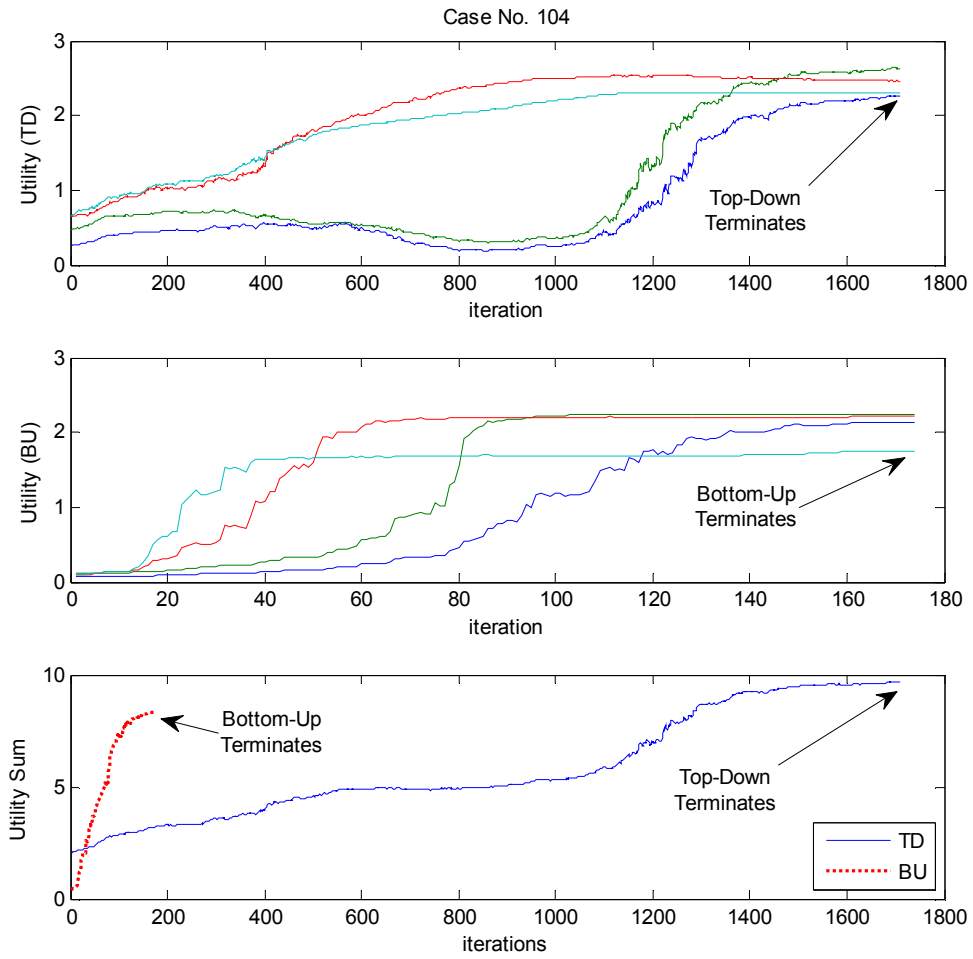
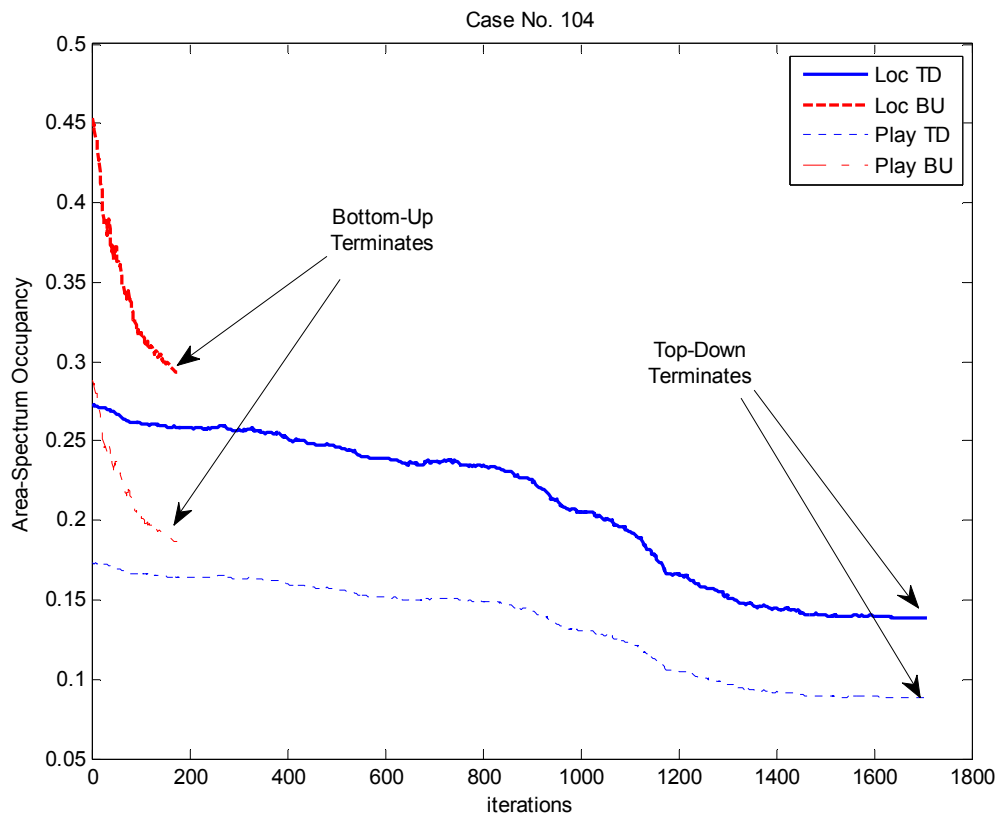


Figure 56: Spectrum Utility Evolution for Sample Case 104

The product of the playbox area and the total available bandwidth can be considered as a three-dimensional manifold, as in Figure 15. Figure 57 depicts the fraction of this space-frequency manifold occupied by all the MANET as a sequence of SPSA iterations. In this plot “local” refers to the product of the occupied spectrum and the geographical area of all the MANET.



**Figure 57: Playbox Occupancy Evolution for Sample Case 104**

## Appendix D: Timing Estimate for Autonomous Spectrum Allocation

The time required to propagate interference sensing data and tuning commands for a single SPSA iteration through a MANET,  $t_{iter}$ , can be modeled as the sum of times required to sense interference ( $t_{sense}$ ), compute the desired incremental change in the tuning state ( $t_{comp}$ ), and pass the new tuning command through the network ( $t_{cmd}$ ):

$$t_{iter} = t_{sense} + t_{comp} + t_{cmd} \quad (87)$$

- Assuming that each sensing node in “bottom-up” spectrum management is equipped with a real-time spectrum analyzer of resolution  $\Delta f=10$  kHz<sup>13</sup>, the minimum dwell time needed to resolve adjacent-band interference is:

$$t_{sense} \approx 1/\Delta f = 10^{-4}sec = 100 \mu s \quad (88)$$

- The “master” node in each MANET is assumed to be equipped with a processor capable of at least one million floating point operations per second (1 MFLOPS), well within the range of commercially available technology. Without the need to simulate interference, a computational budget of 100 mathematical operations should be sufficient to determine the next tuning state increment:

$$t_{comp} < \frac{100 ops}{10^6 ops/sec} = 100 \mu s \quad (89)$$

---

<sup>13</sup> The Rockwell Collins sensors used in the 2004-2006 research and development, test and evaluation (RDT&E) phase of the DARPA XG cognitive radio program have a channel resolution of 10 kHz.



- A generous estimate for the size of the incremental tuning command would be 1024 bits. According to Shannon's channel capacity theorem, a minimum bandwidth greater than 256 kHz at any SINR above 6 dB ( $\gamma=4$ ), should be sufficient to support a data rate of 512 kbps. A conservative estimate of node-to-node command transfer time  $\tau_{link}$  is thus:

$$\tau_{link} < \frac{1024 \text{ bits}}{512 \text{ kbps}} = 2 \text{ ms} \quad (90)$$

- The number of node-to-node data transfers required to span the network is bounded by a logarithmic function of the total number of nodes:

$$t_{cmd} < \tau_{link} \cdot \log_2 \text{Nodes} \quad (91)$$

- For the largest MANET simulated in this study,  $\text{Nodes} = 40$ , so:

$$t_{iter} < 0.2 \text{ ms} + (2 \log_2 40) \text{ ms} \approx 11 \text{ ms} \quad (92)$$

- A maximum of 600 SPSA iterations per MANET present was allowed in this simulation study. Any future deployment would be expected to include an even more efficient tuning algorithm. Thus for a maximum occupancy  $N_{sys} = 10$ , the maximum and average solution times for a bottom-up architecture would be bounded by:

$$T_{max} = 600 N_{sys} \cdot t_{iter} < 66 \text{ sec} \quad (93)$$

$$T_{soln} \approx \frac{1}{2} T_{max} < 33 \text{ sec} \quad (94)$$

It should be noted that the SPSA algorithms used in this proof-of-concept study were not designed for computational efficiency. With further development, there may be room for an order-of-magnitude improvement in these preliminary estimates.

## Appendix E: List of Symbols

The page number is the location of the first use. Where the symbol is defined later, that page is also given.

Symbol	Meaning	Page
$\alpha$	Coefficients of MANET objective function	14
$\alpha_s$	Constant for SPSA iteration	38, 39
$A_{eff}$	Effective MANET area	16
$A_{sig}$	MANET signal footprint area	27
$B$	Bandwidth	15
$B_i$	Interference bandwidth	34, 35
$B_s$	Signal bandwidth	34
$D_{AB}$	Distance between MANET centroids	33
$d_{AB}$	Interference distance between MANET $A$ and $B$	33
$d_{nn}$	Nearest-neighbor distance	27
$f$	Center frequency of transmission	34
$f_i$	Center frequency of interference	35
$f_s$	Center frequency of intended signal	34
$\gamma$	Signal to Interference plus Noise Ratio (SINR)	15
$\gamma_s$	Constant for SPSA iteration	38, 39
$g_n$	Weighting factor for harmonics	31
$\eta_{FDI}$	Frequency dependent interference	34
$I$	Interference power	25
$L_p$	Radio propagation loss	25, 27
$N$	Noise power	25
$N_A$	Number of nodes in network A	33
$N_B$	Number of nodes in network B	33
$N_h$	Number of harmonics	31
$N_{sys}$	Number of MANET present	40
$p_{min}$	Minimum useful bit error rate	16
$Pe_{BPSK}$	Bit error probability for Binary Phase Shift Keying	16
$P_t$	Transmit power	25
$P_{t_{min}}$	Minimum transmit power	25
$\theta_g$	MANET group direction (azimuth)	28
$\Theta$	Composite state vector for a set of MANET	37
$R_{sig}$	MANET signal footprint radius	27
$S$	Received signal power	25
$S_n$	SPSA state vector corresponding to $n^{\text{th}}$ MANET	36
$\Delta S$	Signal margin (dB)	25
$S_{min}$	Minimum useful signal strength (dB)	25
$U_{OBJ}$	MANET utility objective function	14
$U_{ASE}$	Utility with regard to Area Spectral Efficiency	15
$U_{BER}$	Utility with regard to Bit Error Rate	15
$U_{CAP}$	Utility with regard to Channel Capacity	15
$V_g$	MANET group velocity	28

## **Bibliography**

Alion Science and Technology. (2004). *Evaluation of UWB and Adjacent Channel Interference to C-Band Earth Stations*. Landover, MD: Alion Science and Technology.

Alouini, M.-S., & Goldsmith, A. (1997, April). Area Spectral Efficiency of Cellular Mobile Radio Systems. *IEEE Transactions on Vehicular Technology* .

Benkler, Y. (2002). Some Economics of Wireless Communications. *Harvard Journal of Law and Technology* , 16 (1), 25-83.

Byowsky, M. M., & Marcus, M. J. (2002). Facilitating Spectrum Management Refrom via Callable/Interruptible Spectrum. *2002 Telecommunications Policy Research Conference*. Washington, DC.

CRC. (1996). *Standard Mathematical Table and Formulae* (30th ed.). (D. Zwillinger, Ed.) New York, New York: CRC Press.

Crow, E. L., Davis, F. A., & Maxfield, M. W. (1960). *Statistics Manual*. Mineola, New York: Dover.

Defense News. (2007, April 16). Pushing off the Spectrum Crunch Company's Radio Finds 'White Space' Among Frequencies. *Defense News* , p. 1.

Faulhaber, G. R. (2008). Deploying Cognitive Radio: Economic, Legal and Policy Issues. *International Journal of Communication* , 1114-1124.

Faulhaber, G. R. (2005). The Question of Spectrum: Technology, Management and Regime Change. *Journal on Telecommunication and High Technology Law* , 4 (1).

FMI 6-20.70 (FM 24-2) . (2006). *Army Electromagnetic Spectrum Management Operations*. Washington, DC: Headquarters, Department of the Army.

Gupta, P., & Kumar, P. R. (2000). The capacity of wireless networks. *IEEE Transactions on Information Theory* , 46 (2), 388-404.

ITU Radiocommunication Bureau. (2005). *National Spectrum Management*. Geneva: International Telecommunication Bureau.

Jones, L. H. (2002). Algorithm to Optimize the Operational Spectrum Effectiveness of Wireless Communication Systems. *MILCOM 2002*. Anaheim, CA: IEEE.

Jones, L. H. (2002). Operational Spectrum Effectiveness: Management of Adaptive Wireless Networks. *MILCOM 2002*. Anaheim: IEEE.

Jones, L. H., Johnson, L. R., Love, N., & Stegmann, S. (2009). Betting for Bandwidth: A Market Model for QoS and Intelligence Expediency. *Northrop Grumman Engineering Advisory Group Seminar*. Linthicum, MD: Northrop Grumman Corporation.

Katz, M. L., & Rosen, H. S. (1998). *Microeconomics* (3rd ed.). Boston: McGraw-Hill.

Marshall, P., Martin, T., McHenry, M., & Kolodzy, P. (2006). XG Dynamic Spectrum Findings, Experiments and Plans Panel. *DoD Spectrum Summit 2006*. Annapolis, MD: Joint Spectrum Center.

Matheson, R. J. (1994). *A Survey of Relative Spectrum Efficiency of Mobile Voice Communication Systems, NTIA Report 94-311*. Washington: US Department of Commerce.

Miller, L. H. (1956, March). Table of Percentage Points for Kolmogorov Statistics. *Journal of the American Statistical Association* , 51 (273), pp. 111-121.

Mitola, J. (1992). Software Radios: Surveys, Critical Evaluation and Future Directions. *IEEE National Telesystems Conference*.

Moore, L. K. (2009). *Public Safety Communications and Spectrum Resources: Policy Issues for Congress*. Washington, DC: Congressional Research Service.

National Telecommunications and Information Administration. (2008). *Manual of Regulations and Procedures for Federal Frequency Management*. Washington: U. S. Department of Commerce.

OPNET Technologies Inc. (2007). Introduction to IPv6. *OPNETWORK 2007*. Washington, DC.

Osborn, K. (2008, January 7). U. S. Army Faces Spectrum Crunch. *Defense News* , p. 1.

Ostrom, E., & Dietz, T. (2002). *The Drama of the Commons*. Washington, DC: National Academies Press.

Peha, J. M. (2005, March). Protecting Public Safety with Better Communication Systems. *IEEE Communications* .

Poisel, R. A. (2004). *Modern Communications Jamming Principles and Techniques*. Norwood, MA: Artech House.

Reply Comments of AT&T Wireless Services Inc., FCC ET Docket 00-47 (Federal Communications Commission July 14, 2000).

- Shannon, C. E. (1948). A Mathematical Theory of Communication. *The Bell System Technical Journal* , 27, 379-423, 623-656.
- Silverman, S. J. (2006). Game Theory and Software Defined Radios. *MILCOM 2006* (pp. 1-7). Washington, DC: IEEE.
- Spall, J. C. (1998). An Overview of the Simultaneous Perturbation Method for Efficient Optimization. *Johns Hopkins APL Technical Digest* , 19 (4), 482-492.
- Starr, R. M. (1997). *General Equilibrium Theory: An Introduction*. Cambridge, United Kingdom: Cambridge University Press.
- Stine, J. A. (2007). A Location-Based Method for Specifying RF Spectrum Rights. *IEEE DySpan 2007*. Dublin: Institute of Electrical and Electronics Engineers.
- Stine, J. A. (2006, April). Enabling Secondary Spectrum Markets Using Ad Hoc and Mesh Networking Protocols. *Journal of Communications* , 26-37.
- Stine, J. A., & Portigal, D. L. (2004). *Spectrum 101: An Introduction to Spectrum Management*. McLean, VA: MITRE.
- Talbot, D. (2004, November). How Technology Failed in Iraq. *MIT Technology Review* .
- Tanenbaum, A. S. (1996). *Computer Networks (3rd ed)*. Upper Saddle River, NJ: Prentice-Hall.
- Yi, Y., & Chiang, M. (2008). Stochastic Network Utility Maximization. *European Transactions on Telecommunications* , 00, 1-22.